NUMERICAL STUDIES OF FRUSTRATED QUANTUM PHASE TRANSITIONS

NUMERICAL STUDIES OF FRUSTRATED QUANTUM PHASE TRANSITIONS IN TWO AND ONE DIMENSIONS

By MISCHA THESBERG, M.Sc., B.Sc.

A Thesis Submitted to the School of Graduate Studies in Partial Fulfilment of the Requirements for the Degree Doctor of Philosophy

McMaster University DOCTOR OF PHILOSOPHY (2014)
Hamilton, Ontario (Physics & Astronomy)

TITLE: Numerical Studies of Frustrated Quantum Phase Transitions in Two and One Dimensions

AUTHOR: Mischa Thesberg, M.Sc. (McMaster University), B.Sc. (University of Waterloo)

SUPERVISOR: Professor Erik S. Sørensen

NUMBER OF PAGES: ix, 105

Abstract

This thesis, comprising three publications, explores the efficacy of novel generalization of the fidelity susceptibility and their numerical application to the study of frustrated quantum phase transitions in two and one dimensions. Specifically, they will be used in exact diagonalization studies of the various limiting cases of the anisotropic next-nearest neighbour triangular lattice Heisenberg model (ANNTLHM).

These generalized susceptibilities are related to the order parameter susceptibilities and spin stiffness and are believed to exhibit similar behaviour although with greater sensitivity. This makes them ideal for numerical studies on small systems. Additionally, the utility of the excited-state fidelity and twist boundary conditions will be explored. All studies are done through numerical exact diagonalization.

In the limit of interchain couplings going to zero the ANNTLHM reduces to the well studied $J_1 - J_2$ chain with a known, difficult to identify, BKT-type transition. In the first publication of this work the generalized fidelity susceptibilities introduced therein are shown to be able to identify this transition as well as characterize the already understood phases it straddles.

The second publication of this work then seeks to apply these generalized fidelity susceptibilities, as well as the excited-state fidelity, to the study of the general phase diagram of the ANNTLHM. It is shown that the regular and excited-state fidelities are useful quantities for the mapping of novel phase diagrams and that the generalized fidelity susceptibilities can provide valuable information as to the nature of the phases within the mapped phase regions.

The final paper sees the application of twisted boundary conditions to the anisotropic triangular model (next-nearest neighbour interactions are zero). It is demonstrated that these boundary conditions greatly enhance the ability to numerically explore incommensurate physics in small systems.

Acknowledgements

Although there are so many who have contributed to my work and thesis in countless ways I would especially like to thank my supervisor Erik S. Sørensen, my supervisory committee, Catherine Kallin and Sung-Sik Lee, my undergraduate supervisor Michel Gingras, and those wisemen and general sounding boards whom I most frequently pestered (though there were many others) for guidance with physics: Sedigh Ghamari, Andreas Deschner and Ed Taylor.

Contents

List of Figures

List of All Abbreviations and Symbols

QPT – Quantum Phase Transition
ED – Exact Diagonalization
RG – Renormalization Group
DMRG – Density Matrix Renormalization Group
LGW – Landau-Ginzburg-Wilson
VMC – Valence-Bond Monte-Carlo
FS – Fidelity Susceptibility
MG – Majumdar-Ghosh
BKT – Berezinsky-Kosterlitz-Thouless
ATLHM – Anisotropic Triangular Lattice Heisenberg Model
ANNTLHM – Anisotropic Next-Nearest Neighbour Triangular Lattice Heisenberg Model

Declaration of Academic Achievement

First Publication

Mischa Thesberg and Erik S. Sørensen
General Quantum Fidelity Susceptibilities for the $J_1 - J_2$ Chain
Phys. Rev. B 84, 224435 (2011);
DOI: http://dx.doi.org/10.1103/PhysRevB.84.224435

Calculations: All calculations, with the exception of the χ_{AF} data, were performed by the author using a code written entirely by the author. The data within the section related to the antiferromagnetic fidelity susceptibility were performed by Erik S. Sørensen.

Manuscript: The bulk of the text was written by the author with the following exceptions; much of the introductory literature review, the discussion of scaling within the XXZ model and the text related to the antiferromagnetic fidelity susceptibility. The excepted sections were written by Erik S. Sørensen who also provided small miscellaneous corrections and changes throughout.

Second Publication

Mischa Thesberg and Erik S. Sørensen
Excited-State Fidelities and General Quantum Fidelity Susceptibilities for the Next-Nearest-Neighbour Anistropic Triangular Model
Submitted and recommended for publication in Journal of Physics: Condensed Matter (submitted: July 9th, 2014)

Calculations: All calculations were performed by the author using a code written entirely by the author.

Manuscript: The entirety of the text was written by the author excepting miscellaneous edits contributed by Erik S. Sørensen.

Third Publication

Mischa Thesberg and Erik S. Sørensen
An Exact Diagonalization Study of the Anisotropic Triangular Lattice Heisenberg Model Using Twisted Boundary Conditions
arXiv:1406.4083
Submitted and recommended for publication in Physical Review B (submitted: June 19th, 2014)

Calculations: All calculations, with the exception of the expository $J_1 - J_2$ chain calculations, were performed by the author using a code written entirely by the author. The demonstrative data on the $J_1 - J_2$ chain was performed by Erik S. Sørensen.

Manuscript: The bulk of the text was written by the author with the exception of the portion of the introductory text relating to the $J_1 - J_2$ chain. The excepted sections were written by Erik S. Sørensen who also provided small miscellaneous corrections and changes throughout.

1 Introduction

There's an old chestnut in the popular history of physics which boldly asserts that atomic theory traces its origins not with the positing of the Schrödinger equation in 1926, nor the experiments of J. J. Thomson in 1897, nor even in the work of John Dalton in 1800, but rather, millennia earlier, in the fifth century B.C. philosophical musings of Democritus. The evidence for this claim comes from a thought argument which goes approximately as follows:[1]

> If one has a chunk of metal, it has certain properties which tell us it's a metal: it is reflective, it is hard, it can be stretched, etc. If you then take the piece and divide it in two, you will be left with two smaller pieces but both pieces will have the same properties; they'll both be metals. If one then takes one of these smaller chunks and again splits it the result will still be two, smaller, pieces of metal. Democritus then wondered if this subdividing could be done forever, if for any small piece of metal, would splitting it in two always produce two smaller pieces of metal. After thinking about it he decided this probably wasn't true, being a philosopher and not a scientist he didn't have any evidence for this claim, nor did he feel he needed it, but he simply felt that at some point one would have a piece of metal so small that if one split it the two pieces that resulted would stop being metallic. There was a smallest indivisible unit of metal, an atom. Atomic theory was "born".

Aside from the fact that handing credit for atomic theory to a gut feeling of an ancient philosopher is probably doing a great disservice to the many people who actually developed the physics of the atom through experiment and theory, this argument is actually wrong. Democritus and his infinite cutting has not found the atom, he's found, what's called, the *correlation length*.

1.1 More is Different

If one looks at a single atom of copper one would find that, by itself, it's not very coppery. It doesn't reflect the entire visible spectrum (i.e. it isn't shiny), it can't be elongated, it doesn't conduct electricity. This is because these attribute aren't a property of copper atoms but rather a property of *many* copper atoms. When many, many atoms are put together their interactions with one another can cause the *average* behaviour of a large quantity of constituents

[1] This is, of course, a bastardization of the original argument, updated to a modern perspective.

to be completely different than the behaviour of a *single* constituent. This is often called *emergence*, or as Philip Anderson put it: more is different.[1]

The properties we associate with copper are actually properties of the metallic phase, which is the result of many collective actions. First the atoms, through their mutual interactions, find it advantageous energy-wise to form a regular crystal lattice. Additionally, these atoms have electrons in their outermost orbitals, valence electrons. The combination of these two things means that the *bulk* behaviour of this collection of atoms will exhibit an effective property that is completely unlike the behaviour of an individual atoms with its discrete energy levels and orbital fillings; it will have a *band-structure*. If the combination of the geometry of the lattice formed, the available electrons in the valence shell and the strength of the interactions is such that the Fermi level of the material falls *within* a band then the material will be a metal. Crucially, one can then know everything one wants to know about the material's properties (reflectivity, conductivity, etc.) by only knowing the band-structure and knowing nothing about the atomic physics of a copper atom. More is different.

1.2 Spin Systems

In this work we will be entirely focused on the emergent properties of nature, specifically, the various phase that arise when you bring many atoms together. However, we will not focus on all phases of matter, rather we will be interested in those phases whose nature is so different than our every-day experiences; exotic and strange phases driven by the weirdness that occurs at the atomic scale: quantum phases of matter.

Ultimately all phases are due to the quantum mechanical interactions of atoms, so how does it make any sense to talk about "quantum phases"? Are not all phases quantum phases? One of the key aspects of quantum physics, and one of the main sources of wonder it instils, is that a quantum system can exist in a *superposition* of states, its very reality blurred or averaged over a limitless number of possibilities. In many phases, although the ultimate source of their physics is quantum mechanical, this superposed nature is drowned out. The essential phase behaviour is classical. However, in certain systems, in certain phases, this does not happen. In these phases the indeterminacy born from quantum mechanics survives to the macroscopic level. These are quantum phases.

A "go-to" class of systems for observing quantum behaviour are spin systems[2] and they are the subject of study within this work. In a spin system one imagines a crystal lattice with a free electron at each site. Quantum mechanics allows these electrons to tunnel from one atom to the next and in the case we're concerned with, where there is exactly one electron per lattice site or

atom, this hopping allows for each site to have either zero, one, or two. Two is the maximum amount because the Pauli Exclusion Principle forbids two fermions, such as electrons, to every be in the same state. Thus only two can be at the same site, provided they have opposite spins.

A physical system will behave in a manner that minimizes its energy, of which their are two components. The first component of a system's energy is its kinetic energy. A system can lower its energy by *maximizing* the amount of motion and dynamics it contains. The second component is potential energy, due to interactions or an external field. A system can lower its energy by *minimizing* its potential energy. In the situation we consider here, if interactions are strong in the system and the electrons are strongly repulsed by one another, then having two in close proximity (i.e. on the same site) is energetically costly. In such a case the ground-state would involve a single electron on each site with no doubly- or non-occupied sites.

Naively in such a case one might think that dynamics is then entirely frozen out even though the system could lower its energy by allowing for motion. In fact this isn't true, two electrons can *exchange* locations. This is dynamics. However, in order to do this the system must temporarily (i.e. for an infinitesimally short time) be in a doubly-occupied state. The Pauli Exclusion Principle then dictates that this is only possible if the electrons have opposite spins. Thus in order to maximize dynamics by allowing these electron site-swaps or exchanges the system must have opposite aligned spins on neighbouring sites.[2] Thus, strong repulsive interaction and Pauli Exclusion have produced an *effective* interactions which seeks to anti-align neighbouring spins. This is an antiferromagnetic spin system.

The key features of spin systems, of which we will only be concerned with antiferromagnetic ones here, is that the motion of electron charge and lattice dynamics are considered to be entirely frozen out and only this emergent spin interaction remains. Thus the system is greatly simplified from the complete set of physics that would occur in such a lattice. The reason such systems yield such interesting phases is twofold: because spins are inherently quantum mechanical objects and thus their collective behaviour tends to be equally quantum mechanical and because the spins within the system are strongly coupled with one another. Let us now look further into the nature of these quantum phases of matter as well as the way nature transitions between them.

[2]We are of course assuming, for pedagogical simplicity, that it's possible for an electron to have the opposite spin as all its neighbouring sites. This is not always possible.

2 The Quantum Phases of Matter

2.1 Classical Phase Transitions

Before we discuss phases and phase transitions which have very strong quantum character it is worthwhile to discuss and review the theory of phases and phase transitions in general. Of particular importance for this work are *continuous* phase transitions related to broken symmetries. We will briefly explore these concepts now before seeing how quantum phases in particular fit within the general paradigm.

By far the most widely used conceptualization of continuous phase transitions is the Landau-Ginzburg-Wilson (LGW)[3, 4, 5, 6] paradigm. From the perspective of LGW theory a system is viewed as being described by a Hamiltonian consisting of sums of terms which couple degrees of freedom and their associated set of coupling constants which dictate the strengths of these couplings. Examples of such coupling terms may be $\sum_{i,j} S_i S_j$, which couples spin degrees of freedom to spin degrees of freedom, or $\sum_i S_i^z$ which couples spin degrees of freedom and an external magnetic field.[3] The corresponding coupling constants for those couplings would then be J and h respectively. Rather, more correctly, they would be $J' = J/kT$ and $h' = h/kT$ since it is common practice to absorb the temperature dependence of the partition function or action into the Hamiltonian (i.e. $H' = H/kT$). The coupling constants of interest are then a function of both the true coupling constants, arising from interactions and microscopic physics, and the temperature of the system.

In LGW theory one does not simply consider the coupling terms that are *explicitly* present in the system but instead imagines the infinite set of all possible couplings, even if all but a few coupling constants are zero in the system Hamiltonian. The crux of the LGW method then involves investigating what happens to a system Hamiltonian under a change of scale or coarse-graining.[4] Although this change of scale can be accomplished in a number of ways (i.e. block spin renormalization, momentum renormalization, etc.) the net result is that the new scaled Hamiltonian will resemble the original except with coupling constants that have either grown in magnitude, decreased in magnitude or new coupling constants (in the set of all couplings) that have become nonzero. Thus under a change of scale it can be said that some couplings grow increasingly *irrelevant* (i.e. go to zero), others become increasingly *relevant*

[3] In this exposition we conflate, somewhat, a purely Landau approach based on an order parameter potential and the more general theory of Wilsonian renormalization applying to field theories.

[4] The purpose of this exposition is simply to qualitatively review the central concepts of LGW theory in order to motivate future discussions of the failure of the paradigm. For a more comprehensive introduction and exploration of these concepts see the excellent textbook by Nigel Goldenfeld.[7]

(i.e. grow) and new effective couplings, which were not present in the original Hamiltonian, emerge.

As a given Hamiltonian undergoes an infinite progression of scale transformation, or what we simply call *renormalization*, it will eventually reach a point where any additional scale transformation of the scaled Hamiltonian returns the exact same Hamiltonian. In other words, eventually, repeated scale transformation will ultimately produce a Hamiltonian which is *scale invariant*. In the language of field theory we say that the system Hamiltonian flows to a *fixed-point* under renormalization.

Part of the great power of this perspective of phase transitions comes from the realization that a great variety of Hamiltonians, with both different coupling constants and even entirely different couplings, are found to flow to the same fixed-point. Since a fixed-point can be said to describe the long length scale or "zoomed out" behaviour of a Hamiltonian it effectively dictates the macroscopic properties of the system. Thus much of the microscopic details of a system prove to be qualitatively irrelevant in dictating its bulk properties and in reality there are only comparatively few *universal* behaviour "sets" (i.e. phases)[5] that are ever exhibited. Put another way, Landau-Ginzburg-Wilson theory states that for the great variety of microscopic Hamiltonians that can exist, nature only exhibits a much smaller number of universal phases at the macroscopic level. In light of this rather profound (and bold) statement it is worth considering how a fixed-point describes a phase.

The prototypical example of a phase transition is that of the two-dimensional Ising model whose exact solution is known and which was determined by Onsager.[8] Without bogging ourselves down in the details of this solution and in the precise math of the system renormalization,[6] it suffices to say that the two-dimensional Ising model is described by a single coupling ($S_i^z S_j^z$) with a single coupling constant ($J' = J/kT$) and, with varying temperature, transits between a disordered paramagnetic phase at high temperatures where spin-spin correlations decay exponentially to zero, and a ferromagnetic phase at low temperatures where spin-spin correlations decay exponentially to a constant.[9] Under renormalization, first loosely performed by Kadanoff,[10] this system has two stable fixed-points. At the first fixed-point, for $T > T_c$, the coupling constant $J' \to 0$. Thus this "universal phase" behaves as if the spins are completely uncoupled. This is a paramagnetic phase. At the second

[5]Strictly speaking there are a potentially infinite number of Hamiltonians one could construct which are scale invariant, thus there are potentially an infinite number of possible fixed-points. However, for each fixed-point there are an infinite number of Hamiltonians and specific values of coupling constants which renormalize to the same fixed-point. Thus even if there are an infinite number of fixed-points there are still infinitely *fewer* fixed-points than system Hamiltonians. In a way this is analogous to the cardinality of the integers (i.e. fixed-points) versus the real numbers (i.e. possible Hamiltonians).

[6]Again, for such an analysis, see the textbook by Nigel Goldenfeld.[7]

fixed-point, for $T < T_c$, the coupling constant $J' \to \infty$. This system is an infinitely correlated phase. This is a ferromagnetic phase.

A key aspect of LGW theory is the notion of symmetry breaking and ordered and disordered phases. Disordered phases, like the previously discussed high-temperature phase of the two-dimensional Ising model, are typified by having couplings that become irrelevant under renormalization and possessing all the same symmetries of the original Hamiltonian. Ordered phases are the opposite, with coupling which become infinitely strong under renormalization, and are identified with a loss of some symmetry present in the original Hamiltonian. In the case of the two-dimensional Ising model the Hamiltonian acting on a given state will give the same energy as when it acts on a near identical state which has simply had all its spins flipped (i.e. spin inverted). This is a 2-fold symmetry and is thus called a Z_2 symmetry and the Ising Hamiltonian is said to be invariant under Z_2 transformations. However, in the low-temperature, ferromagnetically ordered phase the spins are aligned either all up or all down and the *ground-state* (which is one of the two and not a superposition of the two in the thermodynamic limit) do not have this Z_2 symmetry. This occurance, where the ground-state has less symmetry than the Hamiltonian which produces it, is what is meant by symmetry breaking.

Two states with different symmetries must be orthogonal and thus one cannot "evolve" continuously from one state with a given set of symmetries to another with alternate symmetries through some sort of unitary transformation (like propagation in time). This is actually a crucial point which we will return to later in Sec. 3.1 when discussing quantum fidelities. However, for now it will suffice to realize that this implies that one cannot connect the ground-state of an ordered phase with a disordered phase[7] by changing the temperature. This means that there must be a point of *non-analyticity* separating any two phases. This is, of course, the phase transition point. However, a crucial component of LGW theory is that such a transition point *also* corresponds to a fixed-point. Or rather two phases are divided by a *critical point* and should the system be exactly at this critical point it will flow under renormalization along a "critical line" to a fixed-point. This is indeed the case with the two-dimensional Ising model where in addition to the two stable, $J' \to 0$ and $J' \to \infty$, fixed-points there is a third *unstable* fixed-point that the system will flow to if the system is at the critical point $J' = J'_c$. What is meant by a fixed-point being unstable is that any infinitesimally small change in J' will produce a Hamiltonian which flows *away* from that point under renormalization. In fact, these unstable or *critical* fixed-points end up being one of the most important facets of the LGW theory.[8]

[7] Or ordered phase with another ordered phase with different symmetries.

[8] It is worthwhile to reiterate a subtle distinction here. Two phases will be separated by a *critical point*. In general this critical point lies upon a critical line in the space of all couplings.

Within LGW theory it can be shown that a number of important things happen at a critical (fixed-)point. Specifically, the correlation length (ξ) diverges, the minimum amount of energy required to excite the system (i.e. the excitation or energy gap, ΔE) becomes zero and a parameter called an *order parameter*, Φ, emerges (i.e. becomes non-zero). Let's take a minute to look at what each of these three things imply.

The correlation length effectively tells one the distance over which two degrees of freedom, usually spin, can be said to be correlated with one another or dependent. A divergence in this quantity means that no matter at what scale, at what "level of magnification", you view a critical system the system will look just as correlated. More precisely, when looking at a system at a different scale one is rescaling the basic unit of distance, or in other words $l \to l/b$ where l is any quantity with units of length and b is the amount the system is being scaled. With this in mind, under a change in scales, the correlation length then goes like $\xi \to \xi/b$, but if $\xi = \infty$ then a change in scale does nothing. Thus the statement that the correlation length diverges at a critical point is directly related to the statement that the system is scale invariant or self-similar at a fixed-point. Now what about the disappearance of the energy gap?

There is a very important theorem in field theory called Nambu-Goldstone's theorem[11, 12, 13] which states that whenever a system breaks a continuous symmetry (i.e. it enters an ordered phase) the system then permits excitations, with vanishingly small energy, corresponding to this broken symmetry. A simple example is something like ferromagnetic order in a Heisenberg model. The Heisenberg model Hamiltonian has an $SU(2)$ spin symmetry, i.e. every term S_i can be transformed like $S_i \to S_i e^{-\frac{i}{\hbar}\hat{\mathbf{n}}\cdot\mathbf{S}}$, where $\hat{\mathbf{n}}$ is a unit vector pointing in any direction, and the Hamiltonian will remain unchanged. However, when a Heisenberg system undergoes a phase transition to a ferromagnetic state a specific ordering direction $\hat{\mathbf{n}}_{fm}$ is chosen and the *ground-state* no longer has this symmetry. The continuous symmetry $SU(2)$ has been broken. However, when ferromagnetically ordered the energy cost of globally rotating all spins by the same amount is zero (i.e. it costs nothing to change the direction of $\hat{\mathbf{n}}_{fm}$) and the energy cost of rotating all spins *relative* to each other by an infinitesimal angle $\delta\theta$ is also infinitesimal. Thus these sort of spin distortions or spin waves (which are called *magnons*) are the *Nambu-Goldstone Boson* (i.e. gapless excitation) corresponding to the broken $SU(2)$ symmetry. Phonons similarly are the Nambu-Goldstone boson/excitation associated with breaking continuous translational symmetry by forming a discrete lattice.

If a system should be it exactly at the critical point it will flow under renormalization along this like until it flows to a self-similar fixed-point. If the system is not *exactly* at this critical point the system will flow away from this point and thus in this work we will call these unstable or critical fixed-points.

Within the context of a transition from ordered state to disordered state the disappearance of an energy gap is straightforwardly connected to the emergence of Nambu-Goldstone excitations and symmetry breaking. Later[9] we will discuss different types of transitions, for example between two different ordered states, where this symmetry breaking story is not so clear. Even in such transitions it is found that a system becomes gapless at the critical point, even if both sides of the critical point are in fact gapped. The fact that this is true can be directly motivated from our previous discussion of the self-similarity of a fixed-point. The units of energy ($[M][L]^2/[T]^2$) are obviously dependent on the units of length $[L]$, thus under a change of scales any constants of energy, like say the size of the energy gap, will also be scaled.[10] However, if the system is to look the same at all scales then the system *can't* depend on any energy constants or else the gap would look different at different scales and the system *wouldn't* be self-similar. Therefore the system must always be gapless at a self-similar or fixed-point.[11] It is important to note that the converse statement is not true; just because a system is gapless does *not* imply it is critical or self-similar, we already discussed a counter-example with the ferromagnetic order with its gapless magnons (i.e. the system is gapless but the entire phase is not critical).

The final important artefact of a phase transition point is the emergence of an order parameter. An order parameter is simply defined as some quantity which is zero in a disordered phase and non-zero when in the corresponding ordered phase. For every phase there is an associated order parameter.[12] For ferromagnetic ordering, for example, the associated ordering is the on-site magnetization $\langle S_i^z \rangle$ or average magnetization $\sum_{i=1}^{N} \langle S_i^z \rangle / N$. A diagram of the onset of a non-zero order parameter can be found in Fig. 1.

Taking stock of the three, previously discussed, features of a critical point (diverging ξ, vanishing ΔE and emerging Φ) it is apparent that in the *vicinity* of a critical point we have a theory of small parameters (i.e. ΔE, Φ and $1/\xi$). Specifically, the smallness of the order-parameter Φ in the ordered phase, near the critical point, permits a field theory description in a series expansion about $\Phi = 0$. In fact the power of this field theory description is one of the great

[9] In fact the case of the two-dimensional Ising model discussed previously is such a transition because the symmetry being broken, Z_2, is *not* a continuous symmetry but a discrete one. Such a system does not then have Goldstone modes.

[10] Here we are using the very common convention of $[M]$ being the units of mass, kg in SI, $[L]$ being the units of length and $[T]$ being units of time.

[11] It is important to clarify here that we are not strictly talking about self-similar points at infinity but rather "critical" fixed-points.

[12] This is a true statement. However, it is worth noting that in a certain class of phases, called topological phases, the order parameter is not a *local* quantity, like say the local magnetization, but a non-local or global quantity, like winding number. Strictly speaking topological phases do indeed have order parameters. They're simply non-local.

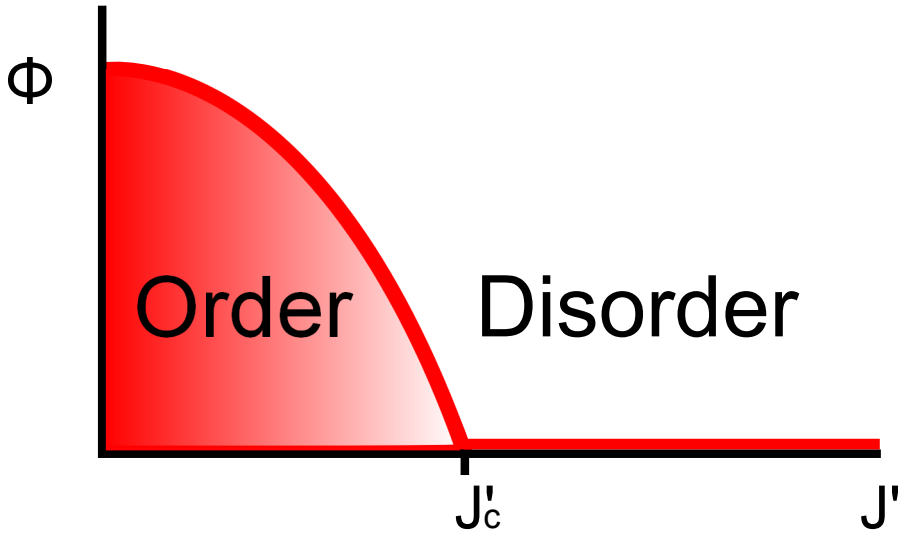

Fig. 1: A diagram of a typical second-order phase transition. At some critical value of J', which is a function of both microscopic system details (i.e. J) and the temperature, an order parameter, such as the average magnetization, abruptly becomes non-zero. The existence of a phase transition is then associated with the broken symmetry captured by the definition of the order parameter.

advantages of LGW theory and it allows for precise calculation of experimental behaviours, such as thermodynamic parameters, in the vicinity of a critical point.[13]

Since all Hamiltonians except the *exact* critical Hamiltonian will flow *away* from a critical fixed-point under renormalization, critical points might seem of little interest since no material will ever be *precisely* critical. However, critical points, and the accompanying *critical* theory constructed in the perturbative vicinity of that point, are a crucial mechanism through which real information about a phase diagram is obtained. The fact that this is true can be seen by considering what a stable fixed-point looks like under renormalization; it looks like a Hamiltonian with either infinite or zero couplings. However, in these limits, far from the vicinity of the critical point, the system can be treated with some combination of mean-field theory or high- and low-temperature ex-

[13]It is worth noting that such treatments are necessarily almost always approximate. A good example is mean-field theory in less than 4 dimensions. Furthermore, as one approaches the critical point the magnitude of fluctuations diverges and the standard Landau based mean-field theory fails. This region must be treated within the Wilsonian renormalization paradigm. However, in this work we take the LGW paradigm to represent a combined formalism including both aspects. Thus LGW describes the complete critical region (assuming, of course, LGW is the correct description of the phase transition).

pansions. Thus the bulk properties of ordered and disordered phases can often be described through these means. These methods fail in the vicinity of a critical point and one then must move to the appropriate critical theory to describe system behaviour. It is then somewhat miraculous that the critical region, through its exhibition of universal behaviour, permits a greatly simplified description with renormalization theory. Furthermore, critical points are a spring-board, of sorts, to the phases they divide and provide a description both of the physics in their vicinity and an additional means of characterizing neighbouring phases through the consideration of renormalization flow. Much then of condensed matter physics revolves around the identification of new critical points and the construction of critical theories around such points to extract information about a phase diagram.

We have now completed our summary of the main concepts of the Landau-Ginzburg-Wilson picture of (continuous)[14] phase phenomena. In summary we found that a phase transition can be understood as follows:

- A microscopic physical system is described by a given Hamiltonian which has some set of couplings and corresponding coupling constants which are dependent both on the microscopic details of the system and the temperature.
- As temperature varies so does the magnitude of the initial value of the coupling constants.
- Depending on the form of the couplings and the values of the coupling constants, repeated scale transformation will cause the Hamiltonian to flow towards one of the following types of fixed points:
  - *Disordered Fixed-Point*: As the system is viewed from longer and longer length scales correlations between degrees of freedom become increasingly *irrelevant* until they are zero. The system is disordered and has no broken symmetries.
  - *Ordered Fixed-Point*: As the system is viewed from longer and longer length scales correlations between degrees of freedom become increasingly *relevant*, growing towards infinity. The system is ordered and has a broken symmetry characterized by the infinite strength couplings at the fixed-point.
  - *Critical Fixed-Point*: As the system is viewed from longer and longer length scales correlations between degrees of freedom remain unchanged and the system is *self-similar*. Under renormalization

[14] As this is not intended to be a textbook on critical phenomena only concepts that will directly inform the ensuing discussion were touched upon. A glaring omission of this treatment is then the behaviour of discontinuous (i.e. first-order) phase transitions.

a system precisely at a critical point will flow along some critical line to a critical fixed-point. Such a fixed-point acts as a cross-over point between two fixed-points and is thus unstable meaning that any perturbation in the initial conditions will cause the system to flow *away* from the critical fixed-point to another ordered or disordered point. One can construct a field-theory description about the vicinity of a fixed point which can yield precise prediction of behaviour of the ordered phase.

- Once the initial Hamiltonian has flowed to a fixed-point it is then scale invariant and this master scale invariant Hamiltonian describes the *universal* behaviour of all initial Hamiltonians that flow to it under renormalization.

It is important to re-emphasize that this rough description of LGW theory glosses over a number of important points, such as: discontinuous phase transitions, marginal couplings, precise renormalization schemes, critical behaviour, scaling laws, critical exponents, and so on. Thus, this discussion is merely intended to prime future discussions about LGW theory and not be an actual introduction to it. For such an introduction see the excellent textbook by Nigel Goldenfeld,[7] as well as the topical reviews by Shankar,[14] Wilson,[6] Fisher[15, 16] and Kogut.[17]

2.2 Quantum Phase Transitions

2.2.1 The Generic Quantum Phase Diagram

In the previous section we discussed the Landau-Ginzburg-Wilson (LGW) within the context of *temperature*, which produced changes in initial coupling constants and was thus the driving force behind changes in phase. However, one could also have varied the system's coupling constants (i.e. h or J) themselves at a constant temperature to produce the same effect. This seems quite sensible for something like a magnetic field, h, which one can vary in a lab but seems strange for something like the exchange constant, J, which ultimately derives from the atomic properties of the material and thus cannot be changed. While this isn't strictly true, for example the exchange constant can be altered slightly through the application of pressure, it is true that when we talk about a model Hamiltonian and mapping its phase diagram in, say, J that no one material will likely be able to exhibit all the phases therein. Instead one often introduces some model Hamiltonian, whose form is often *motivated* by certain real materials, and then explores the phase diagram of the model analytically or numerically. Once potentially interesting phase regions are discovered one then turns around and tries to find a material which is approximately described by the model Hamiltonian and whose coupling constants

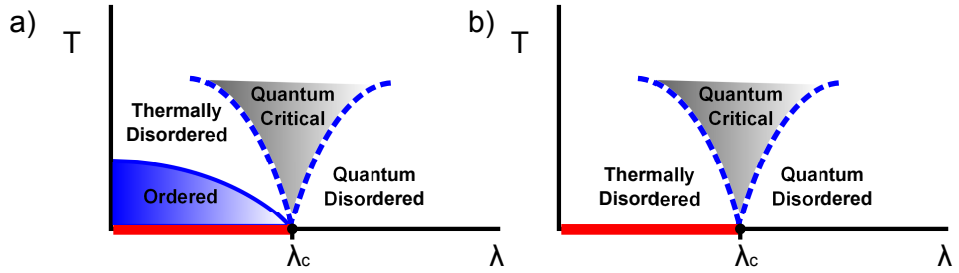

Fig. 2: A schematic of a quantum phase transition. Past some critical value of the driving parameter λ (i.e. λ_c) the system enters a quantum ordered phase provided the temperature is zero. This phase may (a) or may not (b) persist to finite temperatures. Regardless, the critical theory which is often exotic and valid only in the vicinity of the transition point actually caries some of its characters to finite-temperatures. The quantum nature of this critical "fan" diminishes with temperature and eventually quantum fluctuations are entirely drowned out by thermal ones and the system is effectively classical.

have values that would place it within the necessary phase region. This, as one can imagine, is not a trivial undertaking and when exploring the full range of *theoretical* parameters of a given model Hamiltonian, which itself may have somewhat artificial couplings, there is absolutely no guarantee that a material which exhibits those couplings and parameter values actually exists. This is a point we will return to later.

An important class of phase transitions, and the central topic of this thesis, are so called *quantum phase transitions* or QPTs. Such transitions are indeed driven by changes in coupling constants rather than temperature but have the added complication of only occurring at absolute zero (i.e. $T = 0$ K).[18] Clearly such phase transitions are entirely artificial since the third law of thermodynamics, which can be most accurately stated as "specific heat capacity goes to zero as temperature goes to zero", dictates that absolute zero is unattainable. This is, of course, true however the main feature of absolute zero is that all thermal fluctuations cease but still quantum fluctuations remain. We will return to the question of what exactly is meant by thermal and quantum fluctuations, however for now what is important is that at finite, but low, temperatures both these thermal and quantum fluctuations will coexist. However, in this coexistence region quantum fluctuations may still be dominant and thus the physics of the finite temperature system may still contain relics of the exotic $T = 0$ quantum behaviour.

This persistence of such behaviour is perhaps best illustrated by way of an example. A typical quantum phase diagram may consist of a transition

from a disordered phase to an ordered phase as some exchange constant, λ,[15] representing the strength of interactions between spins in the system, is varied with some critical point occurring at $\lambda = \lambda_c$. Another example would be the presence of an external field. With regards to the ordered phase there are two possibilities: the ordered phase persists for $T > 0$ (see Fig. 2a), or it does not (see Fig. 2b). An example of an ordered phase that doesn't persist is that found in the one-dimensional Ising model which exhibits no ordering for $T \neq 0$. Admittedly the physics of such phases are only of academic interest, however, perhaps surprisingly, the fact that the *transition* exists *is* quite important even if the phase itself will never occur. Before we see why this is the case let's first comment on the second case, where the ordered phase exists for $T > 0$.

Should the ordered phase at $T = 0$ persist to non-zero temperatures then in essence the quantum phase transition corresponds to the natural termination point of a continuous phase transition at the zero temperature line. At the higher temperature end of the phase boundary for this ordered phase the transition will be driven by thermal fluctuations (to be discussed shortly) which will produce a critical region of some size. As temperature lowers however this critical region will shrink as thermal fluctuations become unimportant until it eventually becomes a point at the transition's $T = 0$ terminus.

Regardless of the fate of a quantum ordered phase at finite temperatures its mere existence implies a transition or critical point. This point, like its thermal phase transition cousin, exhibits self-similarity and thus gaplessness. In a later section we will discuss in greater detail the exotic behaviours that often emerge at such points but for now we will simply say that such points are characterized by a total *absence* of conventional quasi-particles-like excitations and often have their own, different, novel excitations. Naively though, as one moves away from the quantum critical point, this exotic behaviour is destroyed and one might rightly ask what the point of considering such physics is if it only exists for an infinitely small portion of phase space at, impossible to achieve, absolute zero. The reason is that thermal fluctuations actually act to *enlarge* the region of quantum critical from a point to a finite extent. This is because at the critical point thermal fluctuations are acting on this exotic critical ground-state and if one imagines the energy cost of long-wavelength excitations in the order parameter, $\hbar\omega_c$, the system can *seem* effectively still gapless when $\hbar\omega \ll k_b T$. Thus thermal fluctuations stabilize quantum critical behaviour creating a distinctive *fan* shape (see Fig. 2) in a finite-temperature phase diagram. The critical theories of quantum critical points describe *real*, *finite* phase *regions* at low temperatures.

Obviously this persistence of zero temperature quantum behaviour cannot endure for the entire finite-temperature phase diagram. Typically at a tem-

[15]Here we use λ rather than J to make a connection with later generic descriptions of phase transitions where a notion of λ as a generic driving parameter is introduced.

perature beyond the microscopic energy scales of the system, the exchange constant λ in this case, all quantum nature of the phase region is lost. It is important to understand that this does not actually correspond to a strict transition but rather a gradual loss of "quantumness" with increasing temperature.

2.2.2 What is Meant by Fluctuations?

In the previous section we discussed the competition between thermal and quantum fluctuations. It is therefore worthwhile to discuss what exactly is meant by each term and what exactly is fluctuating. As we examine this question we will work within the formalism of Feynman path integrals and condensed matter and statistical field theory. We will thus assume prior knowledge of these concepts. The uninitiated reader is referred to the textbooks by Altland and Simons,[19] Nagaosa[20] and Negele and Orland.[21]

In statistical mechanics the primary object of interest is the *partition function*. From it all thermodynamic properties of interest can be derived. The partition function can be generically defined within the path integral interpretations as

$$\mathcal{Z}_{th} = \int \mathcal{D}(\overline{\psi}, \psi) e^{-\beta H(\overline{\psi}, \psi)}. \tag{2.1}$$

Conceptually this amounts to a sum over all possible configurations of the variables $(\overline{\psi}, \psi)$ with preferential weighting given to those with *lower* energies and higher energy states being exponentially less important. It then makes sense as a first approximation to only consider the *lowest* energy configuration, the ground-state, and to ignore all higher energy configurations. This is called the saddle point configuration and within this approximation the partition function becomes:

$$\mathcal{Z}_{th} = e^{-\beta H_{\text{sdl.pt.}}} \int \mathcal{D}(\overline{\psi}, \psi) e^{-\beta O(\partial^2 H)} \approx e^{-\beta H_{\text{sdl.pt.}}} \tag{2.2}$$

where $O(\partial^2 H)$ is a catch-all for all higher order terms in a series expansion in paths about $H_{\text{sdl.pt.}}$. What then have we lost in making this approximation? The answer is *thermal fluctuations*, which from this perspective are all the statistical contributions of all other higher energy configurations to the thermodynamic properties of the system. From this perspective we can think of our partition functions as

$$\mathcal{Z}_{th} = e^{-\beta H_{\text{sdl.pt.}}} \int \mathcal{D}(\overline{\psi}, \psi) e^{-\beta(\text{fluctuations})}. \tag{2.3}$$

It is also common, though unfortunately not universal, to call this saddle-point version (without fluctuations) the mean-field theory.[16]

For $T \gg 0$ thermal fluctuations dominate the physics of a given system. At $T = 0$ there are no thermal fluctuations as β goes to infinity and the saddle-point contribution is infinitely greater than all higher energy contributions. However, there are quantum fluctuations. To see what is meant by quantum fluctuations we can again consider the path-integral representation, this time within the confines of quantum field theory. The partition function at $T = 0$ (which is the quantum field theory propagator from the ground-state to the ground-state) is then

$$\mathcal{Z}_{T=0} = \int \mathcal{D}(\overline{\psi}, \psi) e^{-itS(\overline{\psi},\psi)} \tag{2.4}$$

where $S(\overline{\psi}, \psi)$ is the action(in $d+1$ dimensions)

$$S(\overline{\psi}, \psi) = \int\int dt d^d x \mathcal{L}. \tag{2.5}$$

The interpretation of this action follows in a very similar fashion to that of the thermal case, though slightly complicated since now higher energy contributions are not *exponentially* suppressed, since the exponential is now oscillatory, but rather "symmetrically" suppressed. What is meant by this is that paths that deviate greatly from the extremal path (i.e. the saddle-point) will be cancelled by some other similar path of opposite phase. For a more thorough discussion of this, at a very accessible level, the reader is referred to the excellent popular lecture monograph by Richard Feynman: "QED: The Strange Theory of Light and Matter".[22]

In an identical matter to the statistical field theory, the quantum field theory can be written in terms of the path of extremal action (i.e. the classical path) and fluctuations

$$\mathcal{Z}_{T=0} = e^{-itH_{\text{cl.}}} \int \mathcal{D}(\overline{\psi}, \psi) e^{-it(\text{fluctuations})}. \tag{2.6}$$

[16]The term mean-field theory is generally not precisely defined. Sometimes what is meant is the kind of saddle-point approximation discussed here. Other times it refers to the decomposition of an interacting field-theory through a Hubbard-Stratonovich transformation with the resulting decoupling field being the mean-field. Other times still it is the more ad hoc fact of taking couplings between spin operators S_i (i.e. interactions) and converting them by fiat to couplings to an average, mean-field $\langle S_i \rangle$.

From this perspective it is easy to see what quantum fluctuations are; they are the small "fuzziness" about the classical path resulting from nearby (i.e. only perturbatively different) paths that don't completely cancel.[17]

We have now considered the origin of quantum and thermal fluctuations separately. In the distinctive quantum critical "fan" region discussed previously, both types of fluctuations will co-exist simultaneously. One can construct a field theory formalism which accounts for both, the partition function in this combined formalism would have the form

$$\mathcal{Z} = \int \mathcal{D}(\overline{\psi}, \psi) e^{-S(\overline{\psi},\psi)}, \quad S(\overline{\psi}, \psi) = \int_0^\beta d\tau \overline{\psi} \partial_\tau \psi + H(\overline{\psi}, \psi). \tag{2.7}$$

However, no field-theory calculations will be performed in this thesis and therefore a discussion of such a case would be superfluous. The goal of this section is to provide an *intuitive* perspective on the competing nature of thermal and quantum fluctuations within the context of quantum phase transitions. With that accomplished we will now move on to discuss the classification of such transitions.

2.2.3 Classification of Quantum Phase Transitions

When the notion of quantum phase transitions was first introduced it was pointed out that the coupling constants of a Hamiltonian could be varied directly rather than by changing the temperature. However, the astute reader may have noticed that at $T = 0$ a coupling constant of the form $J' = J/kT$ would in fact become infinite. This peculiarity actually has an important consequence which we will now discuss.

When considering thermal phase transition it is necessary that the system become non-analytic at the critical point of a continuous phase transition or else the two phases, whose ground-states must necessarily have different symmetries, cannot be connected. In finite temperature systems the emergence of this non-analyticity is a more subtle point than one might think. The reason is that a non-analyticity can be said to ultimately manifest as a divergence in the partition function (or its derivatives) since it is the generator of all thermodynamic properties. However, the partition function is a sum of the form

$$\mathcal{Z} = \sum_s e^{-\beta H} \tag{2.8}$$

[17] Strictly speaking it is not necessarily correct to say that the paths which have a significant contribution are only those quite close to the classical path. This assume the minimal path essentially lies deep within a "well" or "trench" in phase space. Should the minima not be that "deep" other paths will become more important.

over all possible system configurations (s). For a finite system the number of possible configurations may be extraordinarily large due to the combinatorics involved but it will never be infinite (for discrete variables). How then is it possible for $\mathcal{Z}$ to diverge? The answer is that non-analyticities in finite-temperature systems, and thus phase transitions themselves, can strictly only occur in system of *infinite size*.

It is of course true that though true mathematical phase transitions cannot occur in finite systems, transitions "for all intents and purposes" occur. Without this being true ice and fridge magnets would not exist. It is easiest to see what is meant by "for all intents and purposes" by considering the simple case of the two-dimensional Ising model (on a square lattice). One of the two crucial axioms of statistical mechanics[18] is the notion of *ergodicity*; a system on long enough time scales will "explore" all possible states of identical energy. This means that below the ferromagnetic transition point there are two equal energy ground-states available to the system; a state where all spins are up and a state where all spins are down. Within the ergodic hypothesis the system will, on average, spend equal times in each state and the average magnetization (i.e. 50% of the time all up, 50% of the time all down) is *zero*. Thus there is no phase transition. The reason being is that if the system is not infinite then there is a non-zero probability of the entire system, initially, say, in the down state, of quantum tunnelling to the state with all up spins. As long as this probability is non-zero both states must be averaged. However, if the system *is* infinite then this probability is zero and once it is in one of the two states the system will stay there. We say that *ergodicity has been broken*. This is the only mathematically true way through which phase transitions can occur.

The pragmatic flaw in the above argument is that even though the probability of spontaneous tunnelling between equal energied possible ground-states is not zero for a finite system, if the system is composed of on the order of 10^{24} particles then this probability is outrageously low. So low that one might statistically only expect a sudden en masse tunnelling between ground-states to happen once every several billion lifetimes of the universe. Which is to say, if one wanted to see it happen, one might want to bring a magazine. Thus in real world finite system ergodicity can be broken "for all intents and purposes" and pragmatically phase transitions obviously occur.

In light of this subtle point it is interesting to note that in quantum phase transitions true mathematical phase transitions *can* occur in finite systems. The reason is because the non-analyticity in $\mathcal{Z}$ doesn't need to come from the requirement that there be an infinite number of configurations, and thus an infinite number of terms in the sum, but from the simple fact that $\beta = \infty$. However, this presents another problem. In thermal phase transitions

[18] The other is *detailed balance*.

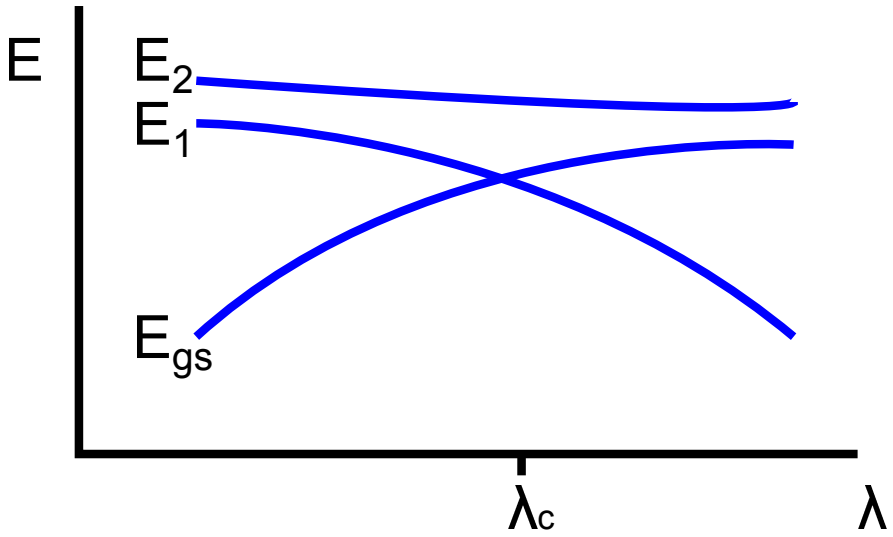

Fig. 3: A pictorial representation of a ground-state level crossing. As λ increases (starting from the left) the ground-state (E_{gs}) and first excited-state (E_1) approach each other in energy until at λ_c they cross and the eigenstate associated with the energy E_1 becomes the new ground-state.

the non-analyticity is defined with respect to some derivative of the partition function, usually with respect to temperature (ie. the specific heat). Indeed the Ehrenfest classification of phase transitions classifies the order of a phase transition as the order of derivative of the free energy (which is directly related to the partition function) with respect to temperature which becomes non-analytic. How then does one go about classifying transitions at $T = 0$ where the derivative with respect to temperature does not exist?

The simple answer to this question is that we define the order of a *quantum* phase transition as the order of the derivative of the *ground-state* with respect to the *driving parameter* λ which becomes non-analytic. It is important to note that the free energy, $F = E - TS$ is simply the energy at $T = 0$ and that no excited states are accessible and thus all physics is controlled by E_{gs}. Thus we say an nth-order QPT has occurred at λ_c if

$$\left.\frac{\partial^n E_{gs}}{\partial \lambda^n}\right|_{\lambda=\lambda_c} \tag{2.9}$$

is non-analytic.

The prototypical example of a first-order QPT is a level crossing in the ground-state as shown in Fig. 3. There is an obvious kink in the ground-state energy at the transition point which will manifest as a discontinuity in

$\partial E_{gs}/\partial\lambda$ at the transition point. It is difficult however, to come up with a prototypical example for higher-order QPTs and indeed, as will be discussed more thoroughly in Sec. 3.1, such continuous transitions are better viewed as a reconstruction of the low lying excited-states of the system, often due to a level crossing in those states.[23] Thus in this work we will use both the nth-order classification system, with the most important being first-order QPTs which are due to ground-state level crossings, and the generic term *continuous* QPTs being a catch-all for all non-first-order transitions.

2.2.4 Critical Theories

An important facet of quantum phase transitions, and indeed one of the primary driving forces of continuing interest, relates to the critical theories themselves that occur at points of transition. Such critical theories will, however, play almost no role in this body of work beyond the simple fact of their existence as quantum disordered phases. However, their central importance in the field begs at least a brief consideration.

As has been discussed, it is a common occurrence in quantum phase transitions to have a transition between two *ordered* phases. It is often the case that each ordered phase can be accurately described by a certain condensed matter field theory. However, one often finds that they cannot be described by the *same* field theory.[19] This cross-over in the field theory description (i.e. having different field theories for different sides of the transition) also lends itself to the *emergence* of a new field theory description at the critical point.

The new field theories that emerge at the critical point are necessarily scale invariant and gapless. Furthermore, they often are most easily described in terms of a new, emergent, effective degree of freedom that was not found in the original field theory descriptions of either phase. This is to say that they tend to be exotic.

A prototype of such, so called, deconfined quantum phase transitions is in the square lattice at the transition from valence bond solid order to antiferromagnetic Néel orderings. It has been shown that the natural critical theory that emerges at the critical point of these phases is that of deconfined spinons with fractional quantum numbers.[24, 25] These new excitations are not an obvious degree of freedom away from the critical point where these spinons are confined (thus the term deconfined phase transition). However, we will not be concerned, in this work, with the exotic field theory descriptions of quantum critical points.

[19] Strictly speaking, this isn't quite true. However, if one truly desires to continuously describe both phases with the same field theory extremely difficult terms in the field theory, such as the Berry phase, which could be safely ignored in one phase, will often become crucial in the other. This often means that one does not know how to *solve* the same field theory on both sides of the transition, even if it is in principle possible.

2.2.5 Failures of Landau-Ginzburg-Wilson Theory

The critical theories discussed in the previous sections are often taken as an example of the failure of the Landau-Ginzburg-Wilson (LGW) theory of phase transitions. Such a deconfined transition occurs in the transitions between two ordered state. However, LGW theory seems to state that a transition between states of different symmetries must be discontinuous or exhibit a region of co-existence, and yet the transition is continuous.

A similar "failure" of LGW theory is the possible existence of a critical *phase*. Such a situation occurs in the $J_1 - J_2$ chain which will be thoroughly introduced later. In a typical LGW scenario a renormalization flow for a given Hamiltonian will flow to a stable fixed point unless it should *exactly* fall on an unstable fixed point. However, in a critical phase there is an entire region of phase space where the system flows *to* a critical or non-trivially self-similar point under renormalization.

Topological phase transitions, though they will not be discussed further here, are another key example of LGW violating phases. In such topological situations the system has degenerate ground-states, all with the same symmetry, however the disparate ground-states are not *accessible* through the local acting dynamical term (i.e. kinetics) within the system Hamiltonian. Thus, the system have no means of dynamically exploring all its degenerate ground-states[20] and a so-called topological phase transition exists between them. In such cases the difference between degenerate ground-states cannot be identified by a local order parameter but instead one must construct a global order parameter to distinguish them.

It is worth making the point as to whether such scenarios are truly a "failure" of LGW theory. For example, LGW theory *does* allow for a transition between two ordered phases to be continuous. In such a situation one simply has a multicritical point (i.e. a point where the transitions point of two different phase transitions, characterized by two different order parameters, fall on the same spot in phase space). Similarly, the existence of an entire critical region (rather than just a point) in one-dimensions, though odd, is still described within the paradigm of renormalization and universality. Ultimately such questions get bogged down in issues of semantics but suffice it to say that the field of quantum phase transitions is fraught with deviations from a naive or "vanilla" conceptualization of LGW theory.

[20] Ground-states which are separated from one another in such a manner are said to be in different topological sectors.

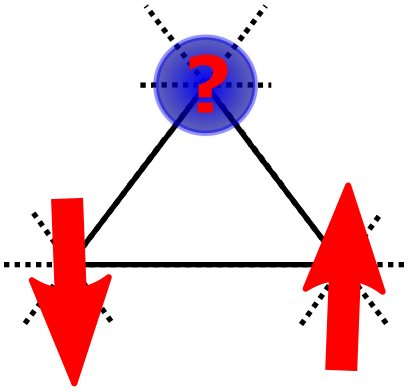

Fig. 4: A typical case of frustation. On a triangular lattice with antiferromagnetic interactions it is impossible to tile the lattice with spins such that all interactions are satisfied. This ambiguity per triangle can potentially lead to a macroscopic number of equally low energy ground-states.

2.3 Frustration

For the last two sections of this chapter we will discuss some of the exotic quantum aspects that will play directly into the systems studied later in this work. Specifically, the entirety of this work focuses on the study of quantum system which are said to be *frustrated*.

At the most general level a system is said to be frustrated if it cannot simultaneously minimize all its interactions. In other words such systems have interactions which actively compete with one another. The most straightforward way in which such a thing can happen is in the case of *geometric* frustration.

Up to this point we have often made reference to the two-dimensional antiferromagnetic Ising model on a square lattice. The ordering in this system is simple with essentially two inter-penetrating sublattices, one with all up spins, the other with all down spins. In other words, the Néel state. However, if we instead consider the same Hamiltonian on a *triangular* lattice things become more complicated.

A diagram of a small portion of a two-dimensional antiferromagnetic Ising model on a triangular lattice can be seen in Fig. 4. In order to minimize the interaction energies of the system all neighbouring Ising spins should be oppositely aligned. This is easily done for two of the three vertices of a given triangle but then the value of the spin on the third vertex is ambiguous. There are two options with equal energy. However, this third vertex is now a corner of an adjacent triangle and its indeterminacy then propagates to an even bigger ambiguity in that one. One could imagine then that the number of

valid ground-states, and thus the ground-state entropy of a triangular system of size N would be on the order of N.. For the antiferromagnetic Ising model on a triangular lattice this turns out not to be the case, as it has been shown that its entropy at absolute zero is finite.[26, 27] However, for many systems this is indeed the case and in the thermodynamic limit there are then an infinite number of ground-states. Another way frustration can happen is through the existence of interactions that directly compete. For example, a chain with both nearest- and next-nearest neighbours antiferromagnetic interactions (i.e. the $J_1 - J_2$ chain which will be discussed later). Such a system seeks to align antiferromagnetically with its nearest-neighbour to satisfy its nearest-neighbour interaction but this consideration is frustrated by the fact that such an orientation would cost energy with respect to its desire to be oriented antiferromagnetically with its *next-nearest* neighbour. Regardless of the ultimate source of frustration it can have a profound effect on a quantum system.

Previously we discussed how quantum fluctuations are the result of an effective "fuzziness" or "blurriness" of a quantum system about its semi-classical, saddle-point solution. What then happens if there are an *infinite number* of classical solutions and each one is easily accessed from another through the allowed dynamics of the system (e.g. only separated by a single spin flip)? The answer is: very interesting things! Such an arrangement leads to a total erosion of classical orderings and the rise of novel quantum orders which are completely dominated by their quantum fluctuations rather than fluctuations playing only a small perturbative role atop classical order. Such a phase is called a spin liquid and we will now look at them in greater detail.

2.4 Spin Liquids

The conventional quantum perspective of materials sees thermal fluctuations as a general disordering force hindering a system's ability to lie in its lowest possible state, its ground-state. Within this perspective, quantum mechanics, with all its caché and bizarreness merely acts to add an inherit coarse-graininess to an otherwise classical ground-state. Thus, Heisenberg's Uncertainty Principle, quantum tunnelling, measurement paradoxes and doomed cats in boxes amount to little more than a minor effect on a classical result.[21]

[21] This statement is in fact quite unfair. Once a system Hamiltonian is described, the effect of quantum mechanics does indeed contribute little to the physical story in most common systems, such as a ferromagnetic. However, quantum mechanics, of course, is contributing far more to the story of a ferromagnet than just fluctuations; it's the entire reason there is a Hamiltonian at all. Quantum mechanics is ultimately the source of: chemical bonding, atomic and electronic spins, spin interactions, etc. So although it is accurate to say that the difference between the terrestrial and low-temperature behaviour of a classical ferromagnetic Heisenberg model is not substantially different than the behaviour of the corresponding

For many systems, like a Heisenberg ferromagnet, this perspective is indeed valid. However, that just means that the small class of systems for which it *isn't* true are that much more exotic. An example of such a system is the spin liquid phase which contradicts almost all conventional intuitions about temperature and ordering.

A spin liquid phase typically arises due to the conditions discussed in the previous section; a frustrated system with a macroscopically degenerate ground-state whose presence erodes any tendency towards classical orderings. Of particular interest in the field of quantum phase transitions is the field theory descriptions of such systems, one of which we briefly discussed as the critical theory between two ordered phases. Such field theories often exhibit exotic excitations, called spinons, which propagate through a lattice like a particle with a spin of 1/2 but *no charge*. This emergence of quasi-particles with spin and charge different than the underlying true particles that make up the system (i.e. atoms and electrons) is called *fractionalization*. Another exotic hallmark of such a phase is the extreme amount of quantum entanglement present in a spin liquid, the interactions are extraordinarily quantum mechanical in nature and defy any classical intuition. This is, of course, only the tip of the iceberg as to the exciting phenomena believed to occur in spin liquid phases.

The field theory description of spin liquids, as well as their intriguing behaviours, are also as complex as they are interesting and they will not play a role in the general narrative of this body of work. Thus, for the purposes of the research contained here-in, spin liquids are merely defined as regions of a quantum phase diagram that have no ordering (i.e. have no order parameter). We will then relegate any considerations of their more exotic characteristics to external references; specifically, the Nature article by Leon Balents[28] and the textbook by X. G. Wen[29] are recommended.

quantum Heisenberg model, none of the actual *terms* in a classical Heisenberg model have a basis in classical physics; even if operators are not used it is a *quantum* theory.

3 The Quantum Fidelity and Fidelity Susceptibility

In the previous chapter we explored the enormous interest in quantum phase transitions; both as new launching points for perturbative theoretical approaches and as a source of interesting physics themselves. In this next chapter we will focus on the latter of these motivations and an emerging new perspective and tool for the identification and characterization of QPTs. However, before we proceed it is fruitful to first discuss a quantity known as the *Loschmidt Echo*.

The Loschmidt Echo,[30] like the fidelity we will discuss shortly, is a quantity originally developed within the field of quantum information.[31, 32, 33, 34] It is defined as the (squared) inner product of two vectors: $|\psi(t_f)\rangle$ and $|\psi'(t_f)\rangle$ where $\langle\psi(t_f)| = \langle\psi_i(t_i)|\, U(t_f - t_i)$ and $|\psi'(t_f)\rangle = U'(t_f - t_i)\,|\psi_i(t_i)\rangle$. The unitary matrices $U(t_2 - t_1)$ and $U'(t_2 - t_1)$ correspond to the time evolution operators, $\exp(-iH(\lambda)(t_2-t_1))$ and $\exp(-iH(\lambda+\delta\lambda)(t_2-t_1))$ respectively. In other words, one starts from some initial state, ψ_i, and time evolves it with two different time evolution operators, one evolved under the Hamiltonian $H(\lambda)$ and another evolved under a Hamiltonian slightly perturbed from the other, $H(\lambda + \delta\lambda)$, and then takes the inner product of the two states.

The Loschmidt Echo[22] was constructed to be a measure of the detrimental effect felt by a highly entangled quantum state in the face of an unintentional errant interaction or perturbation. In other words it is meant to be a measure of the stability of the quantum coherent behaviour of something like a qubit against undesirable contamination from the environment. From this perspective such a quantity has an obvious place in the study of quantum entanglement and quantum information.

From a different perspective, the Loschmidt Echo has a passing resemblance to a propagator or transition amplitude between states tied to the two different Hamiltonians. We can decompose the Echo as

$$L = |\langle\psi(t_f)|\,\psi'(t_f)\rangle|^2 = \left|\langle\psi_i(t_i)|\, e^{it_f H(\lambda)} e^{-it_i H(\lambda+\delta\lambda)}\,\psi_i(t_i)\rangle\right|^2 \tag{3.1}$$

$$= \left|\sum_{n_\lambda}\sum_{n_{\delta\lambda}} e^{i(t_f-t_i)(E_{n_\lambda}-E_{n_{\delta\lambda}})}\,\langle\psi_i(t_i)|\,n_\lambda\rangle\,\langle n_\lambda|\,n_{\delta\lambda}\rangle\,\langle n_{\delta\lambda}|\,\psi_i(t_i)\rangle\right|^2 . \tag{3.2}$$

For a randomly chosen ψ_i in an infinite system the probability of picking a vector that has *no* overlap with a given $|n_\lambda\rangle$ or $|n_{\delta\lambda}\rangle$ is mathematically zero

[22] The term "echo" relates to the fact that it probes the kind of response, or echo of the system to a detrimental perturbation.

and therefore we do not expect $\langle n_\lambda |\, \psi_i(t_i)\rangle$ or $\langle n_{\delta\lambda} |\, \psi_i(t_i)\rangle$ to be zero. Thus, if we ignore the phase term, the most important terms are then

$$\langle n_\lambda |\, n_{\delta\lambda}\rangle\,. \tag{3.3}$$

Imagine a case where the two eigenspaces $\{|n_\lambda\rangle\}$ and $\{|n_{\delta\lambda}\rangle\}$ correspond to spaces in *different phases*. In other words, imagine λ and $\lambda + \delta\lambda$ straddle some λ_c. We then expect, at the very least, that the ground-state and low lying excited-states to undergo substantial qualitative changes resulting from a change in symmetry. In such a case we would expect a sharp drop in the magnitude of Eq. 3.3 and thus a distinctive dip in the Loschmidt Echo if $H(\lambda)$ and $H(\lambda+\delta\lambda)$ should straddle a phase transition. In light of this it is then not surprising that the Loschmidt Echo has found application outside of the field of quantum information; in the field of quantum phase transitions.[35, 36, 37, 38, 39, 40]

3.1 The Quantum Fidelity

In this work we will not actually be concerned with the Loschmidt Echo but in a very related quantity that derives from it: the quantum fidelity.[41] Similar to the Loschmidt Echo, the quantum fidelity is defined as the overlap in the *ground-state* of two distinct Hamiltonians differing only in a small pertubation. Specifically, the standard quantum fidelity assumes a Hamiltonian of the form

$$H = H_0 + \lambda H_\lambda. \tag{3.4}$$

This Hamiltonian, of a quantum system at absolute zero, exhibits a quantum phase transition at some λ_c. Thus we call H_λ the *driving term* of the Hamiltonian and λ the *driving parameter*. Presented this way the fidelity is then[23]

$$F^2 = |\langle \psi_{gs}(\lambda)\; |\psi_{gs}(\lambda + \delta\lambda)\rangle|^2\,. \tag{3.5}$$

In light of our previous discussion of the substantial restructuring of the ground-state (and low lying excited-states) about a phase transition, it is fairly obvious that such a quantity would provide a signature of a quantum phase transition. Should λ and $\lambda+\delta\lambda$ both lie within the same phase we might expect

[23]It is prudent to note that in some works the fidelity is defined as the square of the overlap rather than just the overlap. However, this distinction is just a matter of convention and plays no significant role in the relevant physics.

the fidelity to be near 1, owing to the qualitative similarity of the physics and thus ground-state in that regime. Should the fidelity instead straddle a transition we would expect a sudden drop to zero, for an infinite sized system, owing to the fact that different phases have different symmetries and thus their ground-states must be orthogonal.

The fidelity would also have the added benefit of requiring no *a priori* knowledge of the phase diagrams. One would not need to know anything about the phases that occur or their order parameters and would, in principle, treat more subtle phase transitions, like those topological in nature, on equal footing. Though it is worth noting that this also implies that, as is, the fidelity cannot provide any information about what *phases* exist in a phase diagram, but merely where transitions between these phases lie. It will be a central topic of this work to try and improve upon this shortcoming.

The situation, however, is a little more subtle than the above discussions suggests. In the thermodynamic limit the fidelity should actually be zero regardless of whether it straddles a phase transition or not. This relates to the issue of *distinguishibility*[42] which states that states corresponding to different quantum observables must be orthogonal. Should the fidelity straddle a phase transition then either that phase transition is continuous and thus each phase is distinguishable by a different set of symmetries and the fidelity is zero, or the transition is a result of a level-crossing of the ground-state in which case it is trivially true that the fidelity should be zero.[43] The distinguishing feature is then the non-zeroness or zeroness of the order parameter. However, two states within the same phase will have different *values* of the order parameter and are thus distinguishable. Thus, in the thermodynamic limit, the fidelity should be zero even within a given phase.[24]

In an important paper by Zanardi *et al.*,[41] the case was made that the distinguishibility of states *within* the same phase are solely the result of short-distance details of the physics since both states, under renormalization, flow to the same point. Thus their long-range physics is identical. Conversely, two states in different phases are distinguishable by their *long-distance detail* physics and thus are "more" distinguishable.[25] Thus in *finite* systems we expect the fidelity to take a much lower value in the event it should straddle a phase transition.

The reader may be a little unsettled by the qualitativeness of the discussion of the fidelity so far and the inability to precisely state which types of quantum transitions it can or cannot detect. This point will be detailed a bit further in the following sections, however, to date there does not exist any

[24] The point discussed here is quite subtle and for the curious reader it is strongly suggested that the original paper by Zhou be read.

[25] Obviously this point is more subtle than as is being presented here. For a more complete treatment see the original paper.[41]

exact theoretical derivation of the precise range of applicability of an approach based purely on the fidelity.[44] With that being said the standard fidelity discussed here has seen enormous success in exploring a wide range of quantum systems including: the XXZ chain,[45] the XXZ chain with Dzyaloshinskii-Moriya interactions,[46] the three-site interacting XX chain,[47] the XX chain in an external field,[48] the XY model,[49] topological models (i.e. mosaic, Kitaev's honeycomb),[50] spin ladders,[51, 52] its representation via matrix product states,[53] the quantum q-state Potts model,[54] the Hubbard model,[55] the two-dimensional Heisenberg model on a square lattice,[56] and the two-dimensional anisotropic XYX model.[57] It is also worth noting that although the typical fidelity approach requires the ground-state of the system being studied to be unique, there has also been work[54] related to the use of the fidelity as a measure of the number of degenerate ground-states.

3.2 The Quantum Fidelity Susceptibility

The ability of the quantum fidelity to identify a first-order transition (i.e. one due to a ground-state level-crossing) is straightforward. However, higher-order quantum transitions are identified by non-analyticities in the derivatives of the ground-state energy with respect to the driving parameter, λ. It is then natural to consider the higher-order derivatives of the *fidelity* with respect to the driving parameter as an object of interest. Such quantities can be identified through the Taylor expansion of the fidelity in $\delta\lambda$. The linear term in such an expansion must be zero otherwise one would arrive at values of the fidelity greater than one. Thus, the first surviving term in such an expansion is

$$F = 1 - \frac{\delta\lambda^2}{2}\frac{\partial^2 F}{\partial\lambda^2} + \frac{\delta\lambda^3}{6}\frac{\partial^2 F}{\partial\lambda^3} + \dots \tag{3.6}$$

Neglecting higher-order terms we arrive at the quantity

$$\chi_F = \frac{\partial^2 F}{\partial\lambda^2} = \lim_{\delta\lambda\to 0}\frac{2(1-F)}{\delta\lambda^2}, \tag{3.7}$$

which is called the *fidelity susceptibility*. It can be shown[58] that this quantity is directly connected to the second-derivative of the ground-state:

$$\begin{aligned}\frac{\partial^2 E_{gs}(\lambda)}{\partial\lambda^2} &= \sum_{n\neq 0}\frac{2\left|\langle\Psi_n(\lambda)\right| H_\lambda \left|\Psi_{gs}(\lambda)\rangle\right|^2}{E_n(\lambda) - E_{gs}(\lambda)} \\ \chi_F &= \sum_{n\neq 0}\frac{\left|\langle\Psi_n(\lambda)\right| H_\lambda \left|\Psi_{gs}(\lambda)\rangle\right|^2}{(E_n(\lambda) - E_{gs}(\lambda))^2}\end{aligned} \tag{3.8}$$

Of particular importance in the above relation is the square of the denominator in the case of the fidelity susceptibility. This square implies that for an equivalent finite-sized system, where the second-derivative of the ground-state energy would diverge, that the fidelity susceptibility would diverge more abruptly. In other words, the fidelity susceptibility would have related behaviour but with greatly increased sensitivity. This can be a great boon for numerical studies where system sizes are necessarily small.

In fact the previous statement of "increased sensitivity" can be made more concrete, as the scaling behaviour of the fidelity susceptibility in the vicinity of a phase transition is known. However, the derivation of this scaling relation is contingent on a connection the fidelity susceptibility has with another important quantity: the dynamic structure factor.

In a paper by Gu *et al.*[59] a generalization of the fidelity susceptibility, the *dynamic fidelity susceptibility* was constructed as such:

$$\chi_{Dy}(\omega) = \sum_{n\neq 0} \frac{\left|\langle\Psi_n(\lambda)\right| H_\lambda \left|\Psi_{gs}(\lambda)\rangle\right|^2}{(E_n(\lambda) - E_{gs}(\lambda))^2 + \omega^2}. \tag{3.9}$$

In the limit $\omega \to 0$ it clear that this object then reduces to the regular fidelity susceptibility. Under a Fourier transform this object becomes

$$\chi_{Dy}(\tau) = \sum_{n\neq 0} \frac{\pi \left|\langle\Psi_n(\lambda)\right| H_\lambda \left|\Psi_{gs}(\lambda)\rangle\right|^2}{(E_n(\lambda) - E_{gs}(\lambda))^2} e^{-(E_n(\lambda)-E_{gs}(\lambda))|\tau|}. \tag{3.10}$$

A derivative of this quantity with respect to τ produces the rather interesting result

$$\frac{\partial\chi_{Dy}(\tau)}{\partial\tau} = -\pi G_\lambda(\tau)\theta(\tau) + \pi G_\lambda(-\tau)\theta(-\tau) \tag{3.11}$$

where $\theta(\tau)$ is the Heaviside function and G_λ is a dynamic correlation function of the driving Hamiltonian:

$$\begin{aligned} G_\lambda(\tau) &= \langle\Psi_0(\lambda)\right| H_\lambda(\tau)H_\lambda(0)\left|\Psi_0(\lambda)\rangle - \langle\Psi_0(\lambda)\right| H_\lambda \left|\Psi_0(\lambda)\rangle^2 & (3.12)\\ H_\lambda(\tau) &= e^{H(\lambda)\tau} H_\lambda e^{-H(\lambda)\tau}. & (3.13)\end{aligned}$$

This relation can be further manipulated (see [60]) in order to best take the limit $\omega \to 0$ in a convergent way to produce the final result for the regular fidelity susceptibility

$$\chi_F = \int_0^\infty \tau G_\lambda(\tau) d\tau. \tag{3.14}$$

This expression is extremely illuminating in its own right for it identifies the fidelity susceptibility as a sort of *dynamic structure factor* of the driving

Hamiltonian. Thus, it makes a connection between a quantity which originates in quantum information theory and casts it as a measure of quantum fluctuation within linear response theory. However, this result is also important because it allows for an examination of the scaling behaviour of the fidelity susceptibility through its relation to the scaling of correlation functions.

The original scaling theory for the fidelity susceptibility was derived by Zanardi *et al.*[45] and considered the behaviour of the susceptibility with respect to the scaling transformation

$$r' = sr, \quad \tau' = s^z \tau, \quad H'_\lambda = s^{-\Delta_{H_\lambda}} H_\lambda \tag{3.15}$$

where z is the dynamical exponent and Δ_{H_λ} is the scaling dimension of the H_λ operator. Using this transformation and Eq. 3.14 it was shown that the ultimate finite-size scaling behaviour was

$$\frac{\chi_F}{N} \sim L^{d+2z-2\Delta_{H_\lambda}}. \tag{3.16}$$

and thus the conditions for a divergence of the fidelity susceptibility at a phase transition, and thus its range of application as a signal of a transition, is that[26]

$$2(d + z - \Delta_{H_\lambda}) > 1$$

In principle this relation is sufficient to identify the order of transitions that the fidelity susceptibility can detect through divergence. Indeed, it was this form of the scaling function which was used in Paper #1. However, the H_λ scaling dimension, Δ_{H_λ}, is often not known and even when it is it is not a commonly considered "critical exponent". It is difficult then, in this form, to make any sweeping conclusions about the realm of applicability of the fidelity susceptibility. Thankfully, there is another scaling relation which makes a more direct connection to more typical critical exponents.

In two papers by Capponi *et al.*[44, 56] it was argued (see the papers for a more thorough discussion of the arguments) that the scaling dimension could be represented as

$$\Delta_{H_\lambda} = d + z - \frac{1}{\nu} \tag{3.17}$$

where $1/\nu$ is the critical exponent of the divergence of the correlation length, due to the connection to the dynamic structure factor mentioned earlier. Thus, the fidelity susceptibility scales as

[26] N is the number of sites. We are assuming here that $N = L^d$, which would be the case for a cubic system. For other types of lattices this might not be true. If this is the case a slight modification of the equation is necessary.

$$\frac{\chi_F}{N} \sim L^{2/\nu - d}. \tag{3.18}$$

With this expression it is then possible to identify whether the fidelity susceptibility will diverge provided one has prior knowledge of ν. Perhaps the most poignant demonstration of this divergence dependence is from a paper by Tzeng *et al.* where it was shown that in the spin-one XXZ chain, which exhibits a second-, third- and fifth-order QPT, that the fidelity susceptibility could detect the second- *and* third-order but it could *not* detect the fifth-order.[61]

In addition to the studies detailed above the fidelity susceptibility has also been applied in the following systems and situations: XXZ chain with Dzyaloshinskii-Moriya interactions[46, 62, 63] and without,[64] the one-dimensional transverse-field Ising model (1D-TFIM),[65] the two-dimensional transverse-field Ising model (2D-TFIM),[66, 67] the two-dimensional XXZ model,[68] the non-disordered XY spin chain with Dzyaloshinski-Moriya interactions,[69] the disordered XY spin chain with Dzyaloshinski-Moriya interactions,[70] the one-dimensional transverse-field compass model,[71] spin ladders,[51] the asymmetric Hubbard model chain,[72] its extrapolation to study thermal phase transitions,[73] and an array of two-dimensional spin-orbit models[74]

3.3 Generalized Fidelities and Fidelity Susceptibilities

Since the introduction of the fidelity susceptibility it has been generalized in a number of ways, specifically, the operator fidelity susceptibility[75, 76] and the reduced fidelity susceptibility.[77, 78, 79] However, in this work we will be considering generalizations of the fidelity susceptibility designed to identify *which* phase the system is in, rather than just where the transition exists, and to identify some of the more difficult to identify transitions.

So far we have always considered the fidelity as an object defined relative to a perturbation in the driving parameter, λ, which drives the system across a phase transition. However, almost all of the aspects of the fidelity (i.e. its scaling, the definition of its susceptibility, etc.) are general even if a different perturbation is used. In deference to this we consider an alternate perturbation scheme, one based around the *conjugate field* of an ordered phase.

A conjugate field is a "field" which explicitly breaks the symmetry broken during a phase transition. For a ferromagnetic phase the conjugate field is simply an infinitesimal field in a given direction which is applied to every site (i.e. of the form $\delta\lambda \sum_i S_i^z$); for antiferromagnetic phase that field is then staggered (i.e. of the form $\delta\lambda \sum_i (-1)^i S_i^z$); for a dimer phase it is an infinitesimal staggered change in the exchange coupling (i.e. of the form $\sum_{ij}(J+(-1)^i\delta\lambda)S_iS_j$). The susceptibility associated with the conjugate field is the order parameter susceptibility, which is a quantity which, in the thermodynamic limit, is infinite

for a system in its corresponding phase. However, as with anything, the divergence of the order parameter susceptibility can be more difficult to interpret in finite-size systems where it can frequently be non-zero and non-infinite for the entire phase diagram. In such a case, if numerical issues prevent the consideration of many large systems, a thermodynamic limit extrapolation may be extremely tenuous and the usefulness of the order parameter susceptibility is substantially diminished.

In this work we mainly consider a fidelity, which we will simply call a *generalized fidelity susceptibility*, which is defined by a change, $\delta\lambda$, not in the driving parameter but in the addition of a conjugate field. We thus expect this susceptibility to have a similar relation to the order parameter susceptibility that the regular fidelity susceptibility has with the second-derivative of the ground-state energy; a heightened sensitivity, in small finite systems, to divergence. In two of the papers presented later such susceptibilities will be, successfully, used to explore both well known and novel phase diagrams.

In addition to these conjugate field derived susceptibilities, a similar fidelity susceptibility will also be constructed and studied; one related to the spin stiffness susceptibility. Like an order parameter susceptibility, the spin stiffness susceptibility, which is defined relative to a perturbation representing the insertion of an infinitesimal boundary twist, is a parameter whose divergence holds valuable information about a system's phase. However, unlike the order parameter susceptibility, the spin stiffness susceptibility will diverge for any system which exhibits any spin-ordering; whether ferromagnetic, antiferromagnetic or spiral. In an intuitive way the spin stiffness susceptibility establishes whether the energy of a system is raised when one tries to bend or twist a chain of spins; if the system is not spin ordered then its spins are not correlated and such a twist costs no energy and the spin stiffness susceptibility is zero. If it *is* spin ordered, the spin stiffness susceptibility will be non-zero. Similar to the case of the conjugate field based fidelity susceptibilities, we expect these new quantities to have increased sensitivity in finite systems.

This spin stiffness susceptibility actually deserves a little more thorough discussion as its exact nature has been expanded upon since the publication of Paper #1. Strictly speaking, the spin stiffness susceptibility, which we dub χ_ρ, does not fall within the general fidelity form related to a Hamiltonian of the type

$$H = H_0 + \lambda H_\lambda.$$

This is because the perturbation, an infinitesimal twist, is not *added* to the unperturbed Hamiltonian but rather implemented through the change of variable

$$S_i^+ S_j^- \rightarrow S_i^+ S_j^- e^{i\delta\lambda} \quad S_i^- S_j^+ \rightarrow S_i^- S_j^+ e^{-i\delta\lambda}$$

where our $\delta\lambda$ is taking the form of an infinitesimal twist. However, it can be put in a similar form through a Taylor expansion in $\delta\lambda$:

$$H = H_0 + (\delta\lambda)\mathcal{J} - \frac{(\delta\lambda)^2}{2}\mathcal{T} + \dots \tag{3.19}$$

where

$$\mathcal{J} = \frac{i}{2}\left(S_i^+ S_j^- - S_i^- S_j^+\right) \tag{3.20}$$

$$\mathcal{T} = \frac{1}{2}\left(S_i^+ S_j^- + S_i^- S_j^+\right). \tag{3.21}$$

We have given the first- and second-order terms the names $\mathcal{J}$ and $\mathcal{T}$ respectively because they each have a specific physical interpretation. The first-order term $\mathcal{J}$ essentially amounts, for a spin$-1/2$ system, to the number of left-moving up-spins minus the number of right-moving up-spins. It thus represents the net motion of up-spins, and is thus a *spin-current* operator. The second-order term is essentially a repeat of the regular *spin kinetic term* found in the original Hamiltonian, albeit weighted by the small factor $(\delta\lambda)^2$.

In the work discussed later (Paper #1) it was found that there was little numerical difference between a χ_ρ implemented with the true exponential or one implemented keeping only the first-order spin-current term ($\mathcal{J}$) in its Taylor expansion. Thus the definition of the spin stiffness susceptibility can be brought into the regular form as a fidelity of the Hamiltonian

$$H \approx H_0 + \lambda\mathcal{J}.$$

This redefinition turns out to provide crucial insight. In a paper by Greschner *et al.*[63] building off the results of Paper #1 in this thesis, a spin-current fidelity, $\chi_\mathcal{J}$, was considered. This fidelity susceptibility was defined relative to the H_λ of

$$H_\lambda = (S_i \times S_j)^z = S_i^x S_j^y - S_i^y S_j^x.$$

If one substitutes in the spin ladder operators (i.e. $S_i^x = (S_i^+ + S_i^-)/2$, $S_i^y = (S_i^+ - S_i^-)/2i$) and expands this takes the form

$$\begin{aligned} H_\lambda &= \frac{1}{4i}\left(\cancel{S_i^+ S_j^+} - S_i^+ S_j^- + S_i^- S_j^+ - \cancel{S_i^- S_j^-} - \cancel{S_i^+ S_j^+} - S_i^+ S_j^- + S_i^- S_j^+ + \cancel{S_i^- S_j^-}\right) \\ &= \frac{i}{2}\left(S_i^+ S_j^- - S_i^- S_j^+\right) = \mathcal{J}. \end{aligned} \tag{3.22}$$

Which is to say it is identical to the first-order definition of χ_ρ.

In that paper an important connection was made between, what they call the spin-current fidelity susceptibility,

$$\chi_{\mathcal{J}} = \sum_{n\neq 0} \frac{|\langle\Psi_n(\lambda)|\,\mathcal{J}\,|\Psi_{gs}(\lambda)\rangle|^2}{(E_n(\lambda)-E_{gs}(\lambda))^2}, \tag{3.23}$$

and the positive real part of the spin conductivity

$$\begin{aligned}\sigma_1(\omega) &= \text{Re }\sigma(\omega)|_{\omega>0} &(3.24)\\ &= \frac{\pi}{L\omega}\sum_{n\neq 0}|\,\langle\Psi_0(\lambda)|\,\mathcal{J}\,|\Psi_n(\lambda)\rangle\,|^2\delta(\omega-(E_n(\lambda)-E_{gs}(\lambda))). &(3.25)\end{aligned}$$

Looking at these two expressions it's clear that

$$\chi_{\mathcal{J}} = \frac{L}{\pi}\int_0^\infty \frac{\sigma_1(\omega)}{\omega}d\omega. \tag{3.26}$$

Thus the spin-current fidelity susceptibility, which is found to be numerically identical to the spin stiffness susceptibility, is directly related to an integral over the real part of the spin-current. It is worth noting that the general spin-current is composed to two terms, a regular part $\sigma_{reg}(\omega)$, and a singular Drude peak at $\omega = 0$. However, since $E_n(\lambda) - E_{gs}(\lambda)$ is always greater than 0 for a finite system, $\omega = 0$ is not a part of Eq. 3.24 and thus not included.[27]

A final quantity which will become important in the following work is the excited-state fidelity. In a previous paper on the $J_1 - J_2$ chain, a system to be discussed in the next chapter, it was shown that a specific phase transition, which is not due to a ground-state level crossing, could in fact be identified by a level crossing in the first excited-state.[80] This claim is bolstered by a paper by H. Q. Lin *et al.*[23] which proved that the quantum phase transition in a fairly general class of one-dimensional systems was associated with a level-crossing in the low-lying excited-states. Furthermore, this idea is quite consistent with our earlier discussion of quantum phase transitions being associated with radical re-organization of the low-lying excitations of the system. Thus, with this in mind we will also consider a fidelity defined not as an inner-product of ground-states which are perturbed and unperturbed relative to the driving parameter but rather an inner-product of *first excited-states*. We will find that such a quantity indeed yields valuable information about quantum phase transition points.

[27] This is actually only true for systems with periodic boundary conditions. For a more detailed consideration see [63].

4 The Anisotropic Next-Nearest Neighbour Triangular Lattice Heisenberg Model (ANNTLHM)

This thesis comprises three papers which all study slightly different Heisenberg systems. However, all of these systems exist as special limiting cases within one overarching model: the anisotropic next-nearest neighbour triangular lattice Heisenberg model (the ANNTLHM).

The ANNTLHM model, picture in Fig. 5, consists of a triangular lattice with Heisenberg spins where exchange interactions in the horizontal direction have strength J and in the diagonal directions have strength J'. We will exclusively be concerned with the $J' < J$ region, especially where $J' \ll J$. In this region the system can be viewed as a system of weakly coupled chains with strong *intrachain* interactions, J, and weaker *interchain* interactions, J. Additionally, there are also second-nearest or next-nearest neighbour interactions in the intrachain direction with strength J_2. Although this system has rarely been studied,[81, 82] it is an ideal proving ground for new numerical techniques as it permits two limits; one whose physics is well known and another whose physics are still largely not understood.

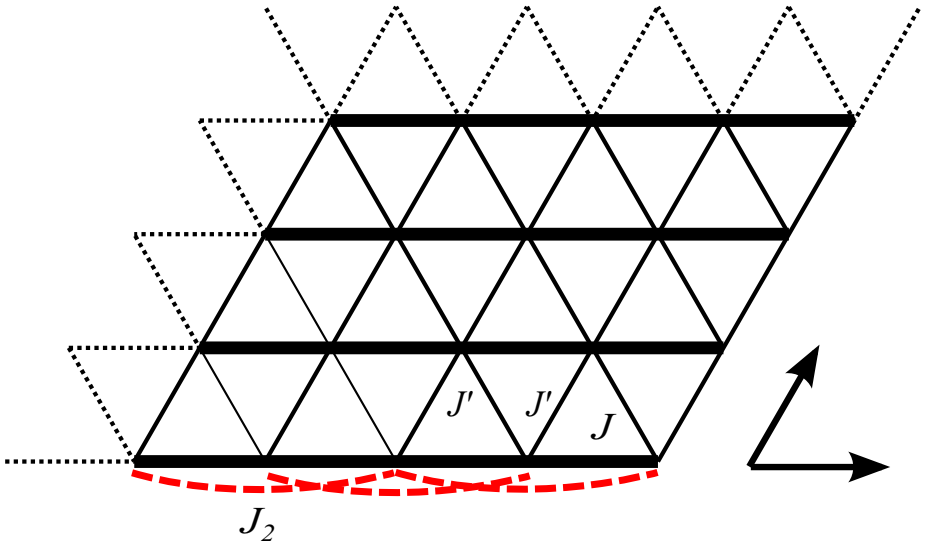

Fig. 5: The anisotropic triangular lattice with next-nearest neighbour interactions. In this work J' and J_2 are taken to be the ratios of J (i.e. $J = 1$). In the limit $J' << 1$ the lattice reduces to one of weakly coupled chains. In such a limit it makes sense to say that the nearest neighbour interaction J and next-nearest neighbour interaction J_2 act in the intrachain direction while the diagonal interaction J' acts in the interchain direction.

4.1 The $J_1 - J_2$ Chain: The $J' \to 0$ Limiting Case

The first of these limit is the limit $J' \to 0$ where the system reduces to what is called the $J_1 - J_2$ chain.[28] Although there are materials whose physics can be partially described by such a system, see for example reference [83], interest in this model really began when a series of paper by Majumdar and Ghosh[84, 85, 86] showed that for the specific case, where $J_2 = J/2$, (for periodic boundary conditions) that the exact ground-state can be solve for analytically. The ground-state, at this so called "Majumdar-Ghosh" (MG) point, consists of an equal weighted superposition of the two possible dimer coverings[29] of a chain. This was a very important discovery since exact solutions are rare and valuable in the field of strongly-correlated systems and thus these paper spurred a great interest in the system.

In this work we will solely be concerned with the $1 > J_2/J > 0$ regime of this model. The physics of this range is divided into three distinct regions. The first two of these regions were recognized by Haldane[87] who originally showed that for $J_2/J \gtrsim 1/6 = J_2^c$ that the system spontaneously dimerized. This field theory estimated value of $J_2^c \approx 0.1\bar{6}$ would later be more accurately determined through a number of numerical studies,[88, 89] including Paper #1 herein, to be ~ 0.24. It is believed that the most accurate estimate of its value is due to Eggert[90] and is $J_2^c \approx 0.241167(5)$ which was found by detecting the point where a marginal operator in the system becomes zero.

At the critical point J_2^c it was found[88, 91] that a gap opened and grew exponentially with J_2/J. However, the MG point actually divides this $J_2/J > J_2^c$ region and the correlation length has a minima at this point.[92] For $J_2^{MG} > J_2/J > J_2^c$ the system is gapped and is dimerized with an exact equal weighted superposition of dimer coverings, as was discussed, occurring at $J_2/J = J_2^{MG}$. For $J_2/J > J_2^{MG}$ it is found that spiral correlations, incommensurate with the underling lattice, emerge. These correlations are short-ranged and compete with the dimer correlations which persist, but reduce in magnitude for $J_2 \gg J_2^c$.

The final region of the $J_1 - J_2$ chain of note here is the $J_2/J < J_2^c$ region. This region is gapless[88, 89, 91] with strong antiferromagnetic correlations. However, these correlations are not sufficient to stabilize order and the region is a disordered example of a Luttinger liquid, or 1D spin liquid, phase. It is also worth noting that this phase is a critical phase of the type discussed previously (i.e. the entire region flows under renormalization to the fixed-point corresponding to the critical point J_2^c).

A final feature of the rich $J_1 - J_2$ system is the nature of the transition

[28] Here we call the J_1 simply J and thus it would technically be called the $J - J_2$ chain. However, that is not the commonly used name. Hopefully this will cause no confusion.

[29] If one imagines a periodic $J_1 - J_2$ chain starting at site 1 and having N sites then the two possible dimer coverings are the one where (1,2),(3,4),(5,6),etc. form a singlet and the one where (N,1),(2,3),(4,5),etc. form a singlet.

at J_2^c. This transition is of the Berezinsky - Kosterlitz - Thouless (BKT) type[93, 94, 95] and is notoriously difficult to identify. It is this transition which will be used as the initial proving ground in Paper #1 for the generalized fidelity susceptibilities discussed here.

In summary the $J_1 - J_2$ chain (for $1 > J_2/J > 0$) is punctuated by three phases: for $J_2/J < J_2^c$ the system is in a gapless 1D spin liquid phase, for $J_2^{MG} > J_2/J > J_2^c$ the system is gapped and notable in its strong dimer correlations, for $J_2/J > J_2^{MG}$ dimer correlation diminish as short-range incommensurate spiral correlations grow. The points J_2^c and J_2^{MG} are also of great significance as a BKT transition point and an exactly solvable point marking the onset of spiral correlations respectively.

4.2 Incommensurate Physics in the Anisotropic Triangular Model: The $J_2 \to 0$ Limiting Case

The other crucial limit of the ANNTLHM is that for which $J_2 \to 0$ where the system reduces to the anisotropic triangular lattice. Interest in this system has a long history dating all the way back to 1972. This original study by Philip Anderson[96] consider the isotropic case $J' = J$ and compared the relative ground-state energies of dimer and three-sublattice order (i.e. spiral ordering with a q-vector of 120° or a wavelength of 3 lattice sites). Based on this analysis Anderson concluded that the isotropic triangular model may exhibit a resonating valence bond state, an early example of the spin-liquid phase. This conclusion turned out to be erroneous and the actual ordering of the isotropic is now rather concretely believed to indeed be the 120° spiral ordering suggested by the classical model.[97, 98, 99] Although the initial conjecture by Anderson turned out to be incorrect, interest in this model, especially in the anisotropic $J' \neq J$ case, continues to this day.

The interest in the anisotropic case was originally sparked by experimental work on the inorganic salt Cs_2CuCl_4 (cesium copper chloride). This neutron scattering work, due to Coldea *et al.*,[100, 101] showed that this material had an unusual blurred or diffuse dispersion relation. Coldea *et al.* would then go on to experimentally show that this material could be well described with the ATLHM Hamiltonian with a $J' \approx 0.33$.[102] Thus interest in this model was renewed.[103]

Although Cs_2CuCl_4 was found to be spin ordered, theoretical and numerical work suggested that it may be proximal to a spin-liquid phase[104] and the the continuum-like dispersion may be due to triplon excitations composed of bound spinons of a quasi-1D spin-liquid.[105]

Cs_2CuCl_4 is not the only material known to be well modelled by the ATLHM Hamiltonian. Other examples include the related inorganic salt Cs_2CuBr_4[106, 107] and the organic compounds $\kappa-(BEDT\text{-}TTF)_2Cu_2(CN)_3$[108, 109, 110]

and $\kappa-(\text{BEDT-TTF})_2\text{Cu}_2[\text{N}(\text{CN})_2]$.[110] A key feature, however, of these systems is that they are not perfectly modelled by the ATLHM Hamiltonian. Especially in Cs_2CuCl_4 and Cs_2CuBr_4 there is also a Dyzaloshinkskii-Moriya interaction present in these systems. Although this interaction is small, for example its strength is believed to be on the order of $\sim 0.05J$ for Cs_2CuCl_4, it does serve to enhance the tendency towards spiral order and pushes these systems away from a disorder phase.[82] However, regardless of the occurrence of a spin-liquid phase in these experimental systems it is still of interest to consider the potential quantum phase diagram of the ATLHM model itself.

Early numerical work on the ATLHM using ED suggested that the system was incommensurate spiral ordered down to $J'/J \sim 0.8 - 0.9$ followed by the emergence of a 2D spin-liquid phase.[111, 112] This is complimented by functional renormalization group work which suggests a similar story.[113] Further investigations by one of the same groups (Sorella) would later argue, through the use of Variational Monte-Carlo (VMC), that the $J' \ll J$ region actually supports two spin-liquid phases; one 1D and another 2D.[114] However, these early numerical works are somewhat unconvincing due to an aspect of ATLHM which is particularly confounding to many numerical approaches: long wavelength incommensurate physics.

In order to truly answer the question as to whether the ATLHM supports a spin-liquid phase, over the more vanilla incommensurate spiral ordering expected in the classical system, one must numerically treat the system in a way that does not penalize incommensurate ordering. This turns out to be quite difficult because even if the system does adopt a spin-liquid phase spiral correlations are still crucial in forming that phase. These spiral correlations seek to establish spiral orderings with very long (tens of thousands to infinite lattice sites) wavelengths, wavelengths that cannot possibly be captured in a finite numerical system. This problem of trying to capture long wavelength behaviour in small finite systems only worsens as $J' \to 0$. Thus the small J' limit is especially difficult to study numerically.

That being said, there have been numerical efforts aimed at minimizing these small system inaccuracies. An example of such an attempt are the series expansion studies by Singh *et al.*[115, 116] which suggest spiral ordering. Another important example, which will be referenced extensively in Paper #3, is the DMRG work of Weichselbaum and White[117] which used DMRG to study the long-distance behaviour of spin-spin correlation function on long thin lattices. This study saw no transition away from the isotropic case and was able to quantitatively determine the q-vectors of the incommensurate spiral correlations. However, they were unable to get convergence for systems for which $J' \lesssim 0.5$ due to long wavelength effects and thus could say nothing about the $J' \ll J$ case. It is the primary motivation of Paper #3 to extend the q-vector data obtained in this study to arbitrarily small J' using the Weichselbaum and

White study as validation. The crux of Paper #3 is to use twisted boundary conditions to capture the long wavelength behaviour. A full discussion of these boundary conditions will be left to the paper but they are designed to allow an arbitrarily long wavelengthed spiral ordering to exist within the small finite lattices available in ED. Thus it can study these physics in a least biased way.

Another leading set of studies of the ATLHM is based on a perturbative renormalization group approach.[81, 82] These papers treat the ATLHM system as an infinite set of coupled chains where each chain is treated as a renormalized block spin. An excellent qualitative discussion of the procedures and findings of those studies can be found in the review by Ghamari *et al.* in reference [118]. However, the crucial finding was that perhaps the most important correlations in the ATLHM are those between next-nearest chains which are believed to be antiferromagnetic (at least for very large systems) and that these correlations, in a manner analogous to the order-from-disorder transitions in the $J_1 - J_2$ square lattice, form a collinear antiferromagnetic ordering in the neighbourhood $J' \to 0$. However, it is worth noting how subtle these correlations are. It is shown in reference [82] that, for smaller systems, next-nearest chain correlations are actually *ferromagnetic* and it's only for fairly large systems that they become antiferromagnetic. This is further evidenced in Paper #2 and Paper #3 where these correlations are studied and the competition between the ferromagnetic and antiferromagnetic case are shown to be fierce.

4.3 The Anisotropic Next-Nearest Neighbour Triangular Lattice Heisenberg Model: The General Case

As was discussed, the ANNTLHM is the general system which encapsulates both the anisotropic triangular lattice and the $J_1 - J_2$ chain. However, very little work has been done on this system in particular. In fact the two main papers on the system are the perturbative RG papers of Balents *et al.*[81] and Ghamari *et al.*,[82] mentioned previously which included extrapolation into the $J' - J_2$ plane of the ANNTLHM. Thus, a purely numerical study of this system is potentially valuable (and is the topic of Paper #2).

The phase diagram proposed in those RG works can be seen in Fig. 6. The dimer phase of the $J_2 \gg J_2^c$ region and the $J' \sim 1$ are both natural extensions of the neighbouring ordered phases in the limits discussed earlier. However, the phase of note is the bounded collinear antiferromagnetic (CAF) phase. As was discussed, the key ingredient in the stabilization of this phase over an apparent disordered phase in the $J_2 \to 0$ limit and known disordered phase in the $J' \to 0$ limit is the antiferromagnetic correlations between *next-nearest* chains.

A key point of interest in any numerical study of the ANNTLM is then

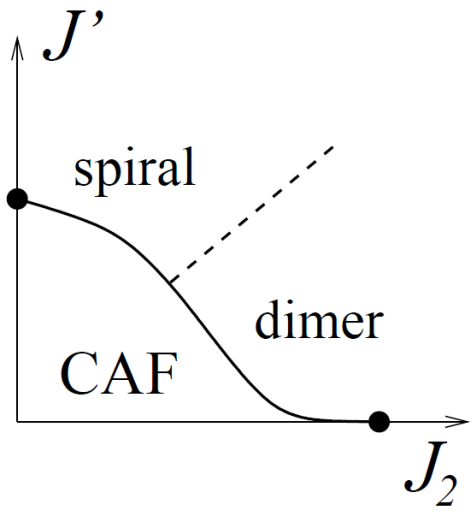

Fig. 6: The phase diagram proposed by perturbative renormalization group techniques. Taken from reference [81]. The bounded collinear antiferromagnetic (CAF) phase is of particular interest.

the nature of the correlations. Specifically, whether next-nearest chain interactions are indeed strong and antiferromagnetic. However, correlations do not necessarily imply ordering and thus the ultimate question, regardless of these correlations, is whether this bounded region exists and is ordered.

The structure of the remaining thesis will be as follows: The first paper presented will be on the $J_1 - J_2$ chain, the next on the ANNTLHM model and, finally, the third on the anisotropic triangular model. Each paper will presented now, preceded by a short discussion of the importance of each work within the overall narrative of the thesis. We will now present the papers.

5 The Papers

5.1 General Quantum Fidelity Susceptibilities for the $J_1 - J_2$ Chain

Mischa Thesberg and Erik S. Sørensen
General Quantum Fidelity Susceptibilities for the $J_1 - J_2$ Chain
Phys. Rev. B 84, 224435 (2011);
DOI: http://dx.doi.org/10.1103/PhysRevB.84.224435

Calculations: All calculations, with the exception of the χ_{AF} data, were performed by the author using a code written entirely by the author. The data within the section related to the antiferromagnetic fidelity susceptibility were performed by Erik S. Sørensen.

Manuscript: The bulk of the text was written by the author with the following exceptions; much of the introductory literature review, the discussion of scaling within the XXZ model and the text related to the antiferromagnetic fidelity susceptibility. The excepted sections were written by Erik S. Sørensen who also provided small miscellaneous corrections and changes throughout.

The following paper sees the application of a new class of fidelity susceptibilities, the generalized fidelity susceptibilities, to a well studied system. Thus this paper serves a validation of these susceptibilities before their application to more disputed systems. Additionally, this system is known to exhibit a transition at $J_2 \sim 0.24 J_1$ which is notoriously difficult to identify and thus the demonstrated ability of these fidelity susceptibilities to identify such a transition further evidences their utility. The paper also contains a review of the relevant literature of the $J_1 - J_2$ chain which will not be repeated here.

The primary questions asked and answered in this paper can be said to be:

- What variety of generalized fidelity susceptibilities can be constructed?
- How useful are these quantities for exploration of a well known phase diagram marked by a subtle transition?
- To what accuracy, compared to other published results, can these objects quantitatively determine the transition point in small finite systems?

We now present the paper.

NOTE: There is a small error in this paper, the y-axis of Fig. 2 reads χ_ρ/L. It is in fact only χ_ρ being plotted there. The caption is correct.

The First Paper: General Quantum Fidelity Susceptibilities for the $J_1 - J_2$ Chain

General Quantum Fidelity Susceptibilities for the $J_1 - J_2$ Chain

Mischa Thesberg[1,*] and Erik S. Sørensen[1,†]

[1] *Department of Physics & Astronomy, McMaster University*
1280 Main St. W., Hamilton ON L8S 4M1, Canada.

(Dated: July 9, 2014)

We study slightly generalized quantum fidelity susceptibilities where the differential change in the fidelity is measured with respect to a different term than the one used for driving the system towards a quantum phase transition. As a model system we use the spin-1/2 $J_1 - J_2$ antiferromagnetic Heisenberg chain. For this model, we study three fidelity susceptibilities, χ_ρ, χ_D and χ_{AF}, which are related to the spin stiffness, the dimer order and antiferromagnetic order, respectively. All these ground-state fidelity susceptibilities are sensitive to the phase diagram of the $J_1 - J_2$ model. We show that they all can accurately identify a quantum critical point in this model occurring at $J_2^c \sim 0.241 J_1$ between a gapless Heisenberg phase for $J_2 < J_2^c$ and a dimerized phase for $J_2 > J_2^c$. This phase transition, in the Berezinskii-Kosterlitz-Thouless universality class, is controlled by a marginal operator and is therefore particularly difficult to observe.

I. INTRODUCTION

The study of quantum phase transitions, especially in one and two dimensions, is a topic of considerable and ongoing interest.[1] Recently the utility of a concept with its origin in quantum information, the quantum fidelity and the related fidelity susceptibility, was demonstrated for the study of quantum phase transitions (QPT).[2–5] It has since then been successfully applied to a great number of systems.[6–11] In particular, it has been applied to the $J_1 - J_2$ model that we consider here.[12]. For a recent review of the fidelity approach to quantum phase transitions, see Ref. 13. Most of these studies consider the case where the system undergoes a quantum phase transition as a coupling λ is varied. The quantum fidelity and fidelity susceptibility is then defined with respect to the same parameter. Apart from a few studies,[14–17] relatively little attention has been given to the case where the quantum fidelity and susceptibility are defined with respect to a coupling different than λ. Here we consider this case in detail for the $J_1 - J_2$ model and show that, if appropriately defined, these general fidelity susceptibilities may yield considerable information about quantum phase transitions occurring in the system and can be very useful in probing for a non-zero order parameter.

Without loss of generality, the Hamiltonian of any many-body system can be written as

$$H(\lambda) = H_0 + \lambda H_\lambda, \tag{1}$$

where λ is a variable which typically parametrizes an interaction and exhibits a phase transition at some critical value λ_c. In this form H_λ is then recognized as a term that *drives* the phase transition.[5] Using the eigenvectors of this Hamiltonian the ground-state (differential) fidelity can then be written as:

$$F(\lambda) = |\langle \Psi_0(\lambda) | \Psi_0(\lambda + \delta\lambda) \rangle| . \tag{2}$$

A series expansion of the GS fidelity in $\delta\lambda$ yields

$$F(\lambda) = 1 - \frac{(\delta\lambda)^2}{2} \frac{\partial^2 F}{\partial \lambda^2} + \dots \tag{3}$$

where $\partial_\lambda^2 F \equiv \chi_\lambda$ is called the *fidelity susceptibility*. For a discussion of sign conventions and a more complete derivation see the topical review by Gu, Ref. 13. If the higher-order terms are taken to be negligibly small then the fidelity susceptibility is defined as:

$$\chi_\lambda(\lambda) = \frac{2(1 - F(\lambda))}{(\delta\lambda)^2} \tag{4}$$

The scaling of χ_λ at a quantum critical point, λ_c, is often of considerable interest and has been studied in detail and previous studies[10,11,14,15,18] have shown that

$$\chi_\lambda \sim L^{2/\nu}, \quad \chi_\lambda / N \sim L^{2/\nu - d}, \tag{5}$$

with $N = L^d$ the number of sites in the system. An easy way to re-derive this result is by envoking finite-size scaling. Since $1 - F$ obviously is *dimensionless* it follows from Eq. (4) that the appropriate finite-size scaling form for χ_λ is

$$\chi_\lambda \sim (\delta\lambda)^{-2} f(L/\xi). \tag{6}$$

If we now consider the case where the parameter λ drives the transition we may at the critical point λ_c identify $\delta\lambda$ with $\lambda - \lambda_c$. It follows that $\xi \sim (\delta\lambda)^{-\nu}$. As usual, we can then replace $f(L/\xi)$ by an equivalent function $\tilde{f}(L^{1/\nu}\delta\lambda)$. The requirement that χ_λ remains finite for

a finite system when $\delta\lambda \to 0$ then implies that to leading order $\tilde{f}(x) \sim x^2 \sim L^{2/\nu}(\delta\lambda)^2$, from which Eq. (5) follows.

Here we shall consider a slightly more general case where the term driving the quantum phase transition is not the same as the one with respect to which the fidelity and fidelity susceptibility are defined. That is, one considers:

$$H(\lambda, \delta) = H_1 + \delta H_I, \quad H_1 = H_0 + \lambda H_\lambda. \tag{7}$$

The fidelity and the related susceptibility is then defined as

$$F(\lambda, \delta) = |\langle \Psi_0(\lambda, 0) | \Psi_0(\lambda, \delta) \rangle|, \tag{8}$$

$$\chi_\delta(\lambda) = \frac{2(1 - F(\lambda, \delta))}{\delta^2} \tag{9}$$

The scaling of χ_δ at λ_c for this more general case was derived by Venuti *et al.*[15] where it was shown that:

$$\chi_\delta \sim L^{2d+2z-2\Delta_v}, \quad \chi_\delta/N \sim L^{d+2z-2\Delta_v}. \tag{10}$$

Here, z is the dynamical exponent, d the dimensionality and Δ_v the scaling dimension of the perturbation H_I. In all cases that we consider here $z = d = 1$. We note that Eq. (10) assumes $[H_1, H_I] \neq 0$, if H_I commutes with H_1 then $F = 1$ and $\chi_\delta = 0$. The case where H_λ and H_I coincide is a special case of Eq. (10) for which $\Delta_V = d + z - 1/\nu$ and one recovers Eq. (5).

A particular appealing feature of Eq. (5) is that when $2/\nu > d$, χ_λ/N will diverge at λ_c and the fidelity susceptibility can then be used to locate the λ_c *without* any need for knowing the order parameter. Secondly, it can be shown[5,14] that the fidelity susceptibility can be expressed as the zero-frequency *derivative* of the dynamical correlation function of H_I, making it a very sensitive probe of the quantum phase transition.[19] On the other hand, if a phase transition is expected one might then use the fidelity susceptibility as a very sensitive probe of the order parameter through a suitably defined H_δ in Eq. (7). This is the approach we shall take here using the $J_1 - J_2$ spin chain as our model system.

The spin-1/2 Heisenberg $J_1 - J_2$ chain is a very well studied model. The Hamiltonian is:

$$H = \sum_i S_i \cdot S_{i+1} + J_2 \sum_i S_i \cdot S_{i+2} \tag{11}$$

where J_2 is understood to be the ratio of the next-nearest neighbor exchange parameter over the nearest neighbor exchange parameter ($J_2 = J_2'/J_1'$). This model is known to have a quantum phase transition of the Berezinskii-Kosterlitz-Thouless (BKT) universality class occurring at J_2^c between a gapless 'Heisenberg' (Luttinger liquid) phase for $J_2 < J_2^c$ and a dimerized phase with a two-fold degenerate ground-state for $J_2 > J_2^c$. Field theory[20,21], exact diagonalization[22,23] and DMRG[24,25], have yielded very accurate estimates of the Luttinger Liquid-Dimer phase transition, the most accurate of these being due to Eggert[23] which yielded a value of $J_2^c = 0.241167$. Previous studies by Chen *et al.*[12] of this model using the fidelity approach used the same term for the driving and perturbing part of the Hamiltonian as in Eq. (1) with the correspondence $H_0 = \sum_i S_i \cdot S_{i+1}$, $H_\lambda = \sum_i S_i \cdot S_{i+2}$, $\lambda = J_2$.[12] . Chen *et al.* demonstrated that, though no useful information about the Luttinger Liquid-Dimer phase transition could be obtained directly from the *ground-state* fidelity (and similarly the fidelity susceptibility), a clear signature of the phase transition was present in the fidelity of the *first excited* state.[12] Sometimes this is taken as an indication that ground-state fidelity susceptibilities are not useful for locating a quantum phase transition in the BKT universality class. Here we show that more general ground-state fidelity susceptibilities indeed can locate this transition.

Specifically, we will study three fidelity susceptibilities, χ_ρ, χ_D and $\chi_{\rm AF}$, which are coupled to the spin stiffness, a staggered interaction term and a staggered field term, respectively. In section II we present our results for χ_ρ while section III is focused on χ_D and section IV on $\chi_{\rm AF}$.

II. THE SPIN STIFFNESS FIDELITY SUSCEPTIBILITY, χ_ρ

We begin by considering the $J_1 - J_2$ model with $J_2 = 0$ but with an anisotropy term Δ, what is usually called the XXZ model:

$$H_{\rm XXZ} = \sum_i [\Delta S_i^z S_{i+1}^z + \frac{1}{2}(S_i^+ S_{i+1}^- + S_i^- S_{i+1}^+)]. \tag{12}$$

The Heisenberg phase of this model, occurring for $\Delta \in [-1, 1]$, is characterized by a non-zero spin stiffness[26,27] defined as:

$$\rho(L) = \left. \frac{\partial^2 e(\phi)}{\partial \delta^2} \right|_{\phi=0}. \tag{13}$$

Here, $e(\phi)$ is the ground-state energy per spin of the model where a twist of ϕ is applied at every bond:

$$H_{\rm XXZ}(\Delta, \phi) = \sum_i [\Delta S_i^z S_{i+1}^z + \frac{1}{2}(S_i^+ S_{i+1}^- e^{i\phi} + S_i^- S_{i+1}^+ e^{-i\phi})]. \tag{14}$$

The spin stiffness can be calculated exactly for the XXZ model for finite L using the Bethe ansatz,[28] and exact

expressions in the thermodynamic limit are available.[26,27] Interestingly the usual fidelity susceptibility with respect to Δ can also be calculated exactly.[29,30]

Since the non-zero spin stiffness defines the gapless Heisenberg phase it is therefore of interest to define a fidelity susceptibility associated with the stiffness. This can be done through the overlap of the ground-state with $\phi = 0$ and a non-zero ϕ. With $\Psi_0(\Delta, \phi)$ the ground-state of $H_{\mathrm{XXZ}}(\Delta, \phi)$ we can define the fidelity and fidelity susceptibility with respect to the twist in the limit where $\phi \to 0$:

$$F(\Delta, \phi) = |\langle \Psi_0(\Delta, 0) | \Psi_0(\Delta, \phi) \rangle| , \tag{15}$$

$$\chi_\rho(\Delta) = \frac{2(1 - F(\Delta, \phi))}{\phi^2}. \tag{16}$$

To calculate χ_ρ the ground-state of the unperturbed Hamiltonian was calculated through numerical exact diagonalization. The system was then perturbed by adding a twist of $e^{i\phi}$ at each bond and recalculating the ground-state. From the corresponding fidelity, χ_ρ was calculated using Eq. (16). Our results for χ_ρ/L versus Δ are shown in Fig. 1. For all data ϕ was taken to be 10^{-3} and periodic boundary conditions were assumed. In all cases it was verified that the finite value of ϕ used had no effect on the final results. The numerical diagonalizations were done using the Lanczos method as outlined by Lin *et al.*[31] Total S^z symmetry and parallel programming techniques were employed to make computations feasible. Numerical errors are small and conservatively estimated to be on the order of 10^{-10} in the computed ground-state energies.

In order to understand the results in Fig. 1 in more detail we expand Eq. (14) for small ϕ:

$$H_{\mathrm{XXZ}}(\Delta, \phi) \sim H_{\mathrm{XXZ}}(\Delta) + \phi \mathcal{J} - \frac{\phi^2}{2} \mathcal{T} + \ldots, \tag{17}$$

$$\mathcal{J} = \frac{i}{2} \sum_i (S_i^+ S_{i+1}^- - S_i^- S_{i+1}^+), \tag{18}$$

$$\mathcal{T} = \frac{1}{2} \sum_i (S_i^+ S_{i+1}^- + S_i^- S_{i+1}^+). \tag{19}$$

Here, $\mathcal{J}$ is the spin current and $\mathcal{T}$ a kinetic energy term. The first thing we note is that, when $\Delta = 0$ both $\mathcal{J}$ and $\mathcal{T}$ commute with $H_{\mathrm{XXZ}}(\Delta = 0)$. The ground-state wave-function is therefore independent of ϕ (for small ϕ) and $\chi_\rho \equiv 0$. This can clearly be seen in Fig. 1.

In the continuum limit the spin current $\mathcal{J}$ can be expressed in an effective low energy field theory[32] with scaling dimension $\Delta_{\mathcal{J}} = 1$. However, we expect subleading corrections to arise from the presence of the operators $(\partial_x \Phi)^2$ with scaling dimension 2 and $\cos(\sqrt{16\pi K}\Phi)$ with scaling dimension $4K$. Here, K is given by $K = \pi/(2(\pi - \arccos(\Delta)))$. For $\Delta \neq 0$ both of these terms will be generated by the term $\mathcal{T}$ in Eq. (17).[15] With these scaling dimensions and with the use of Eq. (10) we then find:

$$\chi_\rho/L = A_1 L + A_2 + A_3 L^{-1} + A_4 L^{3-8K} \tag{20}$$

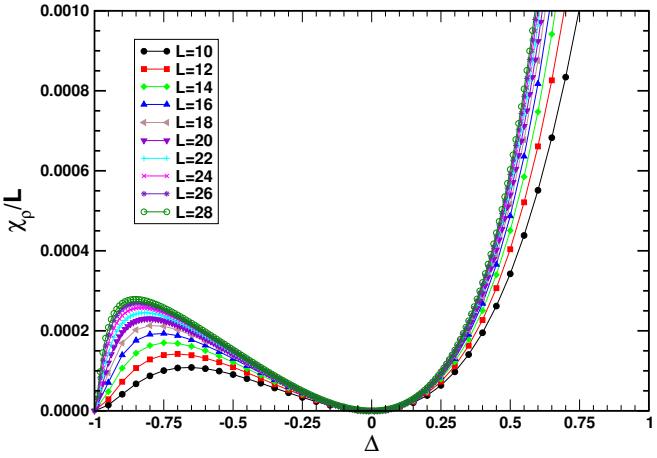

FIG. 1. (Color online.) $\frac{\chi_\rho}{L}$ vs. Δ: The spin stiffness fidelity susceptibility $(\chi_\rho(\Delta)/L)$ as a function of the z-anistropy Δ. At the $\Delta = 0$ point the spin-current operator $\mathcal{J}$ and kinetic energy $\mathcal{T}$ commute with the XXZ Hamiltonian and thus such a perturbation does not change the ground-state, and the fidelity is one. Thus, χ_ρ is zero at this point.

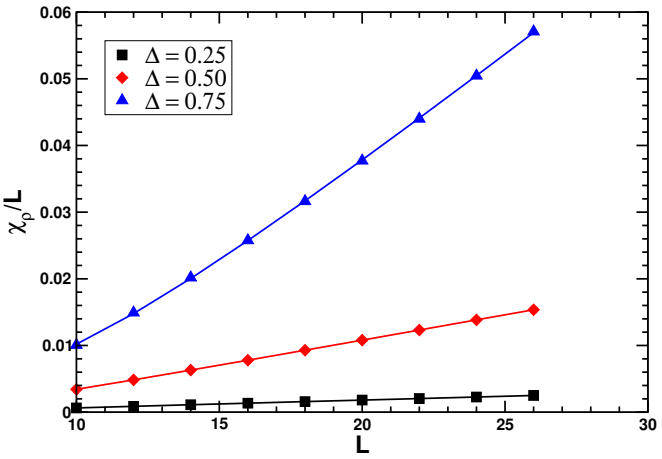

FIG. 2. (Color online.) χ_ρ vs. L (the XXZ model at different values of Δ): This graph shows the scaling of χ_ρ with system size for different values of the z-anisotropy Δ. The points represent numerical data and the lines represent fits to the scaling form predicted for the spin stiffness susceptibility $\chi_\rho/L = A_1 L + A_2 + A_3 L^{-1} + A_4 L^{3-8K}$. It can be seen that there is good agreement.

In Fig. 2 a fit to this form is shown for 3 different values of $\Delta = 0.25, 0.5$ and 0.75 in all cases do we observe an excellent agreement with the expected form with corrections arising from the last term L^{3-8K} being almost un-noticeable until Δ approaches 1. We would expect the sub-leading corrections L^{-1} and L^{3-8K} to be absent if the perturbative term is just $\phi\mathcal{J}$.

We now turn to a discussion of a definition of χ_ρ in the presence of a non-zero J_2 but restricting the discussion to the isotropic case $\Delta = 1$. In this case we define:

$$H(\phi) = \sum_i [S_i^z S_{i+1}^z + \frac{1}{2}(S_i^+ S_{i+1}^- e^{i\phi} + S_i^- S_{i+1}^+ e^{-i\phi})] + J_2 \sum_i [S_i^z S_{i+2}^z + \frac{1}{2}(S_i^+ S_{i+2}^- e^{i\phi} + S_i^- S_{i+2}^+ e^{-i\phi})]. \quad (21)$$

That is, we simply apply the twist ϕ at every bond of the Hamiltonian. As before we can expand:

$$H(\phi) \sim H(0) + \phi(\mathcal{J}_1 + \mathcal{J}_2) - \frac{\phi^2}{2}(\mathcal{T}_1 + \mathcal{T}_2) + \ldots \quad (22)$$

$$\mathcal{J}_1 = \frac{i}{2}\sum_i (S_i^+ S_{i+1}^- - S_i^- S_{i+1}^+), \quad (23)$$

$$\mathcal{J}_2 = \frac{i}{2}\sum_i (S_i^+ S_{i+2}^- - S_i^- S_{i+2}^+), \quad (24)$$

$$\mathcal{T}_1 = \frac{1}{2}\sum_i (S_i^+ S_{i+1}^- + S_i^- S_{i+1}^+), \quad (25)$$

$$\mathcal{T}_2 = \frac{1}{2}\sum_i (S_i^+ S_{i+2}^- + S_i^- S_{i+2}^+). \quad (26)$$

Our results for χ_ρ/L versus J_2 using this definition are shown in Fig. 3 for a range of L from 10 to 32. In the region of the critical point at $J_2 = 0.241167$ the size dependence of χ_ρ/L vanishes yielding near scale invariance. How well this works close to J_2^c is shown in the inset of Fig. 3. This alone can be taken to be a strong indication of χ_ρ/Ls sensitivity to the phase transition. In fact, this scale invariance works so well that one can locate the critical point to a high precision simply by verifying the scale invariance. This is illustrated in Fig. 4B where χ_ρ/L is plotted as a function of L for $J_2 = 0.23$, $J_2 = J_2^c$ and $J_2 = 0.25$. From the results in Fig. 4b the critical point J_2^c where χ_ρ/L becomes independent of L is immediately visible.

As can be seen in the inset of Fig. 3 χ_ρ/L reaches a minimum slightly prior to J_2^c. The J_2 value at which this minimum occurs has a clear system size dependence which can be fitted to a power-law and extrapolated to $L = \infty$ yielding a value of $J_{2c} = 0.24077$. Hence,

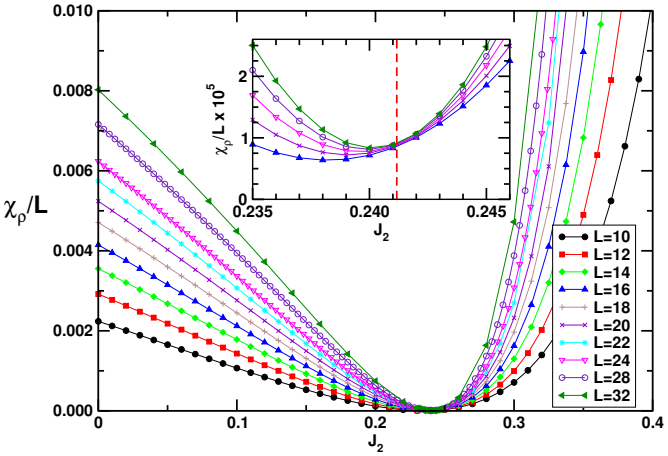

FIG. 3. (Color online.) $\frac{\chi_\rho}{L}$ vs. J_2 and Inset: The generalized spin stiffness susceptibility, χ_ρ as a function of the second nearest-neighbor exchange coupling J_2. The system acquires a clearly size invariant form in the vicinity of the critical point $J_2 \sim 0.24$ (as well as tending to a global minima). Inset shows the the minima for system sizes L=16,20,24,28,32 with J_2^c indicated as the vertical dashed line. A clear dependence of the J_2 value of χ_ρ/L minima on the system size can be seen.

the minimum coincides with J_2^c in the thermodynamic limit. This is shown in Fig. 4a. Comparison of this value with the accepted $J_2^c = 0.241167$ reveals impressive agreement. Another noteworthy feature of the results in Fig. 3 is that χ_ρ/L is *non-zero* at the critical point, J_2^c. This value is very small but we have verified in detail that numerically it is non-zero.

The scale invariance of χ_ρ/L is clearly induced by the disappearance[21] of the marginal operator $\cos(\sqrt{16\pi K}\Phi)$ at J_2^c. We expect that in the continuum limit the absence of this operator implies that the spin current commutes with the Hamiltonian resulting in χ_ρ being effectively zero at J_2^c. The observed non-zero value of χ_ρ/L would then arise from short-distance physics. At present we have no explanation for why this small non-zero value should scale with L at J_2^c.

Note that, as mentioned previously, we take the spin stiffness to be represented by a twist on *every* bond, both first and second nearest neighbor and not merely on the boundary as is sometimes done. This choice is not just a matter of taste. Imposing a twist only on the boundary (usually) breaks the translational invariance of the ground-state and, through extension, effects the value and behavior of the fidelity itself. Another point of note is the use of a twist of only ϕ between next-nearest neighbors. Geometric intuition would sug-

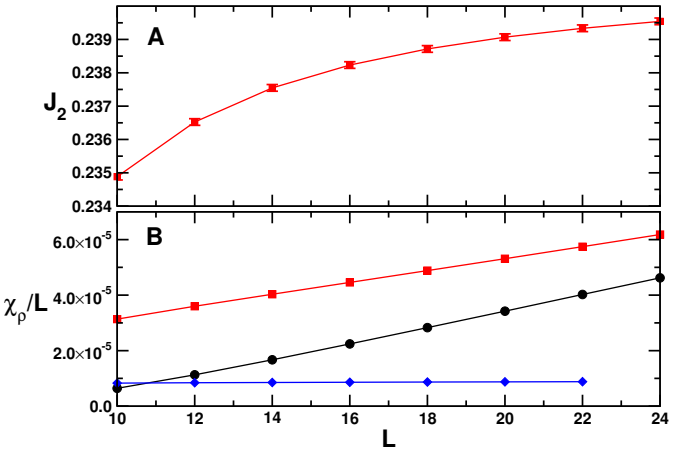

FIG. 4. (Color online.) A: The J_2 value of χ_ρ minima as a function of system size, as well as a (power law) line of best fit. As the system size tends towards infinity the power law best fit predicts a minima at $J_2 = 0.24077$ in good agreement with previously published results. B: Scaling of χ_ρ at $J_2 = 0.23$ (the highest, linear curve), $J_2 = 0.25$ (the second highest, linear curve) and at the critical point $J_2 = 0.241167$ (flat curve). The near constant scaling of $\frac{\chi_\rho}{L}$ at the critical point as well as non-constant scaling on either side of the critical point can clearly be seen.

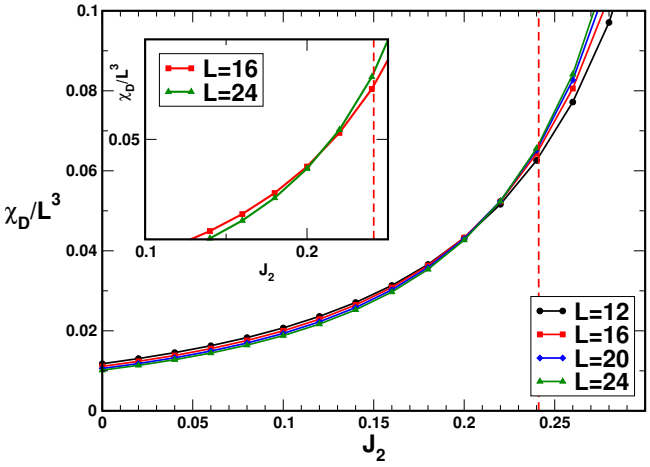

FIG. 5. (Color online.) $\frac{\chi_D}{L^3}$ vs. J_2. The generalized dimer fidelity susceptibility χ_D/L^3 as a function of the second nearest-neighbor exchange parameter J_2. A clear intersection of all curves can be seen in the vicinity of the proposed critical point at $J_2 \sim 0.2 - 0.25$. The inset explicitly shows the crossing of $L = 12$ and $L = 24$. The dashed vertical lines indicate J_2^c.

gest that a twist of 2ϕ should be applied between next-nearest neighbor bonds. However, for the small system sizes available for exact diagonalization it is found that a simple twist of ϕ on both bonds yields *significantly* better scaling.

III. THE DIMER FIDELITY SUSCEPTIBILITY, χ_D

We now turn to a discussion of a fidelity susceptibility associated with the dimer order present in the $J_1 - J_2$ model for $J_2 > J_2^c$. This susceptibility, which we call χ_D, is coupled to the order parameter of the dimerized phase by design. Usually in the fidelity approach to quantum phase transitions one considers the case where the ground-state is unique in the absence of the perturbation. This is not the case here, leading to a diverging χ_D/L in the dimerized phase even in the presence of a gap. Specifically, we consider a Hamiltonian of the form:

$$H = \sum_i [S_i \cdot S_{i+1} + J_2 S_i \cdot S_{i+2} + \delta h (-1)^i S_i \cdot S_{i+1}] \tag{27}$$

Thus, in correspondence with Eq. (7) we have $H_I = (-1)^i S_i \cdot S_{i+1}$ and we choose the driving coupling to be J_2. This perturbing Hamiltonian represents a *conjugate field* for the dimer phase. The scaling dimension of H_I is known[33], $\Delta_D = \frac{1}{2}$, and from Eq. (10) we therefore find:

$$\chi_D \sim L^{4-2\Delta_D} = L^3 \quad (\text{at } J_2^c) \tag{28}$$

Due to the presence of the marginal coupling we cannot expect this relation to hold for $J_2 < J_2^c$. However, the marginal coupling changes sign at J_2^c and is therefore absent at J_2^c where Eq. (28) should be exact.[21] For $J_2 < 0.241167$ it is known[33] that logarithmic corrections arising from the marginal coupling for the small system sizes considered here lead to an effective scaling dimension $\Delta_D > \frac{1}{2}$. At $J_2 = 0$ Affleck and Bonner[33] estimated $\Delta_D = 0.71$. Hence, using this results at $J_2 = 0$, we would expect that $\chi_D \sim L^{2.58}$ which we find is in reasonable agreement with our results at $J_2 = 0$ where a best fit yields an exponent of $\chi_D \sim L^{2.78}$. See Fig. 6a.

We now need to consider the case $J_2 > 0.241167$. At $J_2 = 1/2$ the ground-state is exactly known for *even* L[34] and the two dimerized ground-states are exactly degenerate even for finite L. For $J_2^c < J_2 < 1/2$ the system is gapped with a unique ground-state but with an exponentially low-lying excited state. In the thermodynamic limit the two-fold degeneracy of ground-state is recov-

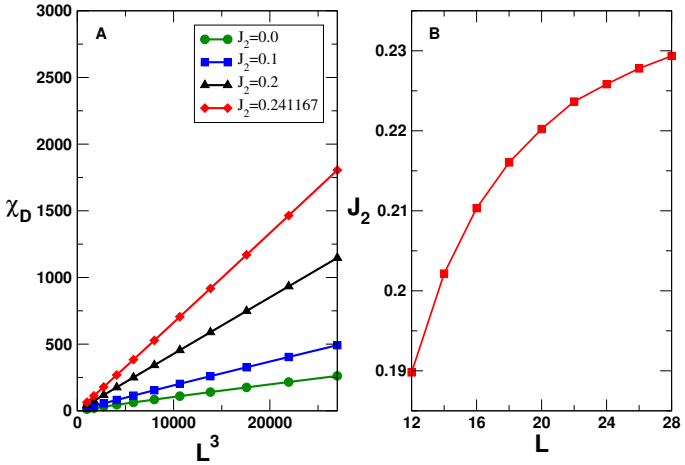

FIG. 6. (Color online.) A: Scaling of χ_D vs. L^3 at the points $J_2 = 0.0, 0.1, 0.2$ and 0.241167. For $J_2 < 0.241167$ the scaling exponent is fitted to be less than 3. B: The J_2 value of the intersection of $\frac{\chi_D}{L^3}$ between systems of size L and $L+2$ plotted as a function of L. The curve can be fitted with a power-law line of best fit. The line of best fit is found to converge to $J_2 = 0.241$.

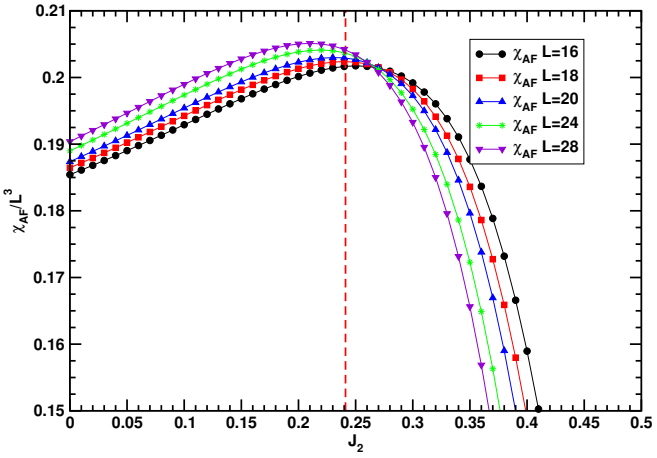

FIG. 7. (Color online.) $\chi_{\rm AF}/L^3$ versus J_2. $\chi_{\rm AF}$ is expected to approach zero exponentially with the system size for $J_2 > J_2^c$, to scale as L^3 at J_2^c and to scale as $L^{\alpha_{\rm eff}}$ with $\alpha_{\rm eff} > 3$ for $J_2 < J_2^c$. A crossing close to the critical point J_2^c (dashed vertical line) is then visible.

ered, corresponding to the degeneracy of the two dimerization patterns. From this it follows that χ_D is formally infinite at $J_2 = 0$ and as $L \to \infty$ for $J_2^c < J_2 < 1/2$ we expect χ_D to diverge exponentially with L. At J_2^c we expect χ_D to exactly scale as L^3 and for $J_2 < J_2^c$ we expect $\chi_D \sim L^{\alpha}_{\rm eff}$ with $\alpha_{\rm eff} < 3$. Hence, if χ_D/L^3 is plotted for different L we would expect the curves to cross at J_2^c. However, the crossing might be difficult to observe since it effectively arise from logarithmic corrections.

Our results for χ_D/L^3 are shown in Fig. 5, where a crossing of the curves are visible around $J_2 \sim 0.2 - 0.25$. As an illustration, the inset of Fig. 5 shows the crossing of $L = 12$ and $L = 24$. In order to obtain a more precise estimate of J_2^c the intersection of each curve and the curve corresponding to the next largest system were tabulated (L and $L+2$). These intersection points as a function of system size were then plotted in Fig. 6b and found to obey a power-law of the form $a - bL^{-\alpha}$ with $\alpha \sim 1.8$ and $a = 0.241$. This estimate of the critical coupling is in good agreement with the value of $J_2^c = 0.241167$.[23]

To further verify the scaling of χ_D at J_2^c we show in Fig. 6a χ_D for various values of $J_2 \leq J_2^c$ as a function of the cubed system size, L^3. A strong linear scaling with an exponent of 3 is observed at J_2^c while for $J_2 < J_2^c$ logarithmic corrections leads to an effective exponent that is *less than* 3 consistent with expectations.[33]

IV. THE AF FIDELITY SUSCEPTIBILITY, $\chi_{\rm AF}$

Finally, we briefly discuss another fidelity susceptibility very analogous to χ_D. We consider a perturbing term in the form of a staggered field of the form $\sum_i (-1)^i S_i^z$ with an associated fidelity susceptibility, $\chi_{\rm AF}$. The scaling dimension of such a staggered field is $\Delta_{\rm AF} = \frac{1}{2}$ and as for χ_D we therefore expect that $\chi_{\rm AF} \sim L^3$ at J_2^c. However, in this case it is known[33] that the effective scaling dimension for $J_2 < J_2^c$ is *smaller* than $\frac{1}{2}$ resulting in $\chi_{\rm AF} \sim L^{\alpha_{\rm eff}}$ with $\alpha_{\rm eff} > 3$ for $J_2 < J_2^c$. On the other had, in the dimerized phase $\chi_{\rm AF}$ must clearly go to zero exponentially with L. Hence, if $\chi_{\rm AF}$ is plotted for different L as a function of J_2 a crossing of the curves should occur.

Our results are shown in Fig. 7 where $\chi_{\rm AF}/L^3$ is plotted versus J_2 for a number of system sizes. It is clear from these results that $\chi_{\rm AF}$ indeed goes to zero rapidly in the dimerized phase as one would expect. Close to J_2^c the scaling is close to L^3 where as for $J_2 < J_2^c$ it is faster than L^3. Hence, as can be seen in Fig. 7, a crossing occurs close to J_2^c.

V. CONCLUSION AND SUMMARY

In this paper we have demonstrated the potential benefits of extending the concept of a fidelity susceptibility beyond a simple perturbation of the same term that drives the quantum phase transition. By using the spin-

1/2 Heisenberg spin chain as an example we first created a susceptibility which was directly coupled to the spin stiffness but of increased sensitivity. This fidelity susceptibility, which we labelled χ_ρ can be used to successfully estimate the transition point at $J_2 \sim 0.241$. Next we constructed another fidelity susceptibility, χ_D, this time coupled to the order parameter susceptibility of the dimer phase. Again, we were able to estimate the critical point at a value of 0.241. Finally, we discussed an anti ferromagnetic fidelity susceptibility that rapidly approaches zero in the dimerized phase but diverges in the Heisenberg phase. Although susceptibilities linked to these quantities appeared the most useful for the $J_1 - J_2$ model we considered here, it is possible to define many other fidelity susceptibilities that could provide valuable insights into the ordering occurring in the system being studied.

ACKNOWLEDGMENTS

MT acknowledge many fruitful discussions with Sedigh Ghamari. ESS would like to thank Fabien Alet for several discussions about the fidelity susceptibility and I Affleck for helpful discussions concerning scaling dimensions. This work was supported by NSERC and by the Shared Hierarchical Academic Research Computing Network.

* thesbeme@mcmaster.ca
† sorensen@mcmaster.ca; http://comp-phys.mcmaster.ca

[1] S. Sachdev, *Quantum Phase Transitions* (Cambridge University Press, 1999).
[2] H. T. Quan, Z. Song, X. F. Liu, P. Zanardi, and C. P. Sun, Phys. Rev. Lett. **96**, 140604 (2006).
[3] P. Zanardi and N. Paunković, Phys. Rev. E **74**, 031123 (2006).
[4] H.-Q. Zhou and J. P. Barjaktarevi, Journal of Physics A: Mathematical and Theoretical **41**, 412001 (2008).
[5] W.-L. You, Y.-W. Li, and S.-J. Gu, Phys. Rev. E **76**, 022101 (2007).
[6] P. Zanardi, M. Cozzini, and P. Giorda, Journal of Statistical Mechanics: Theory and Experiment **2007**, L02002 (2007).
[7] M. Cozzini, P. Giorda, and P. Zanardi, Phys. Rev. B **75**, 014439 (2007).
[8] M. Cozzini, R. Ionicioiu, and P. Zanardi, Phys. Rev. B **76**, 104420 (2007).
[9] P. Buonsante and A. Vezzani, Phys. Rev. Lett. **98**, 110601 (2007).
[10] D. Schwandt, F. Alet, and S. Capponi, Physical Review Letters **103**, 170501 (2009).
[11] A. F. Albuquerque, F. Alet, C. Sire, and S. Capponi, Physical Review B **81**, 064418 (2010).
[12] S. Chen, L. Wang, S.-J. Gu, and Y. Wang, Phys. Rev. E **76**, 061108 (2007).
[13] S. Gu, International Journal of Modern Physics B **24**, 4371 (2010).
[14] P. Zanardi, P. Giorda, and M. Cozzini, Physical Review Letters **99**, 100603 (2007).
[15] L. Campos Venuti and P. Zanardi, Phys. Rev. Lett. **99**, 095701 (2007).
[16] C. De Grandi, A. Polkovnikov, and A. W. Sandvik, arXiv.org **cond-mat.other** (2011).
[17] V. Mukherjee, A. Polkovnikov, and A. Dutta, Phys. Rev. B **83**, 075118 (2011).
[18] S. Gu and H. Lin, EPL (Europhysics Letters) **87**, 10003 (2009).
[19] S. Chen, L. Wang, Y. Hao, and Y. Wang, Phys. Rev. A **77**, 032111 (2008).
[20] F. D. M. Haldane, Phys. Rev. B **25**, 4925 (1982).
[21] S. Eggert and I. Affleck, Physical Review B **46**, 10866 (1992).
[22] T. Tonegawa and I. Harada, J. Phys. Soc. Jpn. **56**, 2153 (1987).
[23] S. Eggert, Phys. Rev. B **54**, R9612 (1996).
[24] R. Chitra, S. Pati, H. R. Krishnamurthy, D. Sen, and S. Ramasesha, Phys. Rev. B **52**, 6581 (1995).
[25] S. R. White and I. Affleck, Phys. Rev. B **54**, 9862 (1996).
[26] B. S. Shastry and B. Sutherland, Phys. Rev. Lett. **65**, 243 (1990).
[27] B. Sutherland and B. S. Shastry, Phys. Rev. Lett. **65**, 1833 (1990).
[28] N. Laflorencie, S. Capponi, and E. S. Sørensen, Eur. Phys. J. B **24**, 77 (2001).
[29] M. Yang, Physical Review B **76**, 180403 (2007).
[30] J. Fjærestad, Journal of Statistical Mechanics: Theory and Experiment **2008**, P07011 (2008).
[31] H. Q. Lin, Phys. Rev. B **42**, 6561 (1990).
[32] J. Sirker, R. Pereira, and I. Affleck, Physical Review B , 035115 (2011).
[33] I. Affleck and J. C. Bonner, Phys. Rev. B **42**, 954 (1990).
[34] C. K. Majumdar, Journal of Physics C: Solid State Physics **3**, 911 (1970).

5.2 A Quantum Fidelity Study of the Anisotropic Next-Nearest-Neighbour Triangular Lattice Heisenberg Model

Mischa Thesberg and Erik S. Sørensen
A Quantum Fidelity Study of the Anisotropic Next-Nearest-Neighbour Triangular Lattice Heisenberg Model
Submitted and recommended for publication in Journal of Physics: Condensed Matter (submitted: July 9th, 2014)

Calculations: All calculations were performed by the author using a code written entirely by the author.

Manuscript: The entirety of the text was written by the author excepting miscellaneous edits contributed by Erik S. Sørensen.

In the previous paper the validity of generalized fidelity susceptibilities as tools for probing a well-known phase diagram was demonstrated. In this paper we then apply this techniques, plus the higher-order fidelity discussed earlier, to a system with a more disputed phase diagram, the ANNTLHM. We apply these susceptibilities and fidelities throughout the entire $J' < J$, $J_2 < J$ phase diagram.

The paper also contains a review of the relevant literature for the models involved and the fidelity techniques. Must of this will be redundant with previous expositions.

This second paper attempts to explore the phase diagram of that ANNTLHM and seeks to answer the following questions:

- Do the generalized fidelity susceptibilities and higher-order fidelities provide useful information about a novel phase diagram?
- What shape and form do any phase regions within the $J' - J_2$ plane have?
- What is the nature of the phase bounded in this phase diagram?
- What do these susceptibilities and fidelities tells us about the physics in the ATLHM ($J_2 \to 0$) case?

We now present the paper.

The Second Paper: A Quantum Fidelity Study of the Anisotropic Next-Nearest-Neighbour Triangular Lattice Heisenberg Model

A Quantum Fidelity Study of the Anisotropic Next-Nearest-Neighbour Triangular Lattice Heisenberg Model

Mischa Thesberg

Department of Physics & Astronomy, McMaster University
1280 Main St. W., Hamilton ON L8S 4M1, Canada.

Erik S. Sørensen

Department of Physics & Astronomy, McMaster University
1280 Main St. W., Hamilton ON L8S 4M1, Canada.

Abstract. Ground- and excited-state quantum fidelities in combination with generalized quantum fidelity susceptibilites, obtained from exact diagonalizations, are used to explore the phase diagram of the anisotropic next-nearest-neighbour triangular Heisenberg model. Specifically, the $J' - J_2$ plane of this model, which connects the $J_1 - J_2$ chain and the anisotropic triangular lattice Heisenberg model, is explored using these quantities. Through the use of a quantum fidelity associated with the first excited-state, in addition to the conventional ground-state fidelity, the BKT-type transition and Majumdar-Ghosh point of the $J_1 - J_2$ chain ($J' = 0$) are found to extend into the $J' - J_2$ plane and connect with points on the $J_2 = 0$ axis thereby forming bounded regions in the phase diagram. These bounded regions are then explored through the generalized quantum fidelity susceptibilities χ_ρ, χ_{120°, χ_D and χ_{CAF} which are associated with the spin stiffness, 120° spiral order parameter, dimer order parameter and collinear antiferromagnetic order parameter respectively. These quantities are believed to be extremely sensitive to the underlying phase and are thus well suited for finite-size studies. Analysis of the fidelity susceptibilities suggests that the $J', J_2 \ll J$ phase of the anisotropic triangular model is either a collinear antiferromagnet or possibly a gapless disordered phase that is directly connected to the Luttinger phase of the $J_1 - J_2$ chain. Furthermore, the outer region is dominated by incommensurate spiral physics as well as dimer order.

PACS numbers:

Submitted to: *J. Phys.: Condens. Matter*

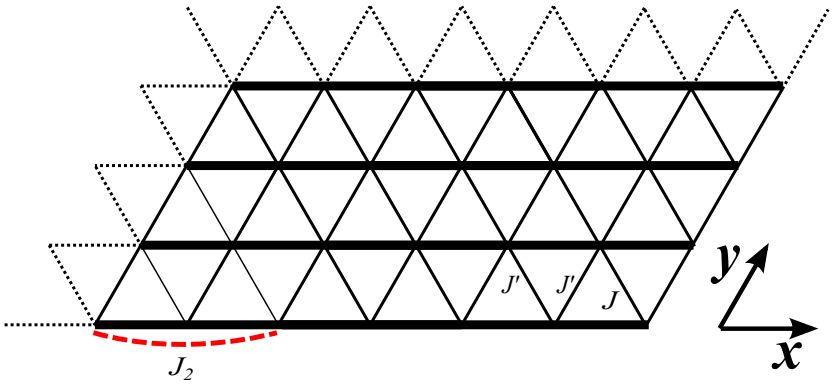

Figure 1. The anisotropic triangular lattice with next-nearest neighbour interactions. In this paper J' and J_2 are assumed to be ratios of J (i.e. $J = 1$). In the limit $J' \ll 1$ the system can be viewed as a set of weakly coupled chains. The *next-nearest neighbour* interactions J_2 are in the intra-chain direction (red dashed line). A system size is denoted as $N = W \times L$ corresponding to a system of W chains of length L. The system size studied here is 4×6.

1. Introduction

The study of quantum phase transitions (QPTs), especially those which occur in two- and one-dimensional systems, remains one of the most active areas of research in condensed matter physics.[1] Of particular interest are systems with competition between interactions that cannot be mutually satisfied. This behaviour, often arising from *frustration*, acts to erode the tendency towards classical orderings and promotes exotic phases dominated by quantum fluctuations. Unfortunately, these quantum fluctuations manifest as highly oscillatory, fermionic field theories. Such theories cause Quantum Monte-Carlo (QMC) methods, numerical methods which allow the study of some of the largest system sizes that are accessible computationally, to fail. In contrast, Exact Diagonalization (ED) methods, that we employ here, are not affected by the presence of frustration and can quite generally be applied to lattice models with a finite Hilbert space. They are, however, restricted to very small system sizes. The use of complimentary methods such as the Density Matrix Renormalization Group (DMRG) and related methods are therefore also extremely valuable and DMRG results for two-dimensional triangular lattice models have already been obtained [2]. However, our focus here is on the information that can be extracted from ED results in combination with new insights arising from the field of quantum information.

The numerical identification of QPTs and the classification of their adjoining quantum phases often involves some *a priori* knowledge about the ordering of the system and the evaluation of quantities, such as the spin stiffness or order parameter, which may have poor behaviour or slow/subtle divergences in small finite systems. A relatively new quantity, with its origin in the field of quantum information, has shown promise as a useful numerical parameter for characterizing QPTs; the quantum fidelity and quantum fidelity susceptibility.[3, 4, 5, 6] These

quantities have already been successfully employed towards the identification of QPTs in a number of systems,[7, 8, 9, 10, 11, 12, 13, 14, 15, 16, 17, 18, 19, 20, 21, 22, 23, 24, 25, 26, 27, 28, 29, 30] and an excellent review of this approach can be found in Ref. [31]. In this paper we will be concerned with attempts to slightly generalize the notion of the standard fidelity in order to construct new quantities that can aid in identifying phase transitions in small systems. Extensions of the basic fidelity concept are not new, with prior developments such as the operator fidelity susceptibility[32] and the reduced fidelity[33, 34, 35] having proved fruitful. Here we consider two additional variants that have been proposed: excited-state fidelities [36] and generalized fidelity susceptibilities [37, 38].

The typical quantum fidelity assumes that the Hamiltonian of a system with a QPT can be written in the form

$$H(\lambda) = H_0 + \lambda H_\lambda, \tag{1}$$

where the phase transition occurs at some critical value of the *driving parameter* λ (λ_c). From this perspective the second term is then seen as the *driving term* and it is entirely responsible for the phase transition. The quantum fidelity is then defined as the overlap or inner-product of the ground-state of a system with another ground-state determined by a Hamiltonian that is slightly perturbed in the driving parameter relative to the first:

$$F_0(\lambda, \delta\lambda) = \langle \Psi_0(\lambda) \, | \Psi_0(\lambda + \delta\lambda) \rangle \, , \tag{2}$$

where $\Psi_0(\lambda)$ is the ground-state of the Hamiltonian $H(\lambda)$. In a study by Chen *et al.*[36] of the $J_1 - J_2$ chain, a system we also consider here, it was shown that a fidelity based not on the ground-state but the first excited-state,

$$F_1(\lambda, \delta\lambda) = \langle \Psi_1(\lambda) \, | \Psi_1(\lambda + \delta\lambda) \rangle \, , \tag{3}$$

could be a potentially valuable quantity. Here we call such a fidelity an excited-state fidelity.

From the quantum fidelity one can calculate the quantum fidelity susceptibility, defined as

$$\chi_\lambda = \frac{2(1 - F_0(\lambda)}{\delta\lambda^2}. \tag{4}$$

However, in a previous study [37] it was shown that this definition could be extended by considering other types of perturbations beyond a perturbation in the driving parameter. Specifically, it is often useful to construct generalized fidelity susceptibilities associated with the order parameters of common orderings.[38]

Our goal here is to explore the phase-diagram of the anisotropic next-nearest-neighbor triangular lattice model (ANNTLHM). This model connects the $J_1 - J_2$ chain ($J' = 0$) with the anisotropic triangular lattice Heisenberg model (ATLHM) ($J_2 = 0$). The phase diagram of the ATLHM for $J' \ll 1$ and accordingly of the ANNTLHM for $J', J_2 \ll 1$ has proven exceedingly difficult to determine and it appears that several possible phases *very* closely compete.

The $J_1 - J_2$ chain has the Hamiltonian

$$H_{J_1-J_2} = \sum_{\mathbf{x}} \hat{S}_{\mathbf{x}} \cdot \hat{S}_{\mathbf{x+1}} + J_2 \sum_{\mathbf{x}} \hat{S}_{\mathbf{x}} \cdot \hat{S}_{\mathbf{x+2}} \tag{5}$$

where J_2 is understood to be the ratio ($J_2 = J_2'/J_1'$) of the next-nearest neighbour (J_2') and nearest-neighbour (J_1') interaction constants. It is a system which has been well studied; both through field theoretic approaches,[39, 40] and through numerical approaches like exact diagonalization,[41, 42] and DMRG.[43, 44] These studies have revealed the existence of a rich phase diagram for the $J_2 > 0$ region. For $J_2 < J_2^c \sim 0.241$[41] the system exhibits a disordered Luttinger liquid phase characterized by quasi-long-range order (i.e. algebraic decay of spin-spin correlations) and no excitation gap. At J_2^c an energy gap opens and for $J_2^c < J_2$ dimerization sets in and correlations become short-ranged. At the so called Majumdar-Ghosh (MG) point $J_2^{MG} = J/2$ the ground-state of the system is known exactly and with periodic boundary conditions it is exactly two-fold degenerate even for finite systems, a fact that is important for our study. Slightly away from the MG point the degeneracy is lifted for finite systems with an exponentially small separation between the odd and even combinations of the two possible dimerization patterns. The correlation length of the system reaches a minimum at the MG point.[45] The MG point can also be identified as a *disorder* point marking the onset of incommensurate correlations in real-space occuring for $J_2 > J_{MG}$. The incommensurate effects occuring for $J_2 > J_2^{MG}$ are short-ranged and the system remains dimerized for any finite $J_2 > J_2^c$. Of particular importance to us here is the Luttinger liquid-dimer transition at J_2^c, which is known to be in the BKT universality class and difficult to detect numerically, and the onset of incommensurate correlations at the MG point J_2^{MG}. As we shall show here it is possible to track these points into the $J' - J_2$ plane of the ANNTLHM.

The ATLHM (see Fig. 1) is described by the Hamiltonian

$$H_\Delta = \sum_{\mathbf{x},\mathbf{y}} \hat{S}_{\mathbf{x},\mathbf{y}} \hat{S}_{\mathbf{x}-1,\mathbf{y}} + J' \sum_{\mathbf{x},\mathbf{y}} \hat{S}_{\mathbf{x},\mathbf{y}} \cdot \left(\hat{S}_{\mathbf{x},\mathbf{y}+\mathbf{1}} + \hat{S}_{\mathbf{x}-1,\mathbf{y}+\mathbf{1}} \right), \tag{6}$$

where, like $H_{J_1-J_2}$, the coupling constant J' is taken to be the ratio of the two exchange constants corresponding to the two different exchange terms. The phase diagram of this system for $J' < 1$ has proven extremely hard to determine and many aspects are still undecided. Early interest in this system was fuelled by initial theoretical and numerical studies[46, 47, 48] which suggested the existence of a two-dimensional spin liquid phase for $J' \ll 1$. This was especially exciting since the ATLHM is believed to be an accurate description of a number of real experimental materials, such as: the organic salts $\kappa-(\text{BEDT-TTF})_2\text{Cu}_2(\text{CN})_3$ [49, 50, 51] and $\kappa-(\text{BEDT-TTF})_2\text{Cu}_2[\text{N}(\text{CN})_2]$;[51] and the inorganic salts Cs_2CuCl_4,[52, 53, 54, 55, 56] and Cs_2CuBr_4.[56, 57] However, later theoretical studies would suggest that experimental results on Cs_2CuCl_4 could be explained within the paradigm of a less exotic quasi-one-dimensional spin liquid.[58, 59] This too gave way to a number of recent renormalization group studies which suggest that the $J' \ll 1$ region is not a spin liquid at all but rather that next-nearest chain antiferromagnetic interactions and order-by-disorder give rise to a collinear antiferromagnetic (CAF) ordering.[60, 61] In prior work [62], we have studied this system through the use of twisted boundary conditions which alleviate some of the finite-size issues associated with incommensurate correlations. The application of twisted boundary conditions suggests the existence of incommensurate spiral

ordering for $J' \sim 1$ giving way, after a phase transition, to a new phase dominated by antiferromagnetism albeit with short-range incommensurate spiral correlations. In Ref. [62] a rough thermodynamic limit extrapolation suggested the new phase was gapless, though whether a true collinear antiferromagnetic ordering, as suggested by Balents *et al.*,[60] emerged could not be definitively determined.

Here we are concerned with the application of excited-state fidelity and generalized fidelity susceptibility techniques to the more general Hamiltonian (ANNTLHM) including a next-nearest neighbor coupling along the chains:

$$\begin{aligned} H(J', J_2) = & \sum_{\mathbf{x},\mathbf{y}} \hat{S}_{\mathbf{x},\mathbf{y}} \hat{S}_{\mathbf{x}-\mathbf{1},\mathbf{y}} \\ & + J' \sum_{\mathbf{x},\mathbf{y}} \hat{S}_{\mathbf{x},\mathbf{y}} \cdot \left(\hat{S}_{\mathbf{x},\mathbf{y}+\mathbf{1}} + \hat{S}_{\mathbf{x}-\mathbf{1},\mathbf{y}+\mathbf{1}} \right) \\ & + J_2 \sum_{\mathbf{x}} \hat{S}_{\mathbf{x}} \cdot \hat{S}_{\mathbf{x}-\mathbf{2}}. \end{aligned} \tag{7}$$

As J' and J_2 are varied the ANNTLHM interpolates between the $J_1 - J_2$ chain ($J' = 0$) and the ATLHM ($J_2 = 0$) through the creation of a $J' - J_2$ plane (see Fig. 1). To our knowledge such a general system has only been studied field theoretically[60, 61] and is believed to exhibit the CAF order discussed previously for small J' and J_2 before transiting to spiral ordering for large J', small J_2, and dimer ordering for large J_2, small J'. We will now more thoroughly introduce and define the excited-state fidelity and generalized fidelity susceptibilities.

2. Excited-State Fidelities

In the context of the quantum fidelity it is sometimes useful to consider a quantum phase transition as a result of a level crossing in the ground- or excited-states as a function of the driving parameter λ.[31] This is a perspective that has proven useful for the study of a class of one-dimensional models[63] and can be partly motivated by the consideration that quantum phase transitions are the result of sudden reconfigurations of the low-lying energy spectrum of a system.

Motivated by this viewpoint it was shown in Ref. [36] (see also Ref. [41]) that the BKT-type transition in the $J_1 - J_2$ can be detected, in finite-systems, by locating a level crossing in the *first* excited-states. Thus, the determination of the transition point at $J_2 \sim 0.24$ was possible by constructing a fidelity, F_1, not of the ground-state but of the first excited-state. Using this excited-state fidelity it was demonstrated [36] that an abrupt drop in F_1 as a result of the excited state level crossing occurs at the BKT transition point. Here, we use the same fidelity to follow the behaviour of this transition as it extends into the $J' - J_2$ plane. We note that, from a numerical perspective, it is considerably more convenient to monitor F_1 rather than the associated level crossing since the latter would require an intricate analysis of several of the low-lying states.

A careful analysis of Ref. [36], specifically Fig. 5 there-in, also indicates the presence of a *ground-state* level crossing at the Majumdar-Ghosh point[64] for finite-systems as mentioned

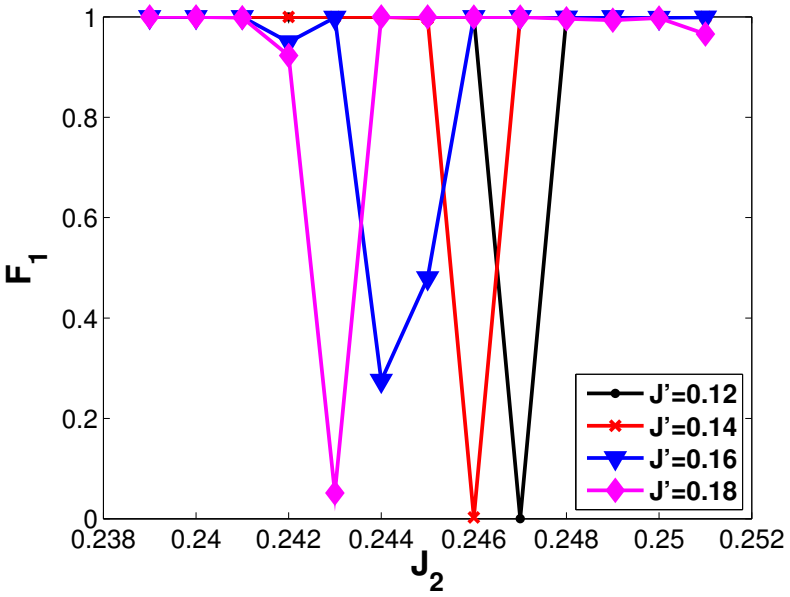

Figure 2. (Colour available on-line) The first excited-state fidelity vs. J_2 for values of J' of 0.12 (black circles), 0.14 (red crosses), 0.16 (bluetriangles) and 0.18 (magenta diamonds). The sharp downward spikes represent a level crossing in the excited state which was shown by Chen *et al.* to signify the BKT-type transition point of the $J_1 - J_2$ chain.[36]

above. This crossing, which occurs where it is known no actual phase transition occurs in the thermodynamic limit, could be detected by the ground-state fidelity (F_0) and coincides with the onset of short-range incommensurate correlations in real space even though no long-range spiral order develops. For a two-dimensional system such as the ATLHM it is known that spiral order occurs close to $J' = 1$ and it is also of considerable interest to see if it is possible to track this level crossing through the $J' - J_2$ plane and what bearing, if any, it has on the physics of the ANNTLHM.

To this end, the ground-state and first excited-state of the ANNTLHM were calculated for a 4×6 triangular lattice with periodic boundary conditions using a parallel, Lanczos, exact diagonalization code as outlined by Lin *et al.*[65] Total-S^z symmetry was invoked and numerical errors in ground-state eigenenergies are estimated to be on the order of 10^{-10}. Numerical errors in the first excited-state energies, as is a drawback of the Lanczos method, are considered to be higher by an order of magnitude. It is worth noting that when constructing the excited-state fidelity, and thus solving for the eigenvector of the first excited-state, the difficulty in the Lanczos method of ghost eigenvalue formation is exacerbated and special care must be taken to throw out erroneous results.

Once the ground-state and first excited-state eigenvectors were obtained numerically, F_0 and F_1 were constructed as a function of J_2. A typical tracking of the drop in F_1 is shown for various

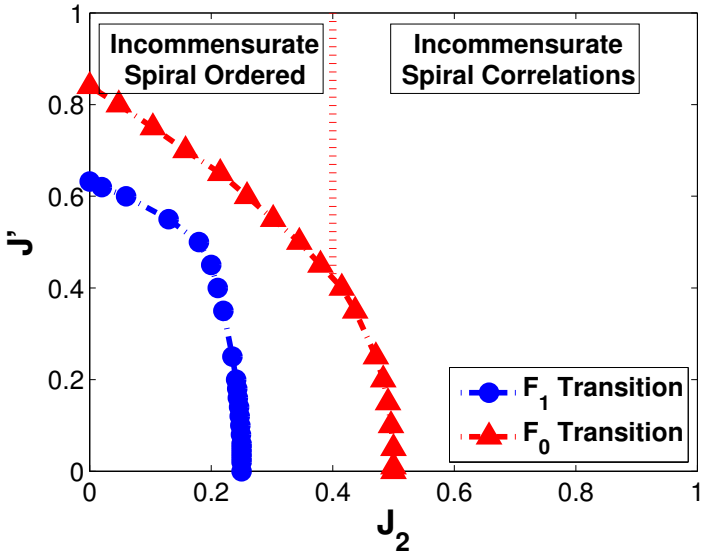

Figure 3. (Colour available on-line) The phase diagram of the $J' - J_2$ plane of the ANNTLHM with regards to the BKT-type transition of the $J_1 - J_2$ chain, identified by the excited-state fidelity F_1, in blue (circles) and the crossover associated with the onset of short-range incommensurate spiral correlations, identified by F_0, in red (triangles). All results are for a 4×6 system. The dotted red line represents a rough estimate, evidenced by the dimer fidelity susceptibility, of the region where long-range spiral order transitions to short-range incommensurate spiral correlations transition with possible dimer order. It is derived from the data in Fig. 9.

values of J' between 0.12 and 0.18 versus J_2 in Fig. 2. The path of the transition in F_0 is traced in a similar manner. As mentioned above, we calculate F_0, F_1 and therefore only gain indirect information about an assoicate level crossing. However, a further examination of the energy spectrum characteristics which produce the spike in F_0 reveals that it is either due to a ground-state level crossing which persists into the $J' - J_2$ plane or an extremely close avoided level crossing. The resulting phase diagram implied by this finite system is shown in Fig. 3. All results are obtained using a 4×6 system.

One can see that both transitions, when followed, persist well into the $J' - J_2$ plane and ultimately terminate along the $J_2 = 0$ line. This line corresponds to the ATLHM and it is therefore fruitful to consider their interpretation within the context of that system. However, a thorough consideration with respect to the nearest-neighbour triangular model will be left to section 4, after the introduction of the generalized fidelity susceptibilities. For now it is sufficient to realize that the level-crossing observed at the Majumdar-Ghosh point in the $J_1 - J_2$ chain ultimately connects with the parity transition observed in previous numerical investigations of the ATLHM.[46, 47] In Ref. [62] we studied the same system through the use of twisted boundary conditions, which allow a more natural treatment of incommensurate behaviour, and it was found that, although a transition does occur, this parity transition is an unphysical artefact of a finite-sized system

with periodic boundary conditions. The same conclusion was arrived at in the DMRG study of Weichselbaum and White.[2] However, it seems that both in the $J_1 - J_2$ chain (where it is known that incommensurate correlations arise past the disorder (MG) point) and in the ANNTLHM this transition may indicate the onset of incommensurate physics.

Using ground-state and excited-state fidelities we have thus demarcated a phase diagram in the $J' - J_2$ plane shown in Fig. 3. It is clear that the quantities F_0 and F_1 are useful tools for determining the phase diagram. However, equally important as the *location* of QPTs is the nature of the adjacent quantum phases. It is possible to extend the fidelity approach, through the introduction of generalized fidelity susceptibilities, to aid in the identification of the phase in each region that has been found so far. These susceptibilities will now be introduced.

3. Generalized Quantum Fidelity Susceptibilities

In the previous section we showed the simplicity with which quantum phase transitions driven by level crossings, either in the ground-state or low-lying excited-states, can be identified and traced with the quantum fidelity (when generalized to the overlap of excited-states). Once the location of QPTs within phase space have been charted often the next task, when encountering a system of interest, is the identification of the various phase regions. Ideally one would like to be able to associate an order parameter, local or not, with each demarcated phase (or none for a disordered phase).

It has been shown by Zanardi *et al.*[66] and Chen *et al.*[67], that there is a close connection between a fidelity susceptibility and the second derivative of the ground-state energy with respect to the "driving parameter" with which the fidelity susceptibility is constructed:

$$\begin{aligned} \chi &= \sum_n \frac{|\langle\Psi_n| H_I |\Psi_0\rangle|^2}{(E_0(\lambda) - E_n(\lambda))^2}, \\ \frac{\partial^2 E_0(\lambda)}{\partial\lambda^2} &= \sum_n \frac{2\,|\langle\Psi_n| H_I |\Psi_0\rangle|^2}{(E_0(\lambda) - E_n(\lambda))}. \end{aligned}$$

As can be seen, the fidelity susceptibility has a higher power in the denominator and is therefore expected to have a higher sensitivity. It is important to note that this relationship holds true even if the "driving" parameter and Hamiltonian (λ and H_λ) are not actually the terms that drive the phase transition. In Ref. [37], it was demonstrated that for the $J_1 - J_2$ chain the different phases can be identified through the use of an appropriately constructed generalized fidelity susceptibility.

When adopting this approach one begins by identifying all the potential phases that one suspects might exist within the phase diagram under study. The primary task is then to construct a fidelity susceptibility for each of these phases which has a similar connection to the order parameter susceptibility of that phase that the regular (i.e. λ *is* the driving parameter) fidelity susceptibility has with the ground-state derivatives. It is then expected that such a generalized fidelity susceptibility will exhibit the same behaviour as the order parameter susceptibility, going

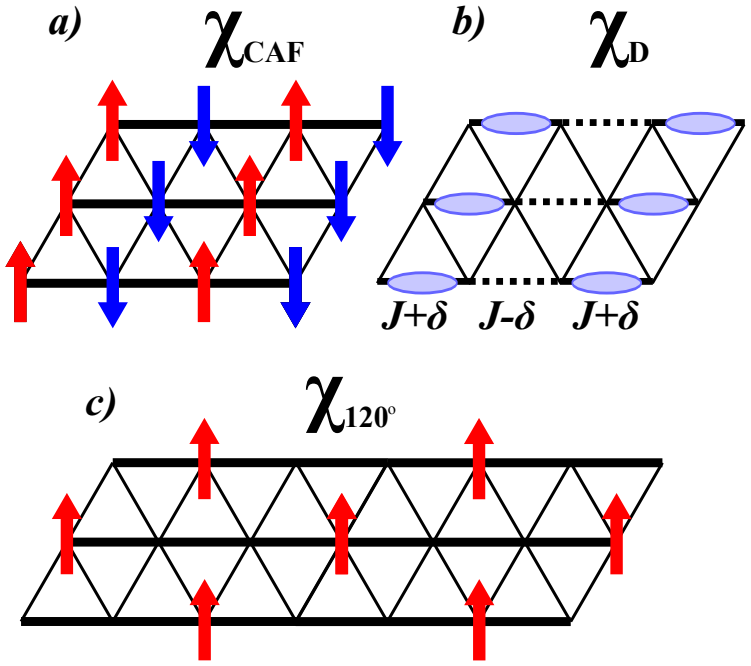

Figure 4. Diagrams of the perturbing term which define the generalized fidelity susceptibilities χ_{CAF}, χ_D and χ_{120°, respectively. χ_{CAF}, shown in a), is defined by a fidelity whose perturbed Hamiltonian is one with an infinitesimal staggered magnetic field in the S^z direction added according to the illustrated pattern. χ_D, shown in b), is defined by a perturbation in the intra-chain, nearest-neighbour, exchange interaction with alternating bonds having their exchange constant modified by a $\pm\delta$. χ_{120°, shown in c), is a rough probe of spiral order close to that known to exist at $J' = 1, J_2 = 0$ and corresponds to an upward magnetic field on every third site, corresponding to a spiral phase whose ordering has a wavelength of three sites. The omission of in-plane fields on the remaining sites is to maintain the conservation of total-S^z in the system Hamiltonian which improves numerics.

to infinity when in the associated phase and zero when outside it in the thermodynamic limit, but with increased sensitivity in finite systems.

As has been discussed, the $J_1 - J_2$ chain studied in Ref. [37] serves as a limiting case of the ANNTLHM as $J' \to 0$. Thus, all the fidelity susceptibilities constructed in Ref. [37] find use here, once generalized to two dimensions. To these susceptibilities (χ_ρ, χ_D, χ_{CAF}) have been added the new susceptibility χ_{120° which is designed to capture the incommensurate spiral phase of the $J' \sim 1$ region. We will now explicitly describe the construction of each of these susceptibilities.

3.1. The CAF Fidelity Susceptibility, χ_{CAF}

The collinear antiferromagnetic susceptibility is the natural two-dimensional extension of the antiferromagnetic fidelity susceptibility (χ_{AF}) introduced in Ref. [37]. It is constructed by choosing a perturbing Hamiltonian representing a staggered magnetic field which tiles the lattice (See

Fig. 4a):

$$\lambda H_{CAF} = \lambda \sum_{\mathbf{y}=0}^{W-1} \sum_{\mathbf{x}=0}^{L-1} (-1)^{\mathbf{x}} S^z_{\mathbf{x},\mathbf{y}}. \tag{8}$$

The generalized fidelity susceptibility associated with this perturbation is then

$$\chi_{CAF} = \frac{2(1 - F(\lambda, J', J_2))}{\lambda^2} \tag{9}$$

where $F(\lambda, J', J_2)$ is given by

$$F(\lambda, J', J_2) = |\langle \Psi_0(0, J', J_2)| \, \Psi_0(\lambda, J', J_2)\rangle| \, . \tag{10}$$

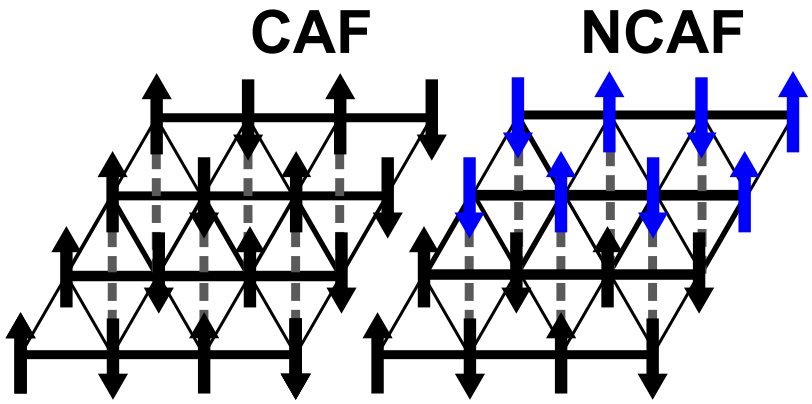

Figure 5. A diagram comparing the staggered magnetic field arrangement of collinear antiferromagnetic (CAF) vs. non-collinear antiferromagnetic (NCAF) orderings. The key difference is whether next-nearest-chain correlations are antiferromagnetic or ferromagnetic. Field theoretical calculations suggests that CAF correlations force an ordered state for $J' \ll 1$.[60] Generalized fidelity susceptibilities were constructed for both CAF and NCAF fields and χ_{CAF} was found to be greater than χ_{NCAF}, though only by a tiny, but meaningful, factor of 0.001%.

As already mentioned, previous studies[60, 61, 62] on the ANNTLHM have emphasized the important physical difference between antiferromagnetic tilings where next-nearest chain interactions are antiferromagnetic and ferromagnetic as indicated by the dashed lines in Fig. 5. In this work we denote the ferromagnetic case as NCAF (non-collinear antiferromagnetic) ordering and the antiferromagnetic as CAF. Thus, we see that the tiling presented in Fig. 4a is indeed χ_{CAF}. Later we will compare the value of this susceptibility with that for a susceptibility with NCAF ordering, χ_{NCAF}:

$$\lambda H_{NCAF} = \lambda \sum_{\mathbf{y}=0}^{W-1} \sum_{\mathbf{x}=0}^{L-1} (-1)^{\lfloor j/2 \rfloor} S^z_{\mathbf{x},\mathbf{y}} \tag{11}$$

where $\lfloor x \rfloor$ represents the *floor* (i.e. rounded down to the nearest integer) of x. Thus, the additional term switches the ordering every *two* chains and thus produces an NCAF tiling as shown in the right panel of Fig. 5.

The procedure for the calculation of χ_{CAF} then simply amounts to solving for the ground-state of the system when $\lambda = 0$ and again when λ is some small number. The inner product of the two resulting wave-functions then yields the fidelity. This fidelity is then converted to a susceptibility. We contend that this fidelity susceptibility will have the same properties as the order parameter susceptibility of a collinear-antiferromagnetic phase but with an increased sensitivity, making it more useful for the small system sizes available through ED.

3.2. The Dimer Fidelity Susceptibility, χ_D

The dimerized susceptibility presented in Ref. [37] is easily extended to two-dimensions. This susceptibility, dictated by the perturbing Hamiltonian

$$\delta H_D = \delta \sum_{\mathbf{y}=0}^{W-1} \sum_{\mathbf{x}=0}^{L-1} (-1)^{\mathbf{x}} S^z_{\mathbf{x},\mathbf{y}} S^z_{\mathbf{x}+\mathbf{1},\mathbf{y}}, \tag{12}$$

corresponds to a dimer tiling *along* chains (here we use δ rather than λ to emphasize the similarity to the classic dimerization operator). See Fig. 4. One could construct a similar susceptibility which assumes dimerization in the J' direction. However, such a tiling was found to be far less important, this could have been expected *a priori* since the energy benefit of such inter-chain singlet formation is less than that for intra-chain singlets. It is also worth noting that, in principle, one could have two different tilings *with* intra-chain singlets corresponding to a vertical (i.e. along $(0,1)$) and diagonal (i.e. along $(1,1)$) stacking. However, no numerical difference was found between these two possibilities.

As before, a quantum fidelity susceptibility, χ_D is constructed from the fidelity associated with this perturbing Hamiltonian and we take it to be related to the order parameter susceptibility of a dimerized phase.

3.3. The Spin Stiffness Fidelity Susceptibility, χ_ρ

The spin stiffness is defined as

$$\rho(L) = \left. \frac{\partial^2}{\partial \theta^2} \frac{E_0(\theta)}{L} \right|_{\theta=0} \tag{13}$$

where $E_0(\theta)$ is the ground-state energy as a function of a twist θ applied at every bond:

$$\begin{aligned} H_0 \quad &\to H_\rho \\ \mathbf{S}_i \cdot \mathbf{S}_j &\to S^z_i S^z_j + \frac{1}{2}\left(S^+_i S^-_j e^{i\theta} + S^-_i S^+_j e^{-i\theta} \right). \end{aligned} \tag{14}$$

It has proven to be a useful quantity in the exploration of quantum phase diagrams for it can be taken as a measure of the level of spin order exhibited by a phase. In a quasi-long-range ordered

system like the Heisenberg chain it is known to take a non-zero value in the thermodynamic limit.[68, 69] The same is true for a system with spin ordering. In a non-spin ordered system in the thermodynamic limit the spin stiffness is zero. The behaviour in finite systems can be less straightforward though it can be said that the sensitivity of a system with respect to an infinitesimal twist can provide valuable information as to the strength of spin-correlations and tendency to order, even in small systems. To benefit from the information stored in a quantity like the spin stiffness while maintaining the sensitivity gains afforded by a fidelity susceptibility we then construct a spin stiffness fidelity susceptibility, χ_ρ. Such a susceptibility is constructed, not by the usual addition of a perturbing conjugate field, but through the transformation Eq. (14) of the system Hamiltonian. One then calculates the overlap of the ground-state of the Hamiltonian with no twist and with an infinitesimal twist in order to construct the appropriate fidelity. Although this does not strictly follow the same form as the other fidelities one could expand the exponential in θ to obtain an $H = H^{(0)} + \theta H_\theta^{(1)} + \theta^2 H_\theta^{(2)}$ form. As is discussed in more detail in Ref. [37], one can then identify $H_\theta^{(1)}$ as a spin current operator and $H_\theta^{(2)}$ as a spin kinetic energy term (see also Ref. [38]). However, the numerical difference between the exponential and Taylor expanded forms was found to be negligible and thus in this paper we will merely treat things as an exponential.

We then take the fidelity susceptibility constructed from this spin stiffness fidelity to be a sensitive measure of spin ordering in a probed phase.

3.4. The 120 Degree Fidelity Susceptibility, χ_{120°

For the isotropic case of $J' = 1$ ($J_2 = 0$) the triangular lattice is known to exhibit a spiral phase with a wavevector of $2\pi/3$ or 120°.[70] As J' becomes less than 1 this spiral order persists, although with incommensurate wavevectors. However, associating a susceptibility with an incommensurate ordering is not feasible without knowledge of the q-vector beforehand. One could invoke estimates of these incommensurate ordering vectors obtained in both the prior studies [2, 62] and construct a separate fidelity susceptibility for each value of J'. However, here we employ a simpler, though likely less accurate, approach by defining a generalized fidelity susceptibility for the 120° ordering case only. In the limit of $J' \to 0$ the classical system will be antiferromagnetically ordered and thus we can expect, in this limit, that χ_{CAF} can correctly identify ordering here. We thus expect a transition from an ordering of wavelength three to an incommensurate ordering with approximate wavelength of two for small systems. Therefore, we can expect a generalized fidelity susceptibility associated with both these limits (i.e. χ_{120° and χ_{CAF}) to provide valuable information about the ordering across the $J_2 = 0$ phase diagram and outwards.

In order to construct χ_{120° an S^z magnetic field is placed on every third site along a chain (see Fig. 4c) while all other sites were left unaffected. The reason that no magnetic field is placed on the other sites is that the addition of magnetic fields in the $S^x - S^y$ plane would break total-S^z symmetry and significantly complicate numerics. Thus, χ_{120° is constructed in an almost identical fashion to χ_{CAF}, χ_{NCAF} except for the location of the perturbing magnetic fields.

3.5. Comparing Generalized Susceptibilities

The fidelity susceptibilities constructed here are the result of significantly different perturbations with different scaling and absolute magnitude i.e. χ_{CAF} and χ_{NCAF} see the addition of 24 perturbing fields for $N = 4 \times 6$ where as χ_{120° sees only the addition of 8. It is therefore sensible to compare χ_{CAF}, χ_{NCAF} with $3 \times \chi_{120^\circ}$. However, there is no obvious way to quantitatively compare these fidelity susceptibilites to χ_D and χ_ρ for a single system size. Instead a detailed finite-size scaling analysis of the different suceptibilities should be done. For the two-dimensional systems we are considering here it is not possible to perform such a finite-size scaling analysis using ED techniques. In fact, when plotting the susceptibilities arbitrary multiplicative coefficients will be added in front of χ_ρ ($\times 3$) and χ_{120° ($\times 30$) in order to produce graphs with all susceptibilities visible. It is therefore only qualitative comparisons that can be made between these new quantities. However, as we will see, this qualitative behaviour tends to be quite drastic and illuminating and thus provides valuable information about the phase diagram of any system under consideration.

4. Results and Discussion

4.1. The $J_1 - J_2$ Chain ($J' = 0$)

In order to interpret generalized fidelity susceptibility data in the $J' - J_2$ plane it is prudent to begin in the limit where things are well understood. In this system the $J' = 0$ case is such a limit for there the systems reduces to the well studied[42, 43, 44, 71] $J_1 - J_2$ chain. A plot of χ_ρ, χ_D, χ_{CAF} and χ_{120° ($\delta\lambda = 10^{-4}$) is shown in Fig. 6 for a 24 site $J_1 - J_2$ chain as a function of J_2. As such this data amounts to an extension of the data found in Ref. [37].

For $J_2 < 0.2411 = J_2^c$ the system is in the spin-liquid Heisenberg phase marked by quasi-long-range order (i.e. algebraic decay of correlation functions to zero with spin separation), a non-zero spin stiffness,[72, 73] and a gapless excitation spectrum. Beyond this phase the system is found to develop a gap for $J_2 > J_2^c$. At the Majumdar-Ghosh point, $J_2 = 1/2 = J_2^{MG}$, the system, in the thermodynamic limit, is a perfect superposition of two dimerized states and the ground-state is known.[64] The MG point is a disorder point and for $J_2 > J_2^{MG}$ incommensurate effects appear in the real-space correlations. The ability of generalized fidelities to identify and characterize the $J_2 < J_2^{MG}$ region and specifically the $J_2 = J_2^c$ BKT-type transition was established in Ref. [37] and thus that analysis will not be repeated here.

For $J_2 < J_2^c$ the dominant fidelity susceptibility is χ_{CAF}, associated with the antiferromagnetic correlations in the Luttinger phase. (For the $J_1 - J_2$ chain χ_{CAF} used here is identical to χ_{AF} discussed in Ref. [37]).

For $J_2 > J_2^c$, χ_{CAF} dramatically decreases while χ_D becomes dominant signalling the onset of dimer order. The distinctive behavior of χ_D for $J_2 > J_2^c$ is reminiscent of the behaviour of the dimer order parameter, whose numerically calculated value can be found in Fig. 5 in Ref. [71] and Fig. 8 in Ref. [44], albeit with increased sensitivity.

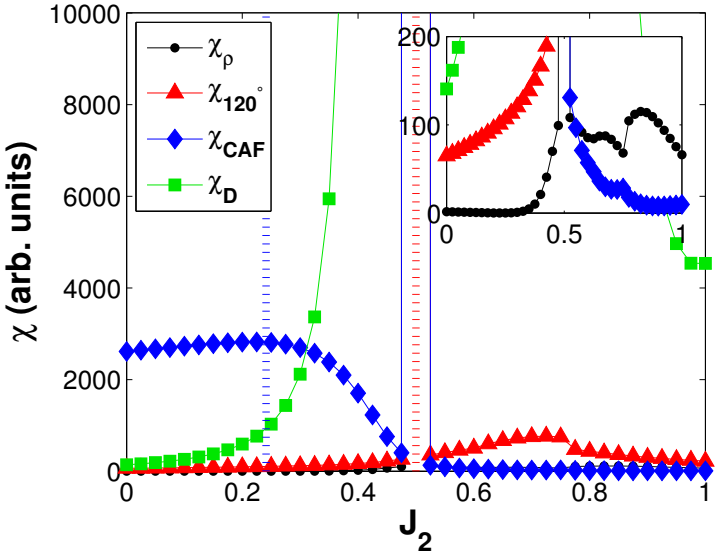

Figure 6. (Colour available on-line) The values of the generalized fidelity susceptibilities χ_ρ (black circles), χ_{120° (red triangles), χ_{CAF} (blue squares), χ_D (magenta diamonds) as a function of J_2 for $J' = 0$ (i.e. the $J_1 - J_2$ chain). All results are for a 24 site $J_1 - J_2$ chain. Also shown are the locations of the transition detected by the excited-state fidelity F_1 (dotted blue line) and the transition detected by the ground-state fidelity F_0 (dotted red line). χ_ρ has been scaled by a factor of three and χ_{120° has been scaled by a factor of thirty. All other susceptibilities have not been scaled. The inset shows the same data but with a different y-axis.

Looking at Fig. 6 it is also clear that there is an abrupt behavior at $J_2 = 1/2$. It is conspicuous in its; sudden spike and then decay of χ_D; sudden, discontinuous increase in χ_{120° and χ_ρ and; drop and spike of χ_{CAF}. Such behavior is to be expected due to the special 2-fold degenerate ground-state occurring *precisely* at the MG-point for a finite system. For the $J_1 - J_2$ chain this point is the one we previously identified using the fidelity F_0. χ_{120° was constructed as a rough probe of incommensurate or non-antiferromagnetic (i.e. $q \neq \pi$) ordering and for $J_2 > J_2^{MG}$ features develop in χ_{120° consistent with incommensurate (short-range) correlations. For $J_1 - J_2$ chain it is known that *short-range* incommensurate correlations emerge at $J_2 > J_2^{MG}$. It is remarkable that the generalized fidelity susceptibility has sufficient sensitivity to detect the onset of incommensurability effects beyond the Majumdar-Ghosh point. To summarize, for the $J_1 - J_2$ it is clear that χ_{CAF} and χ_D detect the quasi-AF and dimer order and at the same time the MG point is clearly identifiable with the onset of incommensurability effects.

It is noteworthy that, as was discussed earlier, the MG point of the $J_1 - J_2$ chain is connected, when tracked through the $J' - J_2$ plane, with the unphysical parity transition of the anisotropic nearest-neighbour triangular model. In particular since in the isotropic triangular limit ($J' = 1$, $J_2 = 0$) the system is known to exhibit 120° order and possess no excitation gap. We therefore now turn our attention to the $J_2 = 0$ anisotropic triangular lattice Heisenberg model.

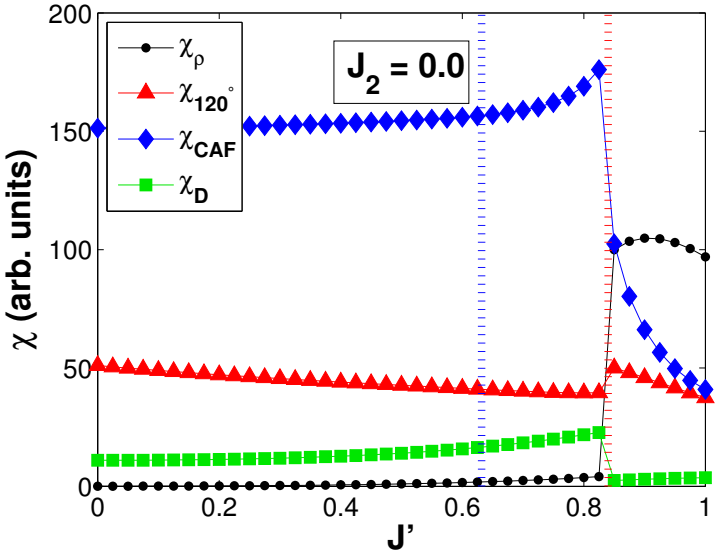

Figure 7. (Colour available on-line) Generalized fidelity susceptibilities as a function of J' for $J_2 = 0$ (i.e the ATLHM). All marker, line, colour and scaling conventions are the same as those in Fig. 6. Results are for a 4×6 system.

4.2. The ATHLM ($J_2 = 0$)

A plot of χ_ρ, χ_D, χ_{CAF} and χ_{120° ($\delta\lambda = 10^{-4}$) for $J_2 = 0$ for $J' < 1$ can be found in Fig. 7. It is immediately apparent there is again a transition, corresponding to the downward spike in F_0 identified earlier, at $J' = 0.840 = J'_c$ and that for $J' < J'_c$, χ_{CAF} and χ_{120° behave in a qualitatively identical manner to the Luttinger phase of the $J_1 - J_2$ chain. On the other hand, χ_D has no spike and simply drops after the transition and although χ_ρ jumps abruptly to a higher value at J'_c, it does not have a minimum anywhere in the $J' < 1$ region.

In Ref. [62] it was shown that the effect of twisted boundary conditions, which allow for incommensurate correlations to exist even in small finite systems, was to change the nature of this J'_c transition from a parity transition to a first-order jump in the ground-state ordering. This jump occurred at a lower J' of 0.765 for $N = 4 \times 6$ and it was observed that incommensurate (short-range) spiral correlations persisted below this new transition though the dominant interaction and ground-state ordering was consistent with antiferromagnetism. From the perspective of quantum fidelity susceptibilities used here it is clear that collinear antiferromagentic correlations are very important below the transition point, $J' < J'_c$. However, from the quantum fidelity susceptibilities alone we cannot rule out the existence of a disordered state similar in character to that found in the $J_1 - J_2$ chain for $J_2 < J_2^c$. We now turn to our results for the generalized quantum fidelity susceptibilities in the rest of the $J' - J_2$ plane (i.e. $J' \neq 0$, $J_2 \neq 0$) for the ANNTLHM.

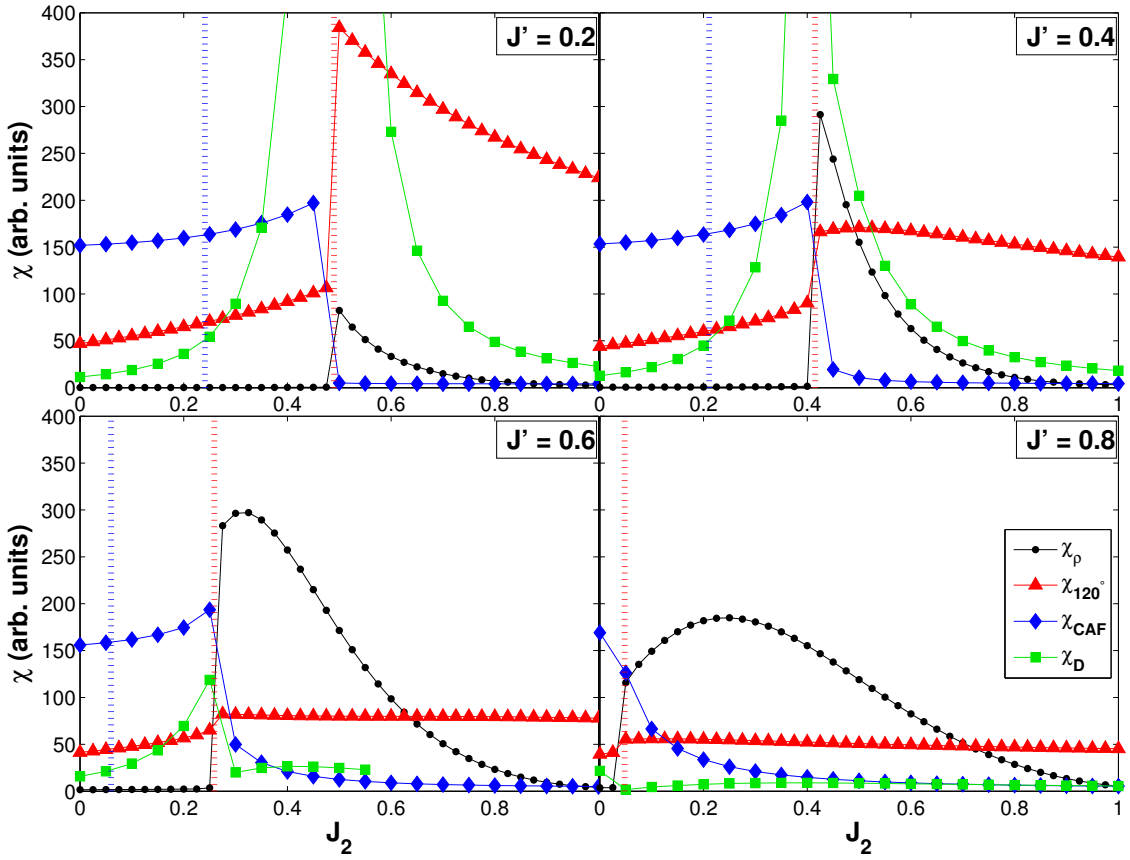

Figure 8. Generalized fidelity susceptibilities as a function of J_2 for values of $J' = 0.2$, 0.4, 0.6 and 0.8 (i.e. cross-sections of the $J' - J_2$ plane). All marker, line, colour and scaling conventions are the same as those in Fig. 6. Results are for a 4×6 system.

4.3. The ANNTLHM ($J_2 = 0$)

The same data gathered for the $J_1 - J_2$ chain in Fig. 6 is shown in Fig. 8 for the cases of $J' = 0.2$, 0.4, 0.6 and 0.8. These plots then serve to divide the $J' - J_2$ plane into cross-sections in J'. Again, the point identified by F_0 is clearly visible. Of note in these plots is the consistent behaviour of χ_ρ, χ_{120° and χ_{CAF} as J' increases lending evidence to the notion that the $J' < J'_c$ phase is directly related to the $J_2 < J_2^c$ phase. The one marked difference is in the behaviour of χ_D whose peaked nature becomes substantially less pronounced as J' grows. This is indicative of a necessary (since they have different symmetries) transition from dimer to spiral order. Unfortunately, there does not seem to be sudden features in χ_D vs. J_2 to identify this region. A plot of χ_D vs. J' for J_2s of 0.3 to 0.45 shown in Fig. 9 does suggest a qualitative change in the way χ_D diverges

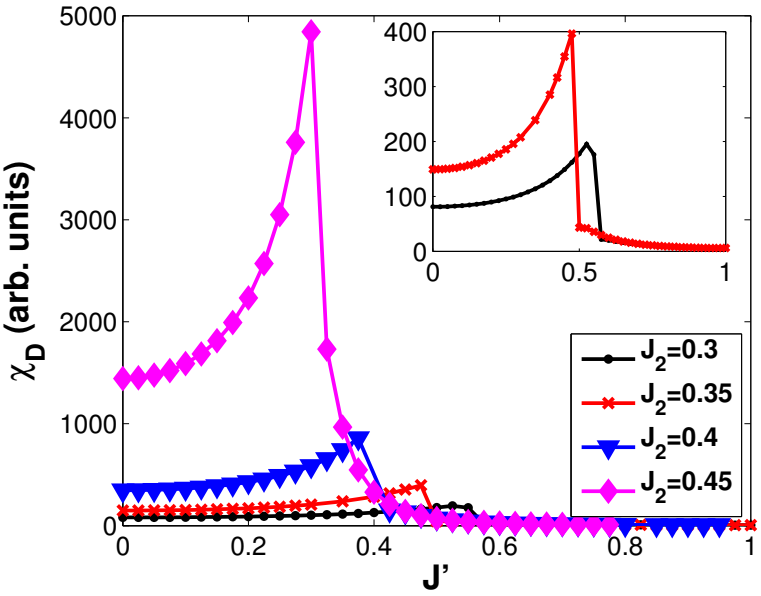

Figure 9. χ_D as a function of J' for $J_2 = 0.3$ (black circles), 0.35 (red crosses), 0.4 (blue triangles) and 0.45 (magneta diamonds). The inset shows the same data for only $J_2 = 0.35$ and 0.3. A qualitative change in the nature of χ_D can be seen at $J_2 \sim 0.4$. For $J_2 > 0.4$ the peak in χ_D is significantly more pronouced. This could suggest a transition from gapped dimer order with incommensurate short-ranged spiral correlations to the true incommensurate spiral order that exists at $J' = 1, J_2 = 0$.

at a J_2 of approximately 0.4. For $J_2 > 0.4$ the peak is much more pronouced than for $J_2 < 0.4$. This could suggest a transition from gapped dimer order with incommensurate short-ranged spiral correlations to the true incommensurate spiral order. In Fig. 3 this is indicated as the dotted red line.

As already stressed, the central observation to make from the results presented in Fig. 8 for $J', J_2 \ll 1$ is the similarity with the results in Fig. 6 for $J_2 < J_2^c$. The presence of a non-zero J' thus only changes the ordering in a very subtle way and possibly not at all.

4.4. Non-collinear Versus Collinear Order (χ_{NCAF} vs. χ_{CAF})

A final issue of interest is the competition between non-collinear and collinear antiferromagnetic correlations in the anisotropic nearest-neighbour triangular lattice. Renormalization group studies[60, 61] of the triangular system suggest that the $J' \ll 1$ phase is ordered antiferromagnetically and that crucial to this ordering is the emergence of antiferromagnetic correlations between *next-nearest chains*. In Ref. [62] it was found that, although next-nearest chain interactions were indeed of great importance within that phase, there is intense competition between collinear (CAF) and non-collinear (NCAF) ordering and that CAF is indeed the dominant

correlation, but only by an extremely small margin. To re-investigate this claim a separate generalized fidelity, χ_{NCAF}, was constructed such that next-nearest chains have ferromagnetic interactions and the two (χ_{CAF} and χ_{NCAF}) were computed for $J_2 = 0$, $J' < 1$. The field defining χ_{NCAF} is shown in Fig. 4. As was the case in Ref. [62] the difference between the two is found to be extremely small but χ_{CAF} is larger by a factor of approximately 0.001%. This minuscule discrepancy, though well within the realm of numerical precision, suggests that the competition between these two types of antiferromagnetic correlations is extremely fierce with a very small advantage to the CAF ordering.

5. Conclusion

In this paper the ground-state and excited-state quantum fidelities were used to track the behaviour of the MG/Lifshitz point and BKT-type transition, found in the $J_1 - J_2$ ($J' = 0$) chain, into the $J' - J_2$ plane. It was found that both points trace bounded regions within $J' - J_2$ plane and ultimately terminate on the J' axis ($J_2 = 0$) corresponding to the anisotropic triangular Heisenberg model. Specifically, the MG point, which occurs as a ground-state level crossing in the $J_1 - J_2$ chain which is known to not survive in the thermodynamic limit, is connected to the unphysical parity transition observed in the $J' < 1$ region of the anisotropic triangular model. However, the region defined by the behavior of F_1 connecting the BKT transition of the $J_1 - J_2$ chain ($J' = 0$) with a point on the J' axis is strongly suggestive of a new distinct phase.

In order to further explore and identify these phase regions, the generalized fidelity susceptibilities χ_ρ, χ_{120°, χ_D and χ_{CAF} were constructed. They are associated with the spin stiffness, 120° spiral phase order parameter, dimer order parameter and collinear antiferromagnetic order parameter respectively. These quantities are believed to be very sensitive and therefore well suited for finite system studies.

When plotting these quantum fidelity susceptibilities within the $J' - J_2$ plane the region defined by F_0 is readily identifiable while the F_1 region is much more subtle. In the $J', J_2 \ll 1$ region the χ_{CAF} is marginally favored over χ_{NCAF} but it is not possible to conclusively eliminate the possibility of a disordered phase. Furthermore, the region above this phase (i.e. $J_2 > J_2^c$, $J' > J_c'$) is spiral ordered within a $N = 4 \times 6$ system. This is known to be the case in the thermodynamic limit for the anisotropic nearest-neighbour triangular model but for the $J_1 - J_2$ chain this is known to be false and for J_2 beyond the MG point incommensurate correlations are only short-ranged for the $J_1 - J_2$ chain. For J_2 greater than approximately 0.4 dimer correlations appear dominant. A possible way to distinguish these two phases would be through a study of larger system sizes (like those done by Weichselbaum and White in Ref. [2]) to track the closure of the energy-gap in the incommensurate phase of the $J_1 - J_2$ chain as that phase connects with the spiral-ordered phase of the triangular lattice through the $J' - J_2$ plane.

An additional aspect not explored in this paper, due to the lack of available system sizes, is the scaling behaviour of these generalized fidelity susceptibilities throughout the $J' - J_2$ plane.

Such a study, potentially viable through DMRG of a finite-cluster, would be very valuable and further solidify the understanding of this phase diagram.

The authors would like to thank Sung-Sik Lee, Catherine Kallin and Sedigh Ghamari for many fruitful discussions. We also acknowledge computing time at the Shared Hierarchical Academic Research Computing Network (SHARCNET:www.sharcnet.ca) and research support from NSERC.

References

[1] S. Sachdev. *Quantum Phase Transitions*. Cambridge University Press, 2011.

[2] Andreas Weichselbaum and Steven R. White. Incommensurate correlations in the anisotropic triangular heisenberg lattice. *Phys. Rev. B*, 84:245130, Dec 2011.

[3] H. T. Quan, Z. Song, X. F. Liu, P. Zanardi, and C. P. Sun. Decay of loschmidt echo enhanced by quantum criticality. *Phys. Rev. Lett.*, 96:140604, Apr 2006.

[4] Paolo Zanardi and Nikola Paunković. Ground state overlap and quantum phase transitions. *Phys. Rev. E*, 74:031123, Sep 2006.

[5] Huan-Qiang Zhou and John Paul Barjaktarevi. Fidelity and quantum phase transitions. *Journal of Physics A: Mathematical and Theoretical*, 41(41):412001, 2008.

[6] Wen-Long You, Ying-Wai Li, and Shi-Jian Gu. Fidelity, dynamic structure factor, and susceptibility in critical phenomena. *Phys. Rev. E*, 76:022101, Aug 2007.

[7] Paolo Zanardi, Marco Cozzini, and Paolo Giorda. Ground state fidelity and quantum phase transitions in free fermi systems. *Journal of Statistical Mechanics: Theory and Experiment*, 2007(02):L02002, 2007.

[8] Marco Cozzini, Paolo Giorda, and Paolo Zanardi. Quantum phase transitions and quantum fidelity in free fermion graphs. *Phys. Rev. B*, 75:014439, Jan 2007.

[9] Marco Cozzini, Radu Ionicioiu, and Paolo Zanardi. Quantum fidelity and quantum phase transitions in matrix product states. *Phys. Rev. B*, 76:104420, Sep 2007.

[10] P. Buonsante and A. Vezzani. Ground-state fidelity and bipartite entanglement in the bose-hubbard model. *Phys. Rev. Lett.*, 98:110601, Mar 2007.

[11] L. Campos Venuti, M. Cozzini, P. Buonsante, F. Massel, N. Bray-Ali, and P. Zanardi. Fidelity approach to the hubbard model. *Phys. Rev. B*, 78:115410, Sep 2008.

[12] David Schwandt, Fabien Alet, and Sylvain Capponi. Quantum monte carlo simulations of fidelity at magnetic quantum phase transitions. *Phys. Rev. Lett.*, 103:170501, Oct 2009.

[13] A Fabricio Albuquerque, Fabien Alet, Clement Sire, and Sylvain Capponi. Quantum critical scaling of fidelity susceptibility. *Physical Review B*, 81(6):064418, 2010.

[14] W. W. Cheng and J.-M. Liu. Fidelity susceptibility approach to quantum phase transitions in the xy spin chain with multisite interactions. *Phys. Rev. A*, 82:012308, Jul 2010.

[15] Manisha Thakurathi, Diptiman Sen, and Amit Dutta. Fidelity susceptibility of one-dimensional models with twisted boundary conditions. *Phys. Rev. B*, 86:245424, Dec 2012.

[16] Bogdan Damski. Fidelity susceptibility of the quantum ising model in a transverse field: The exact solution. *Phys. Rev. E*, 87:052131, May 2013.

[17] Yoshihiro Nishiyama. Criticalities of the transverse- and longitudinal-field fidelity susceptibilities for the $d = 2$ quantum ising model. *Phys. Rev. E*, 88:012129, Jul 2013.

[18] Wen-Long You and Yu-Li Dong. Fidelity susceptibility in two-dimensional spin-orbit models. *Phys. Rev. B*, 84:174426, Nov 2011.

[19] Victor Mukherjee and Amit Dutta. Fidelity susceptibility and general quench near an anisotropic quantum critical point. *Phys. Rev. B*, 83:214302, Jun 2011.

[20] Bo Wang, Mang Feng, and Ze-Qian Chen. Berezinskii-kosterlitz-thouless transition uncovered by the fidelity susceptibility in the xxz model. *Phys. Rev. A*, 81:064301, Jun 2010.

[21] Wing-Chi Yu, Ho-Man Kwok, Junpeng Cao, and Shi-Jian Gu. Fidelity susceptibility in the two-dimensional transverse-field ising and xxz models. *Phys. Rev. E*, 80:021108, Aug 2009.

[22] Shi-Jian Gu, Ho-Man Kwok, Wen-Qiang Ning, and Hai-Qing Lin. Fidelity susceptibility, scaling, and universality in quantum critical phenomena. *Phys. Rev. B*, 77:245109, Jun 2008.

[23] Ke-Wei Sun and Qing-Hu Chen. Quantum phase transition of the one-dimensional transverse-field compass model. *Phys. Rev. B*, 80:174417, Nov 2009.

[24] Bo Li, Sheng-Hao Li, and Huan-Qiang Zhou. Quantum phase transitions in a two-dimensional quantum xyx model: Ground-state fidelity and entanglement. *Phys. Rev. E*, 79:060101, Jun 2009.

[25] Amit Tribedi and Indrani Bose. Entanglement and fidelity signatures of quantum phase transitions in spin liquid models. *Phys. Rev. A*, 77:032307, Mar 2008.

[26] N. Tobias Jacobson, Silvano Garnerone, Stephan Haas, and Paolo Zanardi. Scaling of the fidelity susceptibility in a disordered quantum spin chain. *Phys. Rev. B*, 79:184427, May 2009.

[27] Yan-Chao Li and Shu-Shen Li. Quantum critical phenomena in the xy spin chain with the dzyaloshinski-moriya interaction. *Phys. Rev. A*, 79:032338, Mar 2009.

[28] Yoshihiro Nishiyama. Critical behavior of the fidelity susceptibility for the transverse-field ising model. *Physica A: Statistical Mechanics and its Applications*, 392(19):4345 – 4350, 2013.

[29] Silvano Garnerone, Damian Abasto, Stephan Haas, and Paolo Zanardi. Fidelity in topological quantum phases of matter. *Phys. Rev. A*, 79:032302, Mar 2009.

[30] Min-Fong Yang. Ground-state fidelity in one-dimensional gapless models. *Phys. Rev. B*, 76:180403, Nov 2007.

[31] S.-J. Gu. Fidelity approach to quantum phase transitions. *International Journal of Modern Physics B*, 24(23):4371, 2010.

[32] Xiaoguang Wang, Zhe Sun, and Z. D. Wang. Operator fidelity susceptibility: An indicator of quantum criticality. *Phys. Rev. A*, 79:012105, Jan 2009.

[33] Marko Znidaric and Tomazc Prosen. Fidelity and purity decay in weakly coupled composite systems. *Journal of Physics A: Mathematical and General*, 36(10):2463, 2003.

[34] H.-Q. Zhou. Renormalization group flows and quantum phase transitions: fidelity versus entanglement. *ArXiv e-prints*, April 2007.

[35] Erik Eriksson and Henrik Johannesson. Reduced fidelity in topological quantum phase transitions. *Phys. Rev. A*, 79:060301, Jun 2009.

[36] Shu Chen, Li Wang, Shi-Jian Gu, and Yupeng Wang. Fidelity and quantum phase transition for the heisenberg chain with next-nearest-neighbor interaction. *Phys. Rev. E*, 76:061108, Dec 2007.

[37] Mischa Thesberg and Erik S. Sørensen. General quantum fidelity susceptibilities for the J_1J_2 chain. *Phys. Rev. B*, 84:224435, Dec 2011.

[38] S. Greschner, A. K. Kolezhuk, and T. Vekua. Fidelity susceptibility and conductivity of the current in one-dimensional lattice models with open or periodic boundary conditions. *Phys. Rev. B*, 88:195101, Nov 2013.

[39] F. D. M. Haldane. Spontaneous dimerization in the s=12 heisenberg antiferromagnetic chain with competing interactions. *Phys. Rev. B*, 25:4925–4928, Apr 1982.

[40] Sebastian Eggert and Ian Affleck. Magnetic impurities in half-integer-spin heisenberg antiferromagnetic chains. *Phys. Rev. B*, 46:10866–10883, Nov 1992.

[41] Sebastian Eggert. Numerical evidence for multiplicative logarithmic corrections from marginal operators. *Phys. Rev. B*, 54(14):R9612–R9615, Oct 1996.

[42] T. Tonegawa and I. Harada. Spontaneous dimerization in the $s = 1/2$ heisenberg antiferromagnetic chain with competing interactions. *J. Phys. Soc. Jpn.*, 56:2153, 1987.

[43] R. Chitra, Swapan Pati, H. R. Krishnamurthy, Diptiman Sen, and S. Ramasesha. Density-matrix renormalization-group studies of the spin-1/2 heisenberg system with dimerization and frustration. *Phys. Rev. B*, 52:6581–6587, Sep 1995.

[44] Steven R. White and Ian Affleck. Dimerization and incommensurate spiral spin correlations in the zigzag spin chain: Analogies to the kondo lattice. *Phys. Rev. B*, 54:9862–9869, Oct 1996.

[45] Andreas Deschner and Erik S. Sørensen. Incommensurability effects in odd length j1-j2 quantum spin chains: On-site magnetization and entanglement. *Phys. Rev. B*, 87:094415, Mar 2013.

[46] M. Q. Weng, D. N. Sheng, Z. Y. Weng, and Robert J. Bursill. Spin-liquid phase in an anisotropic triangular-lattice heisenberg model: Exact diagonalization and density-matrix renormalization group calculations. *Phys. Rev. B*, 74:012407, Jul 2006.

[47] Dariush Heidarian, Sandro Sorella, and Federico Becca. Spin-1/2 heisenberg model on the anisotropic triangular lattice: From magnetism to a one-dimensional spin liquid. *Phys. Rev. B*, 80:012404, Jul 2009.

[48] J Merino, Ross H McKenzie, J B Marston, and C H Chung. The heisenberg antiferromagnet on an anisotropic triangular lattice: linear spin-wave theory. *Journal of Physics: Condensed Matter*, 11(14):2965, 1999.

[49] Y. Shimizu, K. Miyagawa, K. Kanoda, M. Maesato, and G. Saito. Spin liquid state in an organic mott insulator with a triangular lattice. *Phys. Rev. Lett.*, 91:107001, Sep 2003.

[50] Yang Qi, Cenke Xu, and Subir Sachdev. Dynamics and transport of the Z_2 spin liquid: Application to $\kappa-(ET)_2cu_2(CN)_3$. *Phys. Rev. Lett.*, 102:176401, Apr 2009.

[51] Hem C. Kandpal, Ingo Opahle, Yu-Zhong Zhang, Harald O. Jeschke, and Roser Valentí. Revision of model parameters for κ-type charge transfer salts: An *Ab Initio* study. *Phys. Rev. Lett.*, 103:067004, Aug 2009.

[52] R. Coldea, D. A. Tennant, A. M. Tsvelik, and Z. Tylczynski. Experimental realization of a 2d fractional quantum spin liquid. *Phys. Rev. Lett.*, 86:1335–1338, Feb 2001.

[53] Oleg A. Starykh, Hosho Katsura, and Leon Balents. Extreme sensitivity of a frustrated quantum magnet: cs_2Cucl_4. *Phys. Rev. B*, 82:014421, Jul 2010.

[54] R. Coldea, D. A. Tennant, R. A. Cowley, D. F. McMorrow, B. Dorner, and Z. Tylczynski. Quasi-1d $s = 1/2$ antiferromagnet cs_2cucl_4 in a magnetic field. *Phys. Rev. Lett.*, 79:151–154, Jul 1997.

[55] R. Coldea, D. A. Tennant, K. Habicht, P. Smeibidl, C. Wolters, and Z. Tylczynski. Direct measurement of the spin hamiltonian and observation of condensation of magnons in the 2d frustrated quantum magnet cs_2cucl_4. *Phys. Rev. Lett.*, 88:137203, Mar 2002.

[56] Weihong Zheng, Rajiv R. P. Singh, Ross H. McKenzie, and Radu Coldea. Temperature dependence of the magnetic susceptibility for triangular-lattice antiferromagnets with spatially anisotropic exchange constants. *Phys. Rev. B*, 71:134422, Apr 2005.

[57] Hidekazu Tanaka, Toshio Ono, Hiroko Aruga Katori, Hiroyuki Mitamura, Fumihiro Ishikawa, and Tsuneaki Goto. Magnetic phase transition and magnetization plateau in cs2cubr4. *Progress of Theoretical Physics Supplement*, 145:101–106, 2002.

[58] M. Kohno, L. Balents, and O.A. Starykh. Dynamical properties of spatially anisotropic frustrated Heisenberg models in a magnetic field. *Journal of Physics: Conference Series*, 145(1):012062, 2009.

[59] Leon Balents. Spin liquids in frustrated magnets. *Nature*, 464:199, Mar 2010.

[60] Oleg A. Starykh and Leon Balents. Ordering in spatially anisotropic triangular antiferromagnets. *Phys. Rev. Lett.*, 98:077205, Feb 2007.

[61] Sedigh Ghamari, Catherine Kallin, Sung-Sik Lee, and Erik S. Sørensen. Order in a spatially anisotropic triangular antiferromagnet. *Phys. Rev. B*, 84:174415, Nov 2011.

[62] M. Thesberg and E. S. Sorensen. An Exact Diagonalization Study of the Anisotropic Triangular Lattice Heisenberg Model Using Twisted Boundary Conditions. *ArXiv e-prints*, June 2014.

[63] Guang-Shan Tian and Hai-Qing Lin. Excited-state level crossing and quantum phase transition in one-dimensional correlated fermion models. *Phys. Rev. B*, 67:245105, Jun 2003.

[64] C K Majumdar. Antiferromagnetic model with known ground state. *Journal of Physics C: Solid State Physics*, 3(4):911, 1970.

[65] H. Q. Lin. Exact diagonalization of quantum-spin models. *Phys. Rev. B*, 42:6561–6567, Oct 1990.

[66] Paolo Zanardi, Paolo Giorda, and Marco Cozzini. Information-theoretic differential geometry of quantum phase transitions. *Phys. Rev. Lett.*, 99:100603, Sep 2007.

[67] Shu Chen, Li Wang, Yajiang Hao, and Yupeng Wang. Intrinsic relation between ground-state fidelity and the characterization of a quantum phase transition. *Phys. Rev. A*, 77:032111, Mar 2008.

[68] B. Sriram Shastry and Bill Sutherland. Twisted boundary conditions and effective mass in heisenberg-ising and hubbard rings. *Phys. Rev. Lett.*, 65:243–246, Jul 1990.

[69] Bill Sutherland and B. Sriram Shastry. Adiabatic transport properties of an exactly soluble one-dimensional quantum many-body problem. *Phys. Rev. Lett.*, 65:1833–1837, Oct 1990.

[70] Zheng Weihong, Ross H. McKenzie, and Rajiv R. P. Singh. Phase diagram for a class of spin-1/2 heisenberg models interpolating between the square-lattice, the triangular-lattice, and the linear-chain limits. *Phys. Rev. B*, 59:14367–14375, Jun 1999.

[71] R Bursill, G A Gehring, D J J Farnell, J B Parkinson, Tao Xiang, and Chen Zeng. Numerical and approximate analytical results for the frustrated spin- 1/2 quantum spin chain. *Journal of Physics: Condensed Matter*, 7(45):8605, 1995.

[72] J. Bonča, J. P. Rodriguez, J. Ferrer, and K. S. Bedell. Direct calculation of spin stiffness for spin-1/2 heisenberg models. *Phys. Rev. B*, 50:3415–3418, Aug 1994.

[73] N. Laflorencie, S. Capponi, and Erik S. Sørensen. Finite size scaling of the spin stiffness of the antiferromagnetic s =1/2 xxz chain. *The European Physical Journal B - Condensed Matter and Complex Systems*, 24(1):77–84, 2001.

5.3 An Exact Diagonalization Study of the Anisotropic Triangular Lattice Heisenberg Model Using Twisted Boundary Conditions

Mischa Thesberg and Erik S. Sørensen
An Exact Diagonalization Study of the Anisotropic Triangular Lattice Heisenberg Model Using Twisted Boundary Conditions
arXiv:1406.4083
Submitted and recommended for publication in Physical Review B (submitted: June 19th, 2014)

Calculations: All calculations, with the exception of the expository $J_1 - J_2$ chain calculations, were performed by the author using a code written entirely by the author. The demonstrative data on the $J_1 - J_2$ chain was performed by Erik S. Sørensen.

Manuscript: The bulk of the text was written by the author with the exception of the portion of the introductory text relating to the $J_1 - J_2$ chain. The excepted sections were written by Erik S. Sørensen who also provided small miscellaneous corrections and changes throughout.

In the previous paper the ANNTLHM model was explored using generalized fidelity susceptibilities and higher-order fidelities. However, it is clear that the phase diagram of that model is dominated by incommensurate physics whose wavelength is much larger than the system sizes accessible through exact diagonalization. It is then prudent to consider if there are methods which can mitigate these difficulties to some extent.

In the third and final paper of this thesis the same $J_2 \to 0$ limit of the ANNTLHM model will be explored using twisted boundary conditions. Twisted boundary conditions effectively diminish the energy penalty to incommensurate correlations in finite systems by allowing such correlations to exist through a twist in the boundary. We consider the case of a twist in both the intrachain and interchain direction and find the values of the boundary twist which minimizes the ground-state energy. From this we can then infer the q-vector of the present incommensurate physics.

This final paper attempts to further explore the incommensurate physics of the anisotropic triangular model and the primary questions asked there-in can be said to be:

- Does the use of twisted boundary conditions successfully allow for incommensurate physics as intended?

- How does the resulting physics compare to what else has been published?
- Can we extend previously results, derived from much larger systems, using exact diagonalization?
- What is the phase diagram of the ANNTLM model?

We now present the paper.

The Third Paper: An Exact Diagonalization Study of the Anisotropic Triangular Lattice Heisenberg Model Using Twisted Boundary Conditions

An Exact Diagonalization Study of the Anisotropic Triangular Lattice Heisenberg Model Using Twisted Boundary Conditions

Mischa Thesberg[1,*] and Erik S. Sørensen[1,†]

[1] *Department of Physics & Astronomy, McMaster University*
1280 Main St. W., Hamilton ON L8S 4M1, Canada.

(Dated: July 9, 2014)

The anisotropic triangular model, which is believed to describe the materials Cs_2CuCl_4 and Cs_2CuBr_4, among others, is dominated by incommensurate spiral physics and is thus extremely resistant to numerical analysis on small system sizes. In this paper we use twisted boundary conditions and exact diagonalization techniques to study the phase diagram of this model. With these boundary conditions we are able to extract the inter- and intrachain ordering q-vectors for the $\frac{J'}{J} < 1$ region finding very close agreement with recent DMRG results on much larger systems. Our results suggest a phase transition between a long-range incommensurate spiral ordered phase, and a more subtle phase with short-range spiral correlations with the q-vector describing the incommensurate correlations varying smoothly through the transition. In the latter phase correlations between next-nearest chains exhibits an *extremely* close competition between predominantly antiferromagnetic and ferromagnetic correlations. Further analysis suggests that the antiferromagnetic next-nearest chain correlations may be slightly stronger than the ferromagnetic ones. This difference is found to be slight but in line with previous renormalization group predictions of a collinear antiferromagnetic ordering in this region.

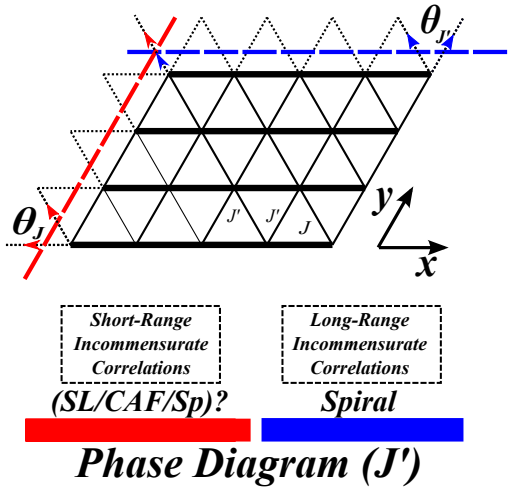

FIG. 1. The anisotropic triangular lattice showing a typical ED cluster. The boundary twists θ_J and $\theta_{J'}$, as discussed in the text, are as shown. The colored arrows indicate the 'positive' direction of the twist. The upper leftmost bond receives a twist of $\theta_J + \theta_{J'}$. Below the lattice diagram is a sample phase diagram showing an incommensurate spiral ordering for $J'/J \sim 1$ with a transition to an unknown phase (speculated to be either long-range collinear antiferromagnetically ordered (CAF), short-ranged incommensurate spiral ordered or a two-dimensional spin liquid, among other things).

I. INTRODUCTION

In the study of two-dimensional quantum magnets, the anisotropic triangular model has been a continuing object of attention. This is partially due to its applicability to real experimental materials such as the organic salts $\kappa-(BEDT\text{-}TTF)_2Cu_2(CN)_3$,[1–3] $\kappa-(BEDT\text{-}TTF)_2Cu_2[N(CN)_2]$,[3] and inorganic Cs_2CuCl_4,[4–8] and Cs_2CuBr_4,[8,9] and partially due to early theoretical and numerical speculation that it could exhibit a coveted 2D spin liquid phase.[10–13] This was followed by suggestions that experimental results on Cs_2CuCl_4[4] could be explained by, less exotic, quasi-1D spin liquid behaviour.[14,15] This led to more recent theoretical work, utilizing renormalization group techniques, suggesting a subtle collinear antiferromagnetic (CAF) ordering in this same region;[16,17] this ordering being in competition with the more classical incommensurate spiral order, which also may exist.[18] Most recently a DMRG study using periodic boundary conditions considered substantially larger systems than before and found a gapped state with strong antiferromagnetic correlations accented by weak, short-range, incommensurate spiral ones.[19]

Thus, the question in the $J' \ll J$ region is whether the systems exhibits a one- or two-dimensional spin liquid phase,[10–13,20] or a collinear antiferromagnetic order driven by next-nearest chain antiferromagnetic correlations and order by disorder,[16] or something entirely different. Suffice it to say that the true physics of this

system remains controversial.

Though Dzyaloshinskii-Moriya and interplane interaction are believed to play a role in the physics of the previously mentioned real materials, the more simplified system of a Heisenberg model on a triangular lattice with exchange interactions J along one direction and differing interactions (J') along the other two primitive vectors (see Fig. 1), is believed to capture much of the relevant physics. For $J' < J$ this can be visualized as an array of weakly interacting chains. In the limit of only two chains this system reduces to the well studied $J_1 - J_2$ chain, which is known to be a gapless Luttinger liquid for $J \ll J'$ before undergoing a phase transition at $J \simeq 0.24J'$ to a gapped phase characterized by dimer-like and incommensurate spiral correlations.[21–28] Though it is known that the behaviour of the true two-dimensional system differs greatly.

In this paper we explore the $J' < J$ region of the anisotropic triangular lattice Heisenberg model (ATLHM) through the use of twisted boundary conditions (TBC) and exact diagonalization (ED). This allows for a minimally biased exploration of the incommensurate behaviour of the system. A typical cluster used in the calculations along with the imposed twists is shown in Fig. 1. By minimizing the total energy of the ground-state with respect to the applied twist we can determine the *optimal twist* θ^{gs} that most closely fit with the natural ordering present in the system. It is then possible to infer a preferred q-vector from the value of the θ^{gs}. The inferred q-vector can tentatively be interpreted as the prefered q-vector for the system in the thermodynamic limit. It is not limited to the usual discrete values $2\pi n/L$ but can take *any* value between 0 and 2π. When such an analysis is performed for the *ground-state* we can directly determine q^{gs} for the ground-state, a substantial advantage of the present approach. We identify non-trivial values of θ^{gs} with the presence of long-range spiral order. Our results seem to indicate a phase transition between two gapless phases: long-range spiral order with a non-trivial ground-state $q^{gs} \neq 0$ and a more subtle phase with $q^{gs} = 0$ and antiferromagnetic intrachain ordering. At the critical point, the minimum in twist-space abruptly jumps between two distinct minima resulting in a similar jump in the inferred q^{gs}. We very roughly estimate this transition to occur at a $J'_c \lesssim 0.5$ in the thermodynamic limit. However, we note that the severe limitation in system sizes when performing exact diagonalizations makes it difficult to to draw a definitive conclusion concerning this transition in the thermodynamic limit. The interchain correlations of the latter phase are further explored with specific attention paid to the competition between next-nearest chain antiferromagnetic and ferromagnetic correlations as well as nearest chain incommensurate spiral interactions. Our results, though not conclusive, seem to favor a CAF-like ordering in this region. A schematic phase-diagram is shown in Fig. 1.

It is important to realize that the behavior of actual correlation functions are not only determined by q^{gs}. In fact, following Ref. 28, we argue that the dominant part of the incommensurate transverse correlations can be estimated by studying the *first excited state*. In general, q-vectors, describing the *transverse correlations*, are best determined by locating the twist minimizing the energy of the first excited-state. If this minimum is located we can infer a q^1-vector from which q, describing the incommensurate correlations, can be determined through the relation $q^1 = q + q^{gs}$. It is quite possible to have $q \neq 0$ and thus clear incommensurate (short-range) correlations in the absence of long-range spiral order. Such short-range incommensurate would then typically be modified by an exponentially decaying envelope. Hence, by studying the minima of mainly the first excited-state, we are able to extract the incommensurate q-vectors describing correlations along both the inter- and intrachain directions. Our results for the intrachain q-vector describing the incommensurate correlations are in *very close* agreement with recent DMRG results[19] on substantially larger systems, a strong validation of our approach. Further, the extracted q-vector for the correlations *varies smoothly* with J' through the tentative phase transition described above where q^{gs} abruptly jumps showing that incommensurate correlations are present on either side of the transition.

The organization of this paper is as follows: In section I we introduce the model and its classical phase diagram, this is then followed by an introduction to the twisted boundary conditions used here in section II along with a detailed explanation of how q^{gs} and q are determined. We then show our results in section III along with analysis of the two phases. We conclude in section IV.

A. The Anisotropic Triangular Lattice Heisenberg Model (ATLHM)

The system under consideration, the anisotropic triangular lattice Heisenberg model (ATLHM), is described by the following Hamiltonian:

$$H = J \sum_{\mathbf{x},\mathbf{y}} \hat{S}_{\mathbf{x},\mathbf{y}} \hat{S}_{\mathbf{x}-1,\mathbf{y}} + J' \sum_{\mathbf{x},\mathbf{y}} \hat{S}_{\mathbf{x},\mathbf{y}} \cdot \left(\hat{S}_{\mathbf{x},\mathbf{y}+\mathbf{1}} + \hat{S}_{\mathbf{x}-1,\mathbf{y}+\mathbf{1}} \right) \tag{1}$$

where for simplicity of exposition all lattice spacings a are taken to be 1 and where $J > 0$ corresponds to antiferromagnetic interactions. A diagram can be found in Fig. 1. In this paper, we are solely concerned with the $J' < J$ region, particularly the region where $J' \ll J$. For reference, the anisotropy found in Cs_2CuCl_4 is estimated to be $J'/J \sim 0.3$.[4] Throughout this paper we use the convention that a system of size N is composed of W chains (i.e. width W) of length L and is notated $N = W \times L$.

B. The Classical System

The classical limit case of the ATLHM (i.e. $S \to \infty$) can be straightforwardly solved.[29,30] The lowest energy configuration can be determined by positing a spiral solution of the form $\mathbf{S} = S\mathbf{u}e^{-i\mathbf{q}\cdot\mathbf{r}}$. This is identical to a local rotation of the quantization direction at each site which is done in spin-wave theory. The resulting energy expression is then

$$E_{cl}(\mathbf{q}) = J\cos(\mathbf{q}_J) + J'\cos(\mathbf{q}_{J'}) + J'\cos(\mathbf{q}_{J'} - \mathbf{q}_J) \tag{2}$$

where the $\hat{S}_i^z\hat{S}_j^z$ term is neglected since it carries no $\mathbf{q}$ dependence. For $J' < J$ we can find the minimum of Eq. (2) by first treating $\mathbf{q}_J$ as a fixed parameter. In that case it immediately follows that the minimum with respect to $\mathbf{q}_{J'}$ is at $2\mathbf{q}_{J'} = \mathbf{q}_J$. Thus, we get

$$E_{cl}(\mathbf{q}) = J\cos(\mathbf{q}_J) + 2J'\cos\left(\frac{\mathbf{q}_J}{2}\right). \tag{3}$$

The global minimum for $J' < J$ can now be found by minimizing this function with respect to $\mathbf{q}_J$. Solving with the use of trigonometric identities yields the classical ground-state solutions:

$$\mathbf{q}_J = 2\arccos\left(-\frac{J'}{2J}\right),\ \mathbf{q}_{J'} = \arccos\left(-\frac{J'}{2J}\right). \tag{4}$$

However, for the region $J'/J = (0, 1]$ the $\mathbf{q}_J$ solution goes from π to $4\pi/3$, we therefore choose a different solution $\tilde{\mathbf{q}}_J = 2\pi - \mathbf{q}_J$, corresponding to a different choice of branch, which ranges from the more physical π to $2\pi/3$. The $\mathbf{q}_{J'}$ solution needs no such adjustment. Thus the final classical solutions are

$$q_J = 2\pi - 2\arccos\left(-\frac{J'}{2J}\right),\ q_{J'} = \arccos\left(-\frac{J'}{2J}\right). \tag{5}$$

where we no longer emphasize q_J and $q_{J'}$ as vectors. In the limit of $J'/J \to 0$ we find $q_J = \pi$, $q_{J'} = \pi/2$, consistent with antiferromagnetic chains with only perturbative coupling.

II. TWISTED BOUNDARY CONDITIONS

The $J' \leq J$ region of the ATLHM is dominated by both incommensurate spiral ordering and short-range incommensurate spiral correlations. These long-wavelength, incommensurate, correlations present formidable challenges to numerical analysis, since attempts to capture physics with wavelengths of $O(10,000) - O(\infty)$ using a system of length $\sim O(10)$ will undoubtedly be dominated by extreme finite-size effects. Even the most recent 2D DMRG results, allowing for the largest systems, can only probe systems of $L \sim 100$ when at $J' = 0.2$ the wavelength of the spiral correlations is expected to be on the order of $10,000$.[19] Thus, it is little wonder that early numerical work produced such disputed results.[10,11]

Many of these finite-size effects can be successfully mitigated through a careful consideration of the boundary conditions. Previous numerical studies[10,11,19] on the ATLHM were produced using either open, periodic or mixed boundary conditions. Such boundary conditions will strongly distort the physics of an incommensurate system in favour of an ordering which is commensurate with the system size, only admitting the ordering q-vectors

$$q_n = \frac{2\pi}{L}n$$

where L is the length of the system in a given direction. It is this tendency of them to "lock" a long wavelength structure into a much smaller box that produces such spurious, unphysical, results such as sudden parity transitions (a point to be discussed in greater detail below).[10,11] Thus to greatly reduce this sort of error our calculations were performed using twisted boundary conditions (TBC).

When using twisted boundary conditions, spin interactions which cross the periodic boundary of the otherwise translationally invariant system become rotated in the $x - y$ plane by an angle θ. This corresponds to the boundary conditions

$$S_{L+1}^- = e^{-i\theta}S_1^-,\ S_{L+1}^+ = e^{i\theta}S_1^+ \tag{6}$$

or, equivalently,

$$S_L^+S_1^- \to S_L^+S_1^-e^{-i\theta},\ S_L^-S_1^+ \to S_L^-S_1^+e^{i\theta}. \tag{7}$$

where we simplify the discussion by only discussing one dimension of the system. Generalization to higher dimensions is straightforward although care has to be taken in order to define positive and negative θ consistently when a twist is introduced along several bonds.

(See Fig. 1.) Physically, the twist corresponds to a spin current where a(n) ↑-spin (↓-spin) acquires an extra phase when traversing the periodic boundary from the left (right). Alternatively, the Heisenberg system can be mapped to one of $N_\uparrow$ fermions with the initial Jordan-Wigner transformation $S_i^+ = c_i^\dagger e^{i\pi \sum_{i<j} c_j^\dagger c_j}$, followed by the gauge U(1) gauge transformation, $c_i^\dagger = f_i^\dagger e^{i\frac{\theta}{L}}$. The interpretation is then of a periodic system, on a ring, of $N_\uparrow$ up spins threaded by a flux θ.

A. $J - J_2$ Spin Chain

For an initially translationally invariant system of linear size L a twist of θ imposed at the boundary can then in general be distributed throughout the system by introducing a twist of θ/L at each bond by performing a non-unitary gauge-transformation. We thereby obtain a model with periodic boundary conditions (PBC). Let us take the well known $J - J_2$ spin chain model as an example:

$$H = J \sum_i \hat{S}_i \cdot \hat{S}_{i+1} + J_2 \sum_i \hat{S}_i \cdot \hat{S}_{i+2}. \tag{8}$$

This model is closely related to the ATLHM and was studied using twisted boundary conditions in Ref. 28 where a twist of θ was introduced at the boundary in the terms coupling sites $[L, 1]$ as well as $[L-1, 1]$ and $[L, 2]$. We can in this case define a translationally invariant model with the *exact* same energy spectrum if we instead introduce a twist of θ/L at each $[i, i+1]$ bond along with a twist of $2\theta/L$ at each $[i, i+2]$ bond. This latter model is now manifestly translationally invariant with periodic boundary conditions and any many-body state can then be characterized by a many-body momentum:

$$\tilde{q} = \frac{2\pi n}{L} \quad n = 0, 1, \ldots, L-1 \tag{9}$$

To be explicit, if T_a denotes the operator translating one lattice spacing a in real space, then $T_a \Psi_{\mathrm{PBC}} = \exp(i\tilde{q}a)\Psi_{\mathrm{PBC}}$ with Ψ_{PBC} the wave-function of the translationally invariant model with periodic boundary conditions. We can then determine the energy as a function of θ as well as the many-body momentum of the corresponding state. As an illustration, results are shown in Fig. 2 for the lowest lying $S = 1$ excitation of the $J - J_2$ at $J = J_2$ for a chain with $L = 12$, displaying the characteristic parabolic shape of the energy. In this case the first energy minimum occurs at $\theta_{min} = 0.6299\pi$ where $\tilde{q} = \pi/2$. We then make the quasi-classical (phenomenological) assumption that the main effect of the twist is to modify the state's natural ordering vector q to fit with the many-body momentum $\tilde{q}$ in the following manner:

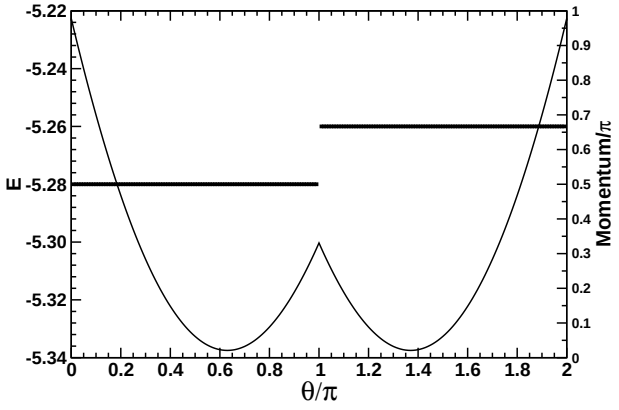

FIG. 2. Energy and momentum of the lowest lying $S = 1$ state for the $J - J_2$ chain at $J_2/J = 1$. The energy minima occur at $\theta = 0.6299\pi, 1.3701\pi$. At $\theta = \pi$ the lowest lying state changes from having $\tilde{q} = 6\pi/12$ to $\tilde{q} = 8\pi/12$.

$$\tilde{q} = q \pm \frac{\theta}{L} = \frac{2\pi n}{L}. \tag{10}$$

In the present case we immediately find

$$q = \pi/2 + 0.6299\pi/12. \tag{11}$$

The second minimum at $\theta_{min} = 2\pi - 0.6299\pi$ and $\tilde{q} = 2\pi/3$ yields the same

$$q = 2\pi/3 - (2\pi - 0.6299)/12 = \pi/2 + 0.6299\pi/12. \tag{12}$$

In the thermodynamic limit the natural ordering vector q is then simply given by $\tilde{q}$ and any effects of the twist θ upon the dermination of q should be negligible as expressed by Eq. (10). This analysis differs in some details from Ref. 28 but yields essentially identical results for the $J - J_2$ chain.

One may also consider the momentum of the model *without* translational invariance and twisted boundary conditions. In this case we find for the wave-function Ψ_{TBC} the relation $T_a \Psi_{\mathrm{TBC}} = \exp(i\alpha a)\Psi_{\mathrm{TBC}}$ with $\alpha = \tilde{q} + \theta N_\uparrow/L$ where $\tilde{q}$ is the many-body momentum of the translationally invariant system. Here $N_\uparrow$ denotes the number of ↑ spins in the state under consideration.

If one, at the classical level, argues that θ is the angle needed for qL to equal an integer number of complete

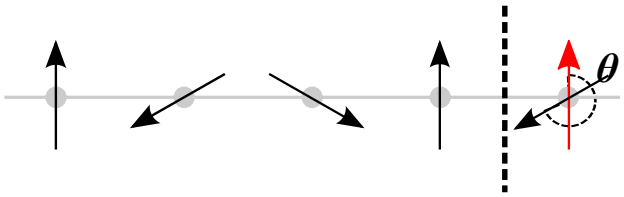

FIG. 3. This diagram shows how a $q = 2\pi/3$ ordering can be made to "fit" into a system of length 4 by twisting by $4\pi/3$ at the boundary. These twisted boundary conditions then allow any incommensurate ordering to fit in any sized system.

turns one arrives at the same relation between q and θ:

$$qL \pm \theta = 2\pi n, \tag{13}$$

In this equation, as well as in Eq. (10), the $\pm$ signifies if q turns in the same direction as θ as we move along the chain. Hence the presence of the twist θ permit a continuum of ordering q-vectors to 'fit' into the system of linear size L, where:

$$q = \frac{1}{L}\left(2\pi n \pm \theta\right). \tag{14}$$

A simple illustration of this is shown in Fig. 3 for $q = 2\pi/3$. In this case the ordering can be made to "fit" a system of length $L = 4$ if a twist $\theta = 4\pi/3$ is introduced as indicated in Fig. 3. From θ we can then infer $q = (2\pi \times 2 - 4\pi/3)/4 = 2\pi/3$. In this example, the wavelength of the twist ($\lambda = 3$) is shorter than the linear length of the system $L = 4$ and we have to use $n = 2$ in Eq. (14) in order to obtain the correct q. In analogy with the example of the $J - J_2$ chain we would therefore expect the energy minimum for $\theta = 4\pi/3$ to occur for the state with many-body momentum $\tilde{q} = 2\pi \times 2/4 = \pi$. Correspondingly we would expect another minimum at $\theta = 2\pi/3$ for a state with many-body momentum $\tilde{q} = 2\pi/4 = \pi/2$.

In practical studies it is not always feasible to use a translationally invariant system and explicitly determine the many-body $\tilde{q}$ of the state corresponding to the minimizing twist and thereby n in Eq. (10) and (14) and for most of the results presented here we have not done so. However, it is almost always possible to infer the correct n to be used in Eq. (10) and (14) by simple continuity from known results and other expected behavior such as $qL \ll 1$.

B. The ATLHM

We now turn to a discussion of the approach we have taken to apply twisted boundary conditions to the ATLHM. With the analysis of the classical system in mind, we include *two* twists in our analysis of the ATLHM. The first, θ_J, is associated with a twisted boundary in the J direction. The second, $\theta_{J'}$, is then associated with the boundary in the J' direction (see Fig. 1). With both twists implemented the Hamiltonian becomes:

$$\begin{aligned} H_\theta = {} & J \sum_{\mathbf{x}>1,\mathbf{y}} \hat{S}_{\mathbf{x},\mathbf{y}} \hat{S}_{\mathbf{x}-1,\mathbf{y}} + J' \sum_{\mathbf{x},\mathbf{y}<W} \hat{S}_{\mathbf{x},\mathbf{y}} \cdot \left(\hat{S}_{\mathbf{x},\mathbf{y}+\mathbf{1}} + \hat{S}_{\mathbf{x}-1,\mathbf{y}+\mathbf{1}} \right) \\ & + \sum_{\mathbf{y}<W} \hat{S}^+_{1,\mathbf{y}} \cdot \left(J \hat{S}^-_{L,\mathbf{y}} + J' \hat{S}^-_{L,\mathbf{y}} \right) e^{i\theta_J} + J' \sum_{\mathbf{x}>1} \hat{S}^+_{\mathbf{x},W} \hat{S}^-_{\mathbf{x},1} e^{i\theta_{J'}} \\ & + J' \hat{S}^+_{1,W} \hat{S}^-_{L,1} e^{i(\theta_J + \theta_{J'})} + H.c. \\ & + \sum_{\mathbf{y}<W} \hat{S}^z_{1,\mathbf{y}} \cdot \left(J \hat{S}^z_{L,\mathbf{y}} + J' \hat{S}^z_{L,\mathbf{y}} \right) + J' \sum_{\mathbf{x}>1} \hat{S}^z_{\mathbf{x},W} \hat{S}^z_{\mathbf{x},1} e^{i\theta_{J'}}. \end{aligned} \tag{15}$$

Although this Hamiltonian looks quite cumbersome when written out explicitly, conceptually it is very simple. If a left moving $\downarrow$-spin traverses, either horizontally or diagonally, the left periodic boundary it is rotated in the $x - y$ plane by θ_J. If an upward moving $\downarrow$-spin traverses, either vertically or diagonally, the upper periodic boundary it is rotated in the $x - y$ plane by $\theta_{J'}$. If a $\downarrow$-spin traverses the upper left periodic boundary diagonally, thus crossing both twisted boundaries, it is rotated in the $x-y$ plane by $(\theta_J+\theta_{J'})$. Spins in the bulk as well as the z-component of all spins are unaffected by the boundary.

These twists, which explicitly break the global SU(2) spin symmetry, are identical to a twist of θ_J/L on *each* horizontal and north-west to south-east bond along with a twist of $\theta_{J'}/W$ on *each* south-west to north-east and north-west to south-east bond. The north-west to south-east bonds therefore recieve a twist of $\theta_J/L + \theta_{J'}/W$ for a system of dimensions $W \times L$. (See Fig. 1.) If this is done one can work with an equivalent translationally invariant model. However, a twist-per-site approach was found to be less fruitful for such small systems and the explicit SU(2) symmetry breaking will play an important role in forcing a S^z quantization direction which will be discussed below.

It is worth noting that the second twist, $\theta_{J'}$, is rarely (if ever) implemented in studies with twisted boundary conditions. Indeed, most existing numerical studies of the ATLHM fail to consider the possibility of incommensurate *inter*chain correlations at all, often enforcing

periodic or open boundary conditions in the interchain direction even when other, more elaborate, boundary conditions are used along chains. The parameter $\theta_{J'}$, then, serves as a tool to explore such new physics.

Our complete Hamiltonian, boundary twists included, then has three free parameters: The energy parameter $\frac{J'}{J}$, the intrachain boundary twist θ_J and the interchain boundary twist $\theta_{J'}$. The numerical task then becomes to explore the two-dimensional landscape $(\theta_J, \theta_{J'})$, at a given J'/J, to find the twists which minimize the ground-state energy. From these twists the q-vectors q_J and $q_{J'}$ can then be extracted using the following generalization of Eq. (10) and (14):

$$q_J = \vec{q}_1 \cdot \vec{a}_1 = \frac{2\pi n_1}{L} \pm \frac{\theta_J}{L}$$
$$q_{J'} = \vec{q}_2 \cdot \vec{a}_2 = \frac{2\pi n_2}{W} \pm \frac{\theta_{J'}}{W}. \quad (16)$$

These equations follow since the twists are applied in *direct* space and reflect the behavior of the system upon L and W translations along the directions $\vec{a}_1$ and $\vec{a}_2$ in real direct space. Our notation here for a system of W chains of length L is the following: As indicated in Fig. 1 we use basis vectors $\vec{a}_1 = a(1,0)$ and $a_2 = a(1/2, \sqrt{3}/2)$ for the direct lattice. As usual reciprocal lattice vecors are then given by $\vec{b}_1 = 4\pi(\sqrt{3}/2, -1/2)/(a\sqrt{3})$ and $b_2 = 4\pi(0,1)/(a\sqrt{3})$. If we now consider the translationally invariant model with twists of θ_J/L and $\theta_{J'}/W$ along the bonds as described above, the many-body momentum of the translationally invariant system with the imposed twist is:

$$\vec{\tilde{q}} = \frac{n_1}{L}\vec{b}_1 + \frac{n_2}{W}\vec{b}_2. \quad (17)$$

Likewise, in our notation, we have:

$$\vec{q} = \vec{q}_1 + \vec{q}_2 = \frac{q_J}{2\pi}\vec{b}_1 + \frac{q_{J'}}{2\pi}\vec{b}_2. \quad (18)$$

Hence, the application of the twists allow us to determine the components of $\vec{q}$ along $\vec{b}_1$ and $\vec{b}_2$.

As an illustration we show in Fig. 4 results for the $S = 1$ ground-state energy of a 4×4 system with $J'/J = 1$. Two identical minima are clearly present at $(\theta_J, \theta'_J) = (2\pi/3, 4\pi/3)$ and $(4\pi/3, 2\pi/3)$. In this case we have done simulations using a translationally invariant model as outlined aboved and explicitly determined the many-body momentum, $\vec{\tilde{q}}$, of the state corresponding to the minima. Here we find $(2\pi n_1/L, 2\pi n_2/W) = (\pi/2, \pi)$ and $(\pi, \pi/2)$ respectively. Thus, following the analysis at the end of the previous section we find $q_J = 2\pi/3$. The mimima in the $S = 0$ ground-state occur at the *exact* same $(\theta_J, \theta_{J'})$ but in this case with $n_1 = n_2 = 0$.

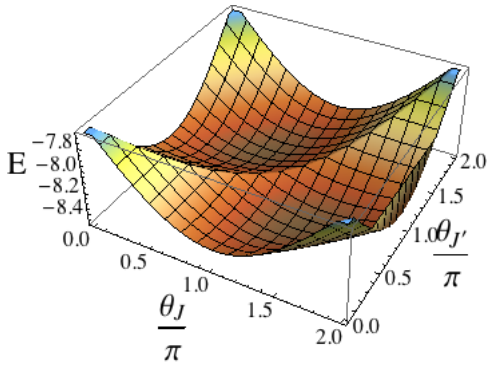

FIG. 4. The energy, E, as a function of the two twists θ_J and θ'_J. Results are shown for the lowest-lying $S = 1$ state of a 4×4 system with $J'/J = 1$. The two identical minima occur for $(\theta_J, \theta'_J) = (2\pi/3, 4\pi/3)$ and $(4\pi/3, 2\pi/3)$.

However, there is an additional complication in such an analysis brought on by such small systems. As has very clearly been shown in Ref. 19, much of the $J'/J < 1$ region is dominated by *antiferromagnetic* correlations superimposed on much subtler incommensurate spiral correlations. Thus, if the system can be made to adopt a specific quantization direction z, through, say, a perturbative magnetic field on a single site as was done in Ref. 19, we expect $\langle GS|\hat{S}^z_{\mathbf{x}}\hat{S}^z_{\mathbf{x}+\mathbf{x}'}|GS\rangle$ correlations to be completely dominated by antiferromagnetism with a small canted incommensurate ordering showing in the transverse correlations:

$$\langle GS|\hat{S}^x_{\mathbf{x}}\hat{S}^x_{\mathbf{x}+\mathbf{x}'} + \hat{S}^y_{\mathbf{x}}\hat{S}^y_{\mathbf{x}+\mathbf{x}'}|GS\rangle$$
$$\rightarrow \left\langle \frac{1}{2}\left(\hat{S}^+_{\mathbf{x}}\hat{S}^-_{\mathbf{x}+\mathbf{x}'} + \hat{S}^-_{\mathbf{x}}\hat{S}^+_{\mathbf{x}+\mathbf{x}'}\right)\right\rangle \quad \propto \langle \hat{S}^+_{\mathbf{x}}\hat{S}^-_{\mathbf{x}+\mathbf{x}'}\rangle. \quad (19)$$

In the absence of an explicit symmetry breaking term it is then extremely difficult to separate the spiral correlations from the "sea" of antiferromagnetic ones. This difficulty is addressed by twisted boundary conditions as can be seen through consideration of the following argument, originally detailed and validated in Ref. 28. First, with the addition of a twist in the $x - y$ plane the global spin SU(2) symmetry is broken and a unique z-quantization is picked out in a direction normal to the system, since a generic twist would frustrate antiferromagnetic ordering in-plane. It is then convenient to rewrite the transverse correlations , $\langle \hat{S}^+_{\mathbf{x}}\hat{S}^-_{\mathbf{x}+\mathbf{x}'}\rangle$, in

the more intuitive Fourier transformed form

$$= \left\langle \left(\frac{1}{\sqrt{L}} \sum_{q'} e^{iqx} \hat{S}^+_{q'} \right) \left(\frac{1}{\sqrt{L}} \sum_{q} e^{-iq(x+x')} \hat{S}^-_{q} \right) \right\rangle$$
$$= \frac{1}{L} \left\langle e^{-iqx'} \left(e^{i(q-q')x} \right) \hat{S}^+_{q'} \left(\sum_m |m\rangle\langle m| \right) \hat{S}^-_q \right\rangle$$
$$= \frac{1}{L} \sum_q \sum_m e^{-iqx'} |\langle m|S^-_q|GS\rangle|^2 \quad (20)$$

where S^-_q can now be physically interpreted as a spin-wave destruction operator. If the ground-state lies in the total $S^z = 0$ sector, which it does for an antiferromagnetic system of even system size, then $\langle GS|S^-_q|GS\rangle = \langle GS| \left(\frac{1}{\sqrt{L}} \sum_q e^{-iqx} S^-_{\mathbf{x}} \right) |GS\rangle = 0$ and the transverse correlations can be rewritten as

$$\langle \hat{S}^+_{\mathbf{x}} \hat{S}^-_{\mathbf{x}+\mathbf{x}'} \rangle = \frac{1}{L} \sum_q \sum_{m \neq GS} e^{-iqr} |\langle m|S^-_q|GS\rangle|^2. \quad (21)$$

As usual, the S^-_q or S^-_x operators take the total $S^z = 0$ ground-state into the total $S^z = -1$ sector. Additionally, if the ground-state has an overall ordering vector q^{gs} then the only terms to survive the sum over $\langle m|S^-_q|GS\rangle$, and thus contribute to the transverse correlations, are those for which $q^1 = q^{gs} + q$. If one then makes the assumption that only the first excited state in the total $S^z = 1$ sector dominates then one now has a method to extract the incommensurate q-vector, q, as well as the ground-state momentum q^{gs}. First one finds the $(\theta_J, \theta_{J'})$ which minimizes the ground-state energy of the total $S^z = 0$ sector, yielding

$$(q^{gs}_J, q^{gs}_{J'}) \quad (S^z = 0). \quad (22)$$

Notice that our two twists, θ_J and $\theta_{J'}$ yield two q-vectors which we denote q_J and $q_{J'}$. After finding the minimum in the total $S^z = 0$ twist-space the procedure is then repeated in the total $S^z = 1$ twist-space yielding

$$q^1_J = q^{gs}_J + q_J \text{ and } q^1_{J'} = q^{gs}_{J'} + q_{J'} \quad (S^z = 1). \quad (23)$$

A demonstration of this can be found in Ref. 28. As an illustration of the procedure we show results for $E(\theta_J, \theta_{J'})$ for the first excited state of a 4×6 system with $J'/J = 0.6$ in Fig. 5. Note that, for our subsequent results the minima are determined on a much finer grid. We also note that in both Fig. 4 and 5 do distinct minima occur for values of $\theta > \pi$. This is due to the non-zero $\theta_{J'}$ which lifts the symmetry with respect to $\theta = \pi$ visible in Fig. 2.

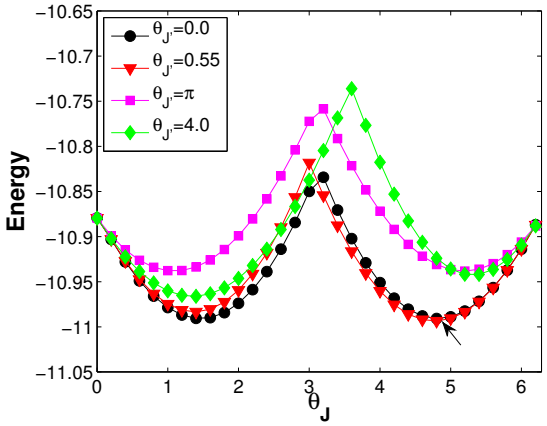

FIG. 5. (Color online.) *Energy* vs. θ_J: The incommensurate and ground-state wavevectors $q^{in}_J/q^{in}_{J'}$ and $q^{gs}_J/q^{gs}_{J'}$ are obtained by minimizing the ground-state energy in the total-$S^z = 1$ and total-$S^z = 0$ subspaces respectively in terms of the boundary twists θ_J and $\theta_{J'}$. This figure shows sample values of θ_J vs. energy for different value of $\theta_{J'}$ for $N = 4 \times 6$ and $J'/J = 0.6$ in the total-$S^z = 1$ subspace. The true minimizing $(\theta_J, \theta_{J'})$ were determined on a much finer grid to an accuracy of 0.001 in the twist, and for this case $(J' = 0.6)$ was found to be $(4.775, 0.550)$ (noted by an arrow) which corresponds to the q-vectors $(q_J, q_{J'}) = (2.890, 1.708)$. This figure merely serves as an illustration.

This method of minimizing the ground-state energy in both the total $S^z = 0$ and $S^z = 1$ sectors, also allows one to compute the *spin gap*, Δ, between these states. Thus, with knowledge of the spin gap, the ground-state long-range ordering q-vectors as well as the incommensurate short range q-vectors, one can imagine two situations of interest that could arise in the ATLHM.

C. Case 1: $q^{gs} \neq 0$ or π, $q = 0$ (incommensurate spiral order)

In the case where the true ground-state (i.e. that in the total $S^z = 0$ sector) is minimized by incommensurate q-vectors q^{gs}_J and $q^{gs}_{J'}$ we then have incommensurate long-range order related to a classical incommensurate spiral.

In such a region we also expect the spin gap (Δ) to vanish owing to the gapless magnon excitations about the spiral order which accompany U(1) symmetry breaking. Note that the symmetry broken *is* U(1), since the initial SU(2) symmetry has already been reduced to U(1) when the twist terms were added. This would coincide, in the limit of infinite system size, with long-

range correlations of the form

$$\left\langle \hat{S}_{\mathbf{x},\mathbf{y}} \hat{S}_{\mathbf{x}+\mathbf{x}',\mathbf{y}} \right\rangle \underset{x'\to\infty}{\approx} e^{iq_J^{gs}x'} \left\langle \hat{S}_{\mathbf{x}} \right\rangle^2, \qquad (24)$$

with a similar form in the J' direction corresponding to $q^{gs}_{J'}$. However, such long-range behaviour of the correlation functions is far beyond the accessible range of any numerical approach. Thus, it will suffice to take a non-zero q^{gs} accompanied by a vanishing spin gap Δ to demonstrate long-range spiral order.

D. Case 2: $q^{gs} = 0$ or π, $q \neq 0$ (non-spiral order)

The case where $q^{gs} = 0$ or π is more complicated. Since q is non-zero the system is displaying incommensurate spiral correlations, however, these correlations are of insufficient strength to stabilize true long-range spiral ordering. Yet, as we find, if the spin gap Δ is found to be zero, then we expect *some* ordering to exist, unless the system is found to be a gapless spin liquid.

Should the value of q^{gs} be consistent with a π ordering vector for all system sizes then, taken along with the gaplessness of the system, one could conclude that the system has ordered antiferromagnetically. However, in our case a more thorough analysis of the correlations of the system becomes necessary. This is expanded upon in Sec. III B

III. RESULTS AND DISCUSSION

The intrachain (θ_J) and interchain ($\theta_{J'}$) boundary twists were varied to minimize the "ground-state" energy in the total-$S^z = 0, 1$ sectors for systems of increasing length and fixed width (4 chains). A fixed width was chosen both since intrachain correlations are the dominant correlations for $J' \ll J$ and to more easily compare with existing DMRG work on larger systems.[19] From these minimizing twist values the q-vectors q_J and $q_{J'}$ were extracted as a function of J'/J which we will simply call J' (i.e. $J = 1$). The resulting data, as well as the classical values, can be found in Fig. 6 for q_J and Fig. 7 for $q_{J'}$. With the exception of the $J' \lesssim 0.3$ region which is discussed later, both q_J and $q_{J'}$ are found to be fitted best by functions of the form $a(J')^2 \exp(-b/J')+c$ rather than power-law fits. This data is in close agreement with the DMRG results found in Ref. 19 where the incommensurate q-vector q_J ($q_{J'}$ was not considered) was extracted by fitting $\langle S^z_{\mathbf{x}} \rangle$, as induced by a boundary field, to an exponentially decaying correlation function of the form $\langle S^z_{\mathbf{0}} \rangle \exp(-x/\xi)\cos(qx)$. The close

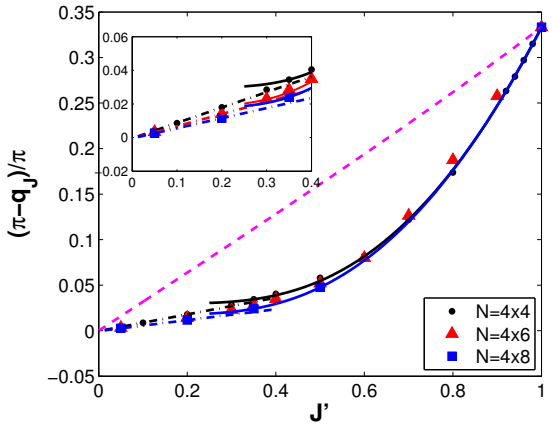

FIG. 6. (Color online.) q_J vs. J': The intrachain ordering q-vector q_J as a function of the interchain interaction J' for systems of width 4 along with the classical value (dashed magenta line). Results are obtained from the θ_J which minimizes the total-$S^z = 0, 1$ sectors. For $J' > J'_c$ q^{gs}_J was found to be non-zero, while $q^{gs}_J = 0$ or π for $J' < J'_c$ The critical value, J'_c was determined to be J'_c =0.9175, 0.7835, 0.7135 for $N = 4\times4$, 4×6 and 4×8 respectively. Exponential fits (black for $N = 4\times4$, light grey for $N = 4\times6$ and dark grey for $N = 4\times8$) are of the form $a(J')^2\exp(-b/J')$, consistent with Ref. 19, and are found to be extremely good for most of the J' region. However at $J' \sim 0.3$ the data markedly deviates from this fit and develops a linear character. The physicality of this linear behaviour for $J' < 0.3$ is further explored in the text.

agreement of our results with the DMRG results on substantially larger systems is surprising and indicative of the power of twisted boundary conditions to circumvent finite-size effects in incommensurate systems.

The lack of distinct features in Fig. 6 and Fig. 7 suggests that the system has identical behaviour for all J'. This is not the case, as can be seen by examining the true ground-state q-vectors in the total-$S^z = 0$ sector. As J' decreases the ground-state twists, θ^{gs}_J and $\theta^{gs}_{J'}$, are found to jump discontinuously at some critical value of J', J'_c (the nature of this jump will be discussed momentarily). For J' J'_c the total-$S^z = 0$ and total-$S^z = 1$ twists coincide. Below J'_c the total-$S^z = 0$ data is found to be either 0 or π for all J' in the region. A sample illustration of this jump can be found in Fig. 8 where it is shown for a 4×4 system. This critical value decreases with system size and is found to be at J'_c =0.9175, 0.7835, 0.7135 for $N = 4\times4$, 4×6 and 4×8 respectively. A finite-size extrapolation of these values to the thermodynamic limit can be found in Fig. 10. At $J'_c = 0.9175$ the θ^{gs}_J minimizing the energy jumps

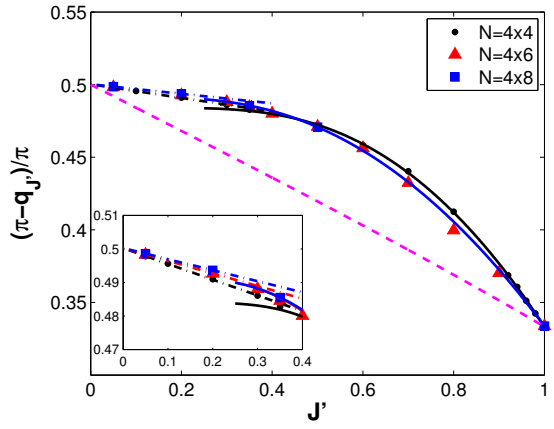

FIG. 7. (Color online.) $q_{J'}$ vs. J': The interchain ordering q-vector $q_{J'}$ as a function of the interchain interaction J' for systems of width 4. Behaviour and fits are identical to those in Fig. 6. As $J' \to 0$, $q_{J'}$

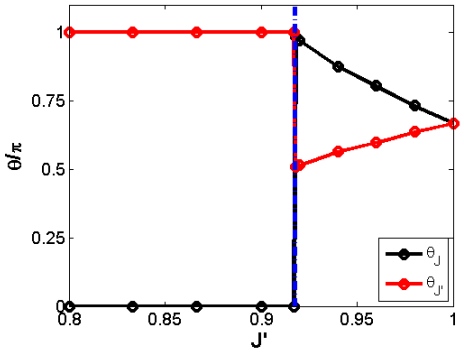

FIG. 8. (Color online.) θ_J, $\theta_{J'}$ vs. J' in the total $S^z = 0$ subspace ($N = 4 \times 4$): As can be clearly seen the total $S^z = 0$ minimizing boundary twists (shown as solid lines with circular markers) undergoes an abrupt jump (occurring here at $J'/J \sim 0.91$) before "locking" to some fixed value for all $J' < J'_c$.

abruptly to 0 due to the appearance of a new distinct minimum in twist space. We can extrapolate J'_c to the thermodynamic limit with a linear $\frac{a}{N} + b$ fit of N^{-1} estimating $J'_c \to 0.475$ as $N \to \infty$. As the system width is increased J'_c is found to increase as well, taking values of 0.912 and 0.917 for systems of size $N = 6 \times 4$ and $N = 8 \times 4$. The infinite system size extrapolation for fixed length, which is obviously non-linear and is thus fitted with a quadratic $\frac{a}{N^2} + \frac{b}{N} + c$ fit, can be found in the inset of 10 and is found to be 0.948. Obviously, for these very limited system sizes, a reliable estimate of the critical coupling in the thermodynamic limit is not within reach. However, it seems plausible that the fixed width estimate of $J'_c = 0.475$ is the more realistic of our estimates. A comparison of both fixed width and fixed length thermodynamic limit extrapolations suggests that the spiral-ordered region extends well into the $J' < J$ region, even in much larger systems.

It is important to note that this discontinuous jump in the ground-state is *not* due to the level crossing observed in previous numerical work.[10,11] This transition, which was found to be a parity transition, occur for a 4×4 system at a value of $J' \sim 0.84$, for 4×6 and at $J' \sim 0.75$ for 4×8 and thus occurs at a higher value of J' for all system sizes. Thus, this level crossing is completely avoided once one allows the boundaries to twist freely.

The nature of the transition is essentially due to a first-order phase transition in "twist-space" as described by Landau theory. At $J' > J'_c$ the ground-state minima is found to lie at some incommensurate twist value, at $J' \sim J'_c$ a second commensurate minimum forms elsewhere, at say $(\theta_J, \theta_{J'}) = (0, \pi)$, this second minima then lowers in energy as the incommensurate minima, which is still the global minima, rises. At $J' = J'_c$ the commensurate minimum overtakes the incommensurate one to become the new global minimum and the ground-state then jumps discontinuously.

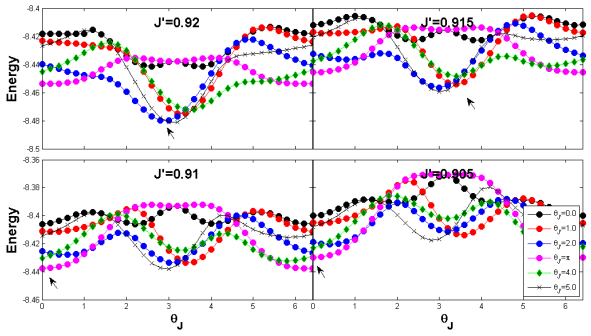

FIG. 9. (Color online.) Energy vs. θ_J for varying values of $\theta_{J'}$ shown for different values of J' near $J'_c = 0.915$ in the total $S^z = 0$ subspace ($N = 4 \times 4$). At $J' > J'_c$ the ground-state minima is found to lie at an incommensurate twist value, at $J' \sim J'_c$ a second commensurate minimum forms at $(\theta_J, \theta_{J'}) = (0, \pi)$, this second minimum then moves lower in energy and becomes the global minimum at $J' = J'_c$. The global minima is indicated in the graphs with an arrow.

We now look at each region separately:

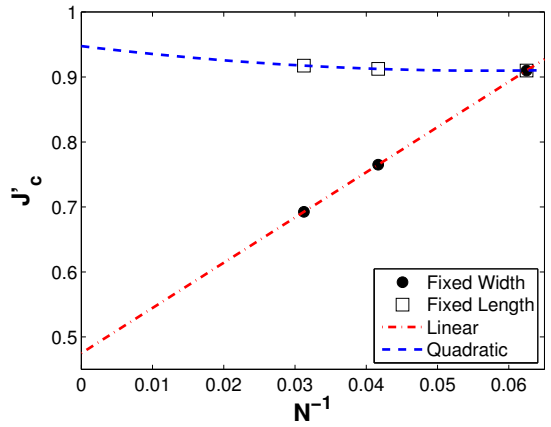

FIG. 10. (Color online.) Critical J' vs N^{-1}: A thermodynamic limit extrapolation of the spiral-ordered to non-spiral ordered transition value (J'_c) for systems of width 4 and length 4. For a width of 4 a linear ($J'_c = 0.475$ as $N \to \infty$) fit was considered. For a length of 4 the extrapolation was clearly not linear and so a quadratic fit ($J'_c = 0.948$ as $N \to \infty$) was used. For consistency the quadratic extrapolation values for both analyses are considered the best fit. The critical temperature was indicated by a discontinuous jump in θ_J and $\theta_{J'}$ from their $J' \ll 1$ values.

A. The Incommensurate Spiral Ordered Phase, $1 \geq J'/J > J'_c/J$

For the isotropic case, where $J' = 1$, the ordering q-vectors $(q_J, q_{J'})$ were found to be $(2\pi/3, 2\pi/3)$ in agreement with previous work. As J' decreases the q-vectors then vary continuously through incommensurate values. In this region the energy minima of the total-$S^z = 0$ and total-$S^z = 1$ regions coincide in twist space. This, taken with the lack of an energy gap (this is shown in section III B 1), indicates that this region is in a long-range spiral order phase. The transition out of this phase seems to occur at an intrachain twist of $\sim \pi$ for all system sizes as illustrated in Fig. 8 for a 4×4 system. The fact that the transition should be related to some critical value of the boundary twist *and not* some critical q_J is interesting and may represent some subtle numerical cause. However, we would comment that spin wave theory is known to encounter a similar region, notable for its non-convergence, for J' smaller than some critical value[12,13]. On the other hand, we also cannot exclude the possibility that for much larger systems this transition would be absent.

B. The Non-Spiral Ordered Phase, $J' < J'_c$

For J' values greater than J'_c the ground-state is found to have incommensurate long-range spiral order as was discussed previously. However, for $J' < J'_c$ the twists which minimize the total $S^z = 0$ sector jumps to $(\theta_J, \theta_{J'}) = (0, \pi)$ for $N = 4 \times 4$, 4×6 and 4×8 (i.e. systems of width 4), and to $(0, 0)$ for systems of size $N = 6 \times 4$ and $N = 8 \times 4$. These values of θ_J are found to be entirely consistent with antiferromagnetic intrachain ordering of the ground-state. However, for increasing system width, the values of $\theta_{J'}$, being π for width 4 but 0 for widths of both 6 *and* 8, are inconsistent with any q-vector suggesting a more careful consideration of interchain physics must be taken. This discussion is postponed until section III B 2.

The fact that no evidence of this transition can be found in the total $S^z = 1$ data suggests that incommensurate correlations are always present and vary smoothly for all $1 > J'/J > 0$, but that the power of those correlations to stabilize long-range spiral order becomes insufficient at J'_c. Below J'_c the dominant correlations are then antiferromagnetic along chains with much smaller incommensurate behaviour resting atop. These antiferromagnetic correlations nested in an incommensurate envelope were demonstrated very clearly for a gapped system in Ref. 19. Though it is our belief that this behaviour is only found below J'_c and the fact that such behaviour was obtained for $1 \geq J'/J > J'_c$ in that paper might be an artefact of the use periodic boundary conditions in the interchain direction there. This point is further discussed in the next subsection.

Numerical access to three system sizes of width 4 makes it possible to extrapolate q_J and $q_{J'}$ to the $4 \times \infty$ limit. Extrapolated values were found to lie, with great precision, on a scaling function of the form $\frac{a}{N^2} + \frac{b}{N} + c$ and can be found in the inset of Fig. 11. The thermodynamic limit results for both q_J^∞ and $q_{J'}^\infty$ are plotted in the main figure. Values above J'_c were not considered, with the exception of the commensurate $J'/J = 1$ case. As before, these q_J^∞ and $q_{J'}^\infty$ data can be well fitted by a function of the form $a(J')^2 exp(-b/J') + c$. However, unlike the finite-size case, this function is found to be valid for all J' considered. This suggests that the linear behaviour in the neighbourhood of $J' \sim 0$ (See Fig. 6) may not be physical. Furthermore, as will be discussed in section III B 2, it is found for $J' \lesssim 0.3$ that the system's energy dependence on $\theta_{J'}$ becomes zero to numerical precision. Thus it is possible that interchain correlations, which are physically non-zero, but of a magnitude smaller than the smallest number that could be represented by a computer are present

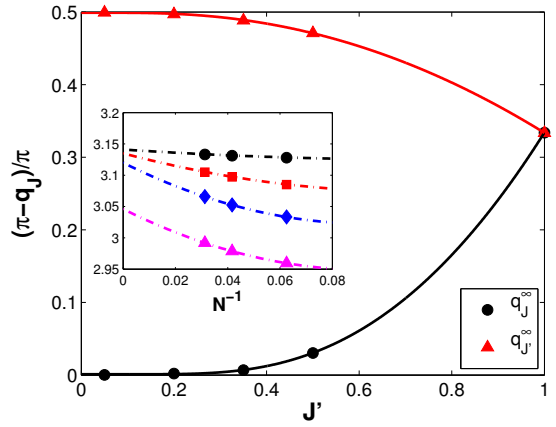

FIG. 11. (Color online.) q_J^∞ and $q_{J'}^\infty$ vs. J': The thermodynamic limit extrapolated values of q_J and $q_{J'}$ vs. J'. Extrapolations were done to quadratic functions of the form $\frac{a}{N^2}+\frac{b}{N}+c$. Sample extrapolations can be seen in the inset for $J'/J = 0.5$ (triangles), 0.35 (diamonds), 0.2 (squares) and 0.05 (circles). Values greater than the estimated infinite system size transition point and less than $J'/J = 1$ are not shown (see text). In similarity to the finite-size Fig. 6 and Fig. 7, $q_J \to \pi$ and $q_{J'} \to \pi/2$ as $J' \to 0$. However, contrary to that figure, the degradation of an exponential fit to a linear one in the $J' \sim 0$ region is less pronounced, if present at all (see text).

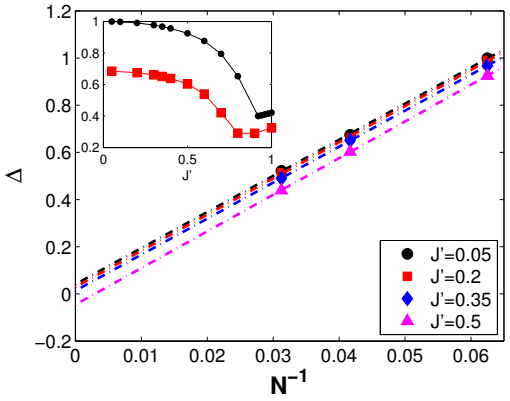

FIG. 12. (Color online.) Spin Gap vs. N^{-1}: The energy difference between the ground-states of the total $S^z = 0$ and total $S^z = 1$ sectors extrapolated to the thermodynamic limit. Dotted lines represent fits of the form $\frac{a}{N}+\Delta_\infty$ with Δ_∞s found in the non-spiral region to be on the order of 10^{-2}. The error, estimated by contrasting fits quadratic vs. linear in N^{-1}, could be as large as 10^{-1}; or approximately one percent. Inset: Δ vs. J': We show the energy gap Δ versus J' for $N = 4\times 4$ (circles) and $N = 4\times 6$ (squares). Without a thermodynamic limit analysis it is easy to see how previous work found the $J' < J_c'$ region to be gapped.

in this region. Regardless, the physicality of the linear behaviour is not certain.

1. *The Energy Gap:* Δ

The numerical determination of a spin gap is in general a difficult task. Often computational reality doesn't permit enough system sizes to be calculated in order for a reliable thermodynamic limit to be established. Furthermore, when the thermodynamic limit can be taken, considerations like the method and boundary conditions used can have a profound effect on the extrapolated results.

With this in mind the bulk of existing numerical work on the ATLHM has suggested the existence of a spin gap either for all of $J'/J < 1$ or for J' less than some critical value in the range of $J'/J \sim 0.6-0.8$.[10,11,19] Indeed, an initial analysis of our own data, as can be seen in the inset of Fig. 12, is consistent with this picture. However, a more careful consideration of these results shows that this could be misleading.

As previously, the accessibility of three width 4 system sizes permits a finite-size extrapolation of the energy gap data. This extrapolation was done for values of $J' \leq 0.5$ and can be found in Fig. 12. Values of $1 > J' \geq 0.5$ were not considered due to the possibility of different system sizes being on opposite sides of the J_c' transition. For $J' \leq 0.5$ the Δ values were found to fit very well to a scaling function of form $\frac{a}{N}+\Delta_\infty$ and Δ_∞ was found to be on the order of 10^{-2}. An estimate of the error in this extrapolation can be generated by contrasting the linear fit y-intercept with that of a quadratic fit which produces a Δ_∞ on the order of 10^{-1}. Such small values are extremely suggestive of a gapless system. Taken alone, this is consistent with both spiral and collinear antiferromagnetic orderings as well as potentially a gapless spin liquid phase.

Data was also collected for $J'/J = 1$ where the situation appeared to be different, with linear scaling fits suggesting a small non-zero spin gap. However, it is well known[31,32] that the spin gap converges very slowly with system size in the spiral-ordered region and the system is known to be gapless in this phase. This, combined with the apparent gaplessness of the $J' < J_c'$ region, suggests that the ATLHM is gapless for all $J'/J \leq 1$

One of the central results of the numerics of Ref. 19 was the unusual behaviour of the energy gap Δ for different system widths. This paper studied the incom-

mensurate behaviour of long systems of a small number of chains, i.e. 4×64, 6×64, 8×32, etc. One of the central results of the paper was that for systems (periodic in $\mathbf{y}$) of width 2, 4 and 8 the system exhibited a spin gap for $J'<1$ which shrank with decreasing J' down to $J'\sim0.5$, the lowest J' studied in the work. This spin gap was accompanied by an exponential decay of intrachain correlations. Conversely, systems of width 6 displayed a small or, likely, no such spin gap and presumably an algebraic decay of correlations. The reason for this discrepancy could not be identified. A possible explanation for the discrepancy between these results and the ones presented here could be the presence of a non-zero $\theta_{J'}$ in our calculations allowing the system to relax more completely as we now comment on in more detail.

For J'/J in the neighbourhood of 1 the classical and quantum ordering vector in the $\mathbf{y}$ direction is $q_{J'}=2\pi/3$, where for $J'/J\ll1$ $q_{J'}\to\pi/2$ as $J'\to0$. Thus, a cylinder, as used in Ref. 19, with a width of 6 chains and periodic (no twist) boundary conditions around the cylinder would be commensurate with the $2\pi/3$ order but not the $\pi/2$ order, and thus we expect the correct spin gap for $J'/J\sim1$ and an artificial, finite size induced gap as J' decreases (though this is not observed in Ref. 19 since the spin gap is only calculated as low as $J'\sim0.9$ for the 6×64 system). Conversely, system sizes of 4 and 8 are incommensurate with $2\pi/3$ order, and therefore are found to have an unphysical spin gap when $J'\sim J$, but *are* commensurate with a $q_{J'}=\pi/2$ ordering and thus we expect the correct spin gap to emerge as $J'\to0$. It is then the case that the 4 and 8 width system would be expected to give the most accurate indication of the spin gap for small J' and the width 6 system for $J'/J\sim1$. The key point is that gapless spiral correlations in the J' direction might appear gapped if analyzed with periodic boundary conditions around the cylinder with widths incommensurate with the spiral in that direction. With this in mind, an alternative interpretation of the data of Ref. 19 could be consistent with a system with no spin gap in the thermodynamic limit.

2. Interchain Correlations

Our analysis of intrachain correlations for systems of size 4×4, 4×6, 4×8 produced a clear and consistent picture of antiferromagnetically ordered chains ($\theta_J=0$, $q_J=\pi$ for all chain lengths) accented by incommensurate interchain correlations. The situation for interchain correlations is not so simple.

The open question in the $J'\ll J$ region is whether the systems exhibits a one or two-dimensional spin liquid phase[10–13] or a collinear antiferromagnetic order driven by next-nearest chain antiferromagnetic correlations and order by disorder[16]. This debate can be better informed by a consideration of the interchain ordering vector, $q_{J'}$ and the importance of next-nearest chain antiferromagnetic interactions to the ground-state.

The twist $\theta_{J'}$ which minimizes the ground-state as a function of system *width* is found to be π for 4×4, and 0 for 6×4 and 8×4 for $J'<J'_c$. This is clearly inconsistent with any classical ordering vector $q_{J'}$. This supports the belief that, for the system sizes under consideration, any long-range classical incommensurate spiral order is suppressed. Previous studies which have shown the lack of long-range spiral order had a potentially critical flaw in that they used periodic boundary conditions which undoubtedly destabilize such orderings. It is then interesting that a lack of spiral order is still found when the system has complete freedom to adopt an incommensurate ground-state.

It is important to remember that, although the long-range incommensurate ordering is suppressed short-range incommensurate correlations are still present. This is manifest by the complete lack of any features of the minimum twist when calculated in the total $S^z=1$ sector around the critical J'_c. An implication of this is that the short-range behavior of correlation functions would show the same incommensurate behavior above and below J'_c. It is then natural to consider how strong these incommensurate interchain interactions are, and how they compare to the predicted next-nearest chain antiferromagnetic interactions that would drive a CAF ordering.

The strength of interchain correlations can typically be determined by examining $\left\langle \hat{S}_{\mathbf{x},\mathbf{y}}\hat{S}_{\mathbf{x},\mathbf{y}+y'}\right\rangle$. However, the value of such an analysis here is hindered by the small system sizes numerically available. This deficiency turns out not to be so significant since the qualitative information relating to the correlation between chains can be inferred from the curvature of $\theta_{J'}$. For completely decoupled chains the ground-state energy will have no dependence on the interchain twist $\theta_{J'}$, similarly if the minima in $\theta_{J'}$ that minimizes the ground-state energy is found to be extremely shallow then it can be argued that the interchain correlations are extremely weak. Thus, by taking the second numerical derivative, in the total-$S^z=0$ sector, we can construct a $J'-$*twist susceptibility*:

$$\frac{\partial^2 E_{gs}}{(\partial\theta_{J'})^2}=\chi_{\theta_{J'}}. \tag{25}$$

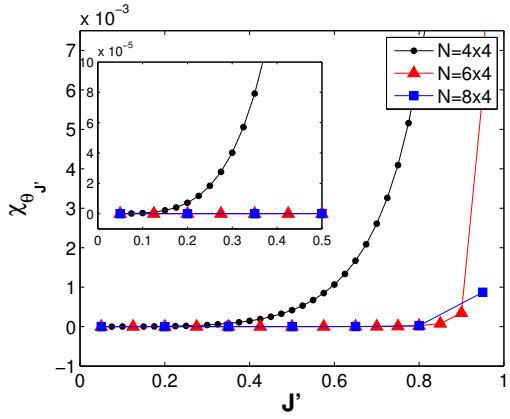

FIG. 13. (Color online.) $\chi_{\theta_{J'}}$ vs. J': The curvature of the ground-state energy (i.e. total-$S^z = 0$) about its minimum ($\theta_{J'} = \pi$ for $N = 4 \times 4$, $\theta_{J'} = 0$ for $N = 6 \times 4$ and $N = 8 \times 4$) with respect to $\theta_{J'}$ ($\chi_{\theta_{J'}}$) versus J' for systems of increasing width. The size of $\chi_{\theta_{J'}}$ gives an indication of the strength and importance of interchain, (i.e. nearest chain) interactions to the ground-state energy. It is clear that these correlations become smaller with width and become exceedingly weak as $J' \to 0$. This is consistent with reasoning from RG and the lack of long-range spiral order in this region.

This susceptibility will probe the strength of interchain correlations with a large value of $\chi_{J'}$ representing strong correlations and a small value of $\chi_{J'}$ representing weak ones.

The $\chi_{\theta_{J'}}$ dependence on J' and system width can be seen in Fig. 13 for a $\delta\theta_{J'}$ of 0.1. It can clearly be seen that interchain correlations become tiny as the number of chains increases. In fact the interchain correlations are found to be zero within the 10^{-13} precision of the numerics for systems of width 6 and 8 for small J' even for such a large value of $\delta\theta_{J'}$. This is consistent with the previous claim that these correlations are too weak to force spiral ordering. However, an RG analysis of the ATLHM[16,17] posit that as the interchain correlations become weak with $J' \to 0$, the next-nearest chains correlate antiferromagnetically with a strength, J_{nnc}, which grows. We will now consider the effect of such correlations.

Recent series expansion work by Pardini and Singh in Ref. 18 have suggested that an incommensurately ordered ground-state has a lower energy than a CAF one for small J'. However, their work also showed that this energy difference was extremely small and dependent on how short-ranged spiral correlations are treated. We found previously that the ground-state is not incommensurately ordered for our system sizes for small J' and instead exhibits intrachain antiferromagnetism. A relevant question is then whether the next-nearest chain interactions are antiferromagnetic (CAF) or ferromagnetic (non-CAF or NCAF) and whether these correlations grow as $J' \to 0$. We previously determined that 6×4 and 8×4 sized systems are minimized, in the total-$S^z = 0$ subspace, by $\theta_{J'} = 0$. This observation makes it difficult to discriminate between CAF and NCAF phases since both would have such a twist. However, the 4×4 system is minimized by a $\theta_{J'} = \pi$, which is inconsistent with CAF ordering. This presents an opportunity to clearly demonstrate the effect of next-nearest neighbour correlations.

We proceed by artificially inserting an exchange coupling between next-nearest chains, $J_{nnn}\hat{S}_{\mathbf{x},\mathbf{y}}\hat{S}_{\mathbf{x}-1,\mathbf{y}+2}$. The question then is, at what strength of J_{nnn} does the 4×4 system adopt a $\theta_{J'} = 0$ ordering (which we take to be CAF). This critical J^c_{nnn} is shown, as a function of J' in Fig. 14. As $J' \to 0$ the necessary "nudge" the system needs to adopt a CAF ordering becomes very small. In fact, for $J' = 0.05$, this critical interaction strength is as tiny as 0.0003. Contrarily, if a *ferromagnetic* interaction is used (i.e. $J_{nnn} < 0$) then $\theta_{J'}$ does not change, regardless the magnitude of J_{nnn}. The fact that such a minuscule increase in antiferromagnetic next-nearest neighbour correlations can force the ground-state minimizing boundary twist to jump to one consistent with CAF ordering and inconsistent with NCAF ordering lends promise to the notion of CAF ordering in the thermodynamic limit.

The ability to easily force a 4×4 system into a CAF consistent ordering is appealing, but hardly conclusive, evidence that CAF ordering will occur for larger systems, especially since this system is so small. We therefore consider another means of analysing these interactions that can be applied to larger systems.

We begin by perturbing our system with two different arrangements of staggered magnetic field. The first arrangement is chosen to be consistent with CAF ordering and involves antiferromagnetic staggering along chains and between next-nearest chains (see Fig. 15, left). We only apply fields to *every other* chain in order to allow the system the freedom to adopt the classical $q_{J'} = \pi/2$ ordering. The second arrangement is designed to be consistent with ferromagnetic ordering between next-nearest chains (see Fig. 15, right) but still antiferromagnetic along chains. Two susceptibilities are constructed from this perturbation.

The first susceptibility, which we call χ_{NNN}, is constructed from the next-nearest neighbour chain correla-

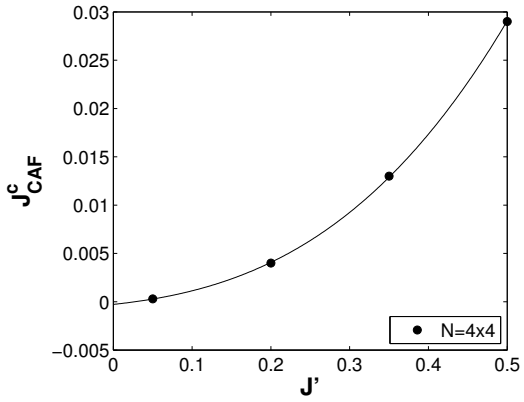

FIG. 14. (Color online.) J^c_{CAF} vs. J' for $N = 4 \times 4$: As is discussed in the text, the $N = 4 \times 4$ system, whose $\theta_{J'}$ of π is found to be incompatible with the predicted collinear-antiferromagnetic (CAF) ordering for $J' \ll 1$, can be forced to a θ_J of 0, consistent with this ordering by applying only a small next-nearest neighbour antiferromagnetic interaction J_{CAF} (see text). Thus, as a demonstration of the subtle importance of these next-nearest chain interactions the critical J^c_{CAF} for which $\theta_{J'}$ jumps from π to 0 is plotted as a function of J'. For $J' = 0.05$ this value becomes as low as $J^c_{CAF} = 0.0003$ representing an extreme susceptibility to such interactions. Conversely a next-nearest chain *ferromagnetic* interaction is found to have no effect on $\theta_{J'}$. This suggests a strong preference for CAF order. This solid line is given as an aid for the eye.

tion functions:

$$\chi_{NNN} = \frac{\delta^2 \langle \hat{S}_{\mathbf{x},\mathbf{y}} \hat{S}_{\mathbf{x}-1,\mathbf{y}+2} \rangle}{\delta h^2} \tag{26}$$

where h is arranged in one of the two (CAF or NCAF) ways. The first derivative term was found to be zero, which could have been predicted on the basis of spin inversion symmetry, and thus calculating this quantity is a simple matter of numerical differentiation. The results, as a function of J', are shown in Fig. 16 where calculations were done only between chains that received a magnetic field (i.e. between chains 0 and 2 or 2 and 4 but not 1 and 3). The specific chain considered and the specific spin within that chain was found to be irrelevant.

This χ_{NNN} is found to be largely system size independent and negative (positive) for CAF (NCAF) correlations. This is consistent with the notion that a perturbative CAF field will cause the next-nearest chain correlations to grow more negative and a NCAF field to grow more positive. The extremely similar magnitude of the two correlations suggests the system exhibits a

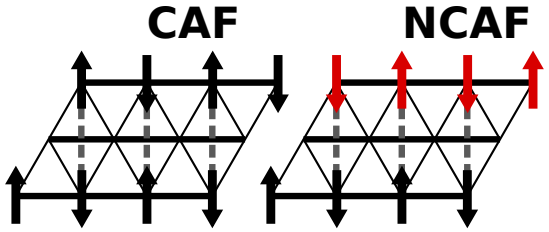

FIG. 15. A diagram of the staggered fields applied in the generation of χ_{NNN}, χ_{CAF} and χ_{NCAF}. The field terms, $h\hat{S}^z_i$, are represented by arrows. Fields are placed on every *other* chain to allow the system freedom to adopt a classical $q_{J'} = \pi/2$ ordering. The collinear antiferromagnetic (CAF) ordering is found on the left and corresponds to antiferromagnetic correlations between next-nearest chains. For clarity, a sample next-nearest chain partner for the non-skewed triangular system is illustrated with a dotted line. The non-collinear antiferromagnetic (NCAF) ordering, corresponding to *ferromagnetic* next-nearest chain correlations, is shown on the right.

delicate competition between collinear and non-collinear next-nearest chain correlations in the non-spiral ordered phase and that this susceptibility grows as $J' \to 0$. The growth of this susceptibility, coupled with the diminution of nearest-chain correlations as demonstrated in Fig. 13 seems consistent with the picture painted by renormalization theory. However, the system seems potentially equally susceptible to ferromagnetic next-nearest chain interactions. One then wonders which of these correlations ultimately prevails. In order to consider this we consider yet another susceptibility.

To quantify the systems preference towards ferromagnetic versus antiferromagnetic next-nearest chain ordering, we considered the effect that perturbing magnetic fields of Fig. 15 have on the ground-state energy. We thus define:

$$\chi_{CAF} = \frac{\delta^2 E_{gs}}{\delta h^2_{CAF}}, \quad \chi_{NCAF} = \frac{\delta^2 E_{gs}}{\delta h^2_{NCAF}}. \tag{27}$$

As before, the first derivative term was found to be zero. This is due to spin inversion symmetry. χ_{CAF} can be found plotted in Fig. 17. χ_{NCAF}, which is not plotted, behaves identically except being positive. The fact that χ_{CAF} is negative implies that CAF-ordering lowers the systems energy where NCAF, having a positive χ_{NCAF}, increases it. Furthermore, when we compare the *magnitudes* of the two susceptibilities, which can be found in the inset of Fig. 17, we see that χ_{CAF} is in fact larger than χ_{NCAF} for all system sizes. Though it is important to note that it is only larger by a margin of $\sim 10^{-7}$, and decreases with system width, further

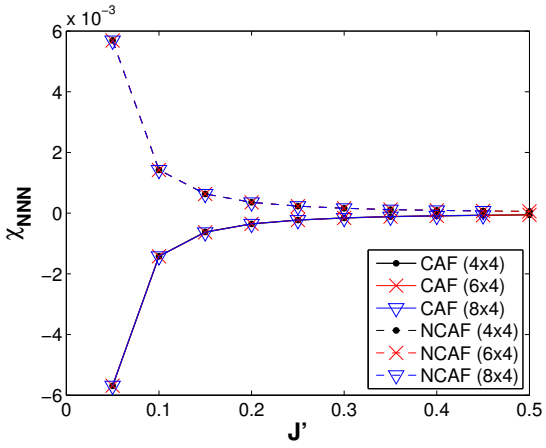

FIG. 16. (Color online.) χ_{NNN} vs. J' and System Size: χ_{NNN}, being a susceptibility of the next-nearest chain correlation function to collinear (CAF) and non-collinear (NCAF) perturbative magnetic fields further discussed in the text, plotted against J' for various system widths. The perturbing field was of strength $h = 0.001$ and applied to half the sites for both CAF and NCAF (see text). Calculations were done in total-$S^z = 0$ about the $\theta_{J'} = 0$ minima. This quantity is found to be largely system size independent and negative (positive) for CAF (NCAF) correlations. This is consistent with the notion that a perturbative CAF field will cause the next-nearest chain correlations to grow more negative and a NCAF field to grow more positive. The extremely similar magnitude of the two correlations suggest the system exhibits a delicate competition between collinear and non-collinear next-nearest chain correlations in the non-spiral ordered phase and that this susceptibility grows as $J' \to 0$.

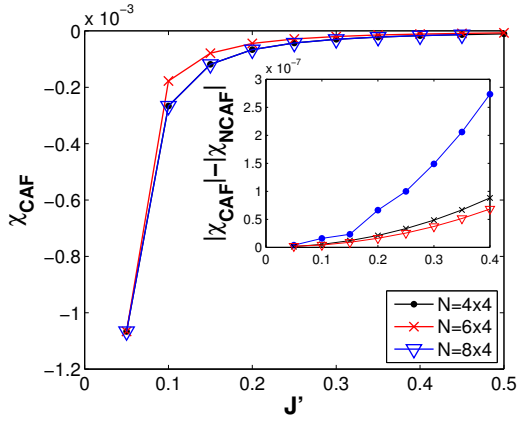

FIG. 17. (Color online.) χ_{CAF} vs. J': χ_{CAF}, being the second derivative of the ground-state energy (i.e. total-$S^z = 0$, $\theta_{J'} = 0$) with respect to a collinear antiferromagnetic (CAF) perturbing magnetic field, versus J' for systems of varying width. For all system sizes the quantity is found to be negative and increasing in magnitude with decreasing J'. This implies that the system's energy is lowered by promoting CAF-like ordering. In order to establish the strength of this affinity for CAF order vs. non-collinear antiferromagnetic (NCAF) order, a similar ground-state susceptibility is defined relative to an NCAF perturbing magnetic field (χ_{NCAF}). The inset show the difference in magnitude between χ_{CAF} and χ_{NCAF}. χ_{CAF} is found to be greater for all system sizes and J' though only by $\sim 10^{-7}$.

evidencing the tenuousness of these competing correlations.

IV. CONCLUSION AND SUMMARY

In this paper we have demonstrated the power of twist boundary conditions to mitigate potentially disastrous finite-size effects in incommensurate systems. Using these twisted boundary conditions we were able to extract the intrachain incommensurate q-vector q_J and found it to be in good agreement with results on substantially larger systems. Furthermore, we were also able to extract the *inter*chain incommensurate q-vector $q_{J'}$. To our knowledge our is the first work to allow fully incommensurate behaviour in both intra- and interchain directions.

Analysis of the incommensurability in both the ground-state and total $S^z = 1$ excited state revealed a potential phase transition between a long-range spiral ordered phase and one with short-range spiral correlations. A scaling analysis of this critical J'_c suggests that this point is at $J'_c \sim 0.475$ for systems of width 4 and ~ 0.948 for systems of infinite width (length 4). We then attempted to characterize the $J' < J'_c$ phase. We believe it to be gapless in the thermodynamic limit, as well as dominated by both next-nearest ferromagnetic and antiferromagnetic correlations. Additionally, the nearest chain correlations are found to become minuscule. Further analysis reveals that the antiferromagnetic interactions are marginally stronger in the systems considered. This is consistent with the renormalization group claim that this region should be CAF ordered.

ACKNOWLEDGMENTS

We would like to thank Sedigh Ghamari, Sung-Sik Lee and Catherine Kallin for many fruitful discussions. We also acknowledge computing time at the Shared Hierarchical Academic Research Computing Network (SHARCNET:www.sharcnet.ca) and research support

from NSERC.

* thesbeme@mcmaster.ca
† sorensen@mcmaster.ca; http://comp-phys.mcmaster.ca

[1] Y. Shimizu, K. Miyagawa, K. Kanoda, M. Maesato, and G. Saito, Phys. Rev. Lett. **91**, 107001 (2003).
[2] Y. Qi, C. Xu, and S. Sachdev, Phys. Rev. Lett. **102**, 176401 (2009).
[3] H. C. Kandpal, I. Opahle, Y.-Z. Zhang, H. O. Jeschke, and R. Valentí, Phys. Rev. Lett. **103**, 067004 (2009).
[4] R. Coldea, D. A. Tennant, A. M. Tsvelik, and Z. Tylczynski, Phys. Rev. Lett. **86**, 1335 (2001).
[5] O. A. Starykh, H. Katsura, and L. Balents, Phys. Rev. B **82**, 014421 (2010).
[6] R. Coldea, D. A. Tennant, R. A. Cowley, D. F. McMorrow, B. Dorner, and Z. Tylczynski, Phys. Rev. Lett. **79**, 151 (1997).
[7] R. Coldea, D. A. Tennant, K. Habicht, P. Smeibidl, C. Wolters, and Z. Tylczynski, Phys. Rev. Lett. **88**, 137203 (2002).
[8] W. Zheng, R. R. P. Singh, R. H. McKenzie, and R. Coldea, Phys. Rev. B **71**, 134422 (2005).
[9] H. Tanaka, T. Ono, H. A. Katori, H. Mitamura, F. Ishikawa, and T. Goto, Progress of Theoretical Physics Supplement **145**, 101 (2002), http://ptps.oxfordjournals.org/content/145/101.full.pdf+html.
[10] M. Q. Weng, D. N. Sheng, Z. Y. Weng, and R. J. Bursill, Phys. Rev. B **74**, 012407 (2006).
[11] D. Heidarian, S. Sorella, and F. Becca, Phys. Rev. B **80**, 012404 (2009).
[12] P. Hauke, Phys. Rev. B **87**, 014415 (2013).
[13] J. Merino, R. H. McKenzie, J. B. Marston, and C. H. Chung, Journal of Physics: Condensed Matter **11**, 2965 (1999).
[14] M. Kohno, L. Balents, and O. Starykh, Journal of Physics: Conference Series **145**, 012062 (2009).
[15] L. Balents, Nature **464**, 199 (2010).
[16] O. A. Starykh and L. Balents, Phys. Rev. Lett. **98**, 077205 (2007).
[17] S. Ghamari, C. Kallin, S.-S. Lee, and E. S. Sørensen, Phys. Rev. B **84**, 174415 (2011).
[18] T. Pardini and R. R. P. Singh, Phys. Rev. B **77**, 214433 (2008).
[19] A. Weichselbaum and S. R. White, Phys. Rev. B **84**, 245130 (2011).
[20] J. Reuther and R. Thomale, Phys. Rev. B **83**, 024402 (2011).
[21] M. Thesberg and E. S. Sørensen, Phys. Rev. B **84**, 224435 (2011).
[22] S. Chen, L. Wang, S.-J. Gu, and Y. Wang, Phys. Rev. E **76**, 061108 (2007).
[23] T. Tonegawa and I. Harada, J. Phys. Soc. Jpn. **56**, 2153 (1987).
[24] S. Eggert, Phys. Rev. B **54**, R9612 (1996).
[25] R. Chitra, S. Pati, H. R. Krishnamurthy, D. Sen, and S. Ramasesha, Phys. Rev. B **52**, 6581 (1995).
[26] S. R. White and I. Affleck, Phys. Rev. B **54**, 9862 (1996).
[27] F. D. M. Haldane, Phys. Rev. B **25**, 4925 (1982).
[28] A. A. Aligia, C. D. Batista, and F. H. L. Eßler, Phys. Rev. B **62**, 3259 (2000).
[29] A. Yoshimori, Journal of the Physical Society of Japan **14**, 807 (1959).
[30] J. Villain, Journal of Physics and Chemistry of Solids **11**, 303 (1959).
[31] L. Capriotti, A. E. Trumper, and S. Sorella, Phys. Rev. Lett. **82**, 3899 (1999).
[32] A. E. Trumper, L. Capriotti, and S. Sorella, Phys. Rev. B **61**, 11529 (2000).

6 Conclusions

The central impetus of the body of work developed throughout this thesis is towards a two-fold goal. The first of these is the demonstration of the utility of a number of extensions to the standard exact diagonalization approach, specifically methods based around generalized fidelity susceptibilities, the higher-order fidelity and twisted boundary conditions. The second goal was to provide new insights into the phase diagram of the anisotropic triangular lattice Heisenberg model (ATLHM) and the more general anisotropic next-nearest neighbour triangular lattice Heisenberg model (ANNTLHM). It is worthwhile, in this final chapter, to reflect upon the relative success and progress towards these two goals.

It has been shown that generalization of the standard fidelity susceptibility can produce useful parameters. It has been shown that such methods successfully identify the BKT-type transition in the $J_1 - J_2$ chain where many other numerical methods have difficulty. It has been shown that twisted boundary conditions can, rather impressively, provide valuable information about incommensurate physics in small systems, even when other methods used on much larger systems fail to capture such behaviour. Finally, it has been shown that the sort of "order parameter fidelity susceptibilities" do provide a simple and direct insight into the ordering behaviour of a given phase. However, it is necessary to note that the somewhat naive expectation of a direct one-to-one correspondence between phase and a signal in these fidelity susceptibilities was not born out. Rather it was found that when exploring a given phase a number of different generalized fidelity susceptibilities will show a large non-zero value and exhibit strong qualitative features. The method then requires a level of interpretation and is thus potentially susceptible to *misinterpretation*. Additionally, these methods could certainly benefit from a more rigorous theoretical study of their behaviour, scaling and comparability. However, regardless of this non-ideal behaviour it can confidently be said that the first goal was successfully accomplished.

Success with regards to the second goal is somewhat less solid. The higher-order fidelity did illuminate the existence of a bounded region which, although previously theorized to exist, has never been quantitatively identified. However, this achievement is diminished somewhat by the matching appearance of an obviously unphysical transition within the same diagram. The nature of this false transition does seem to have been adequately identified as an artefact of incommensurate physics in small systems. Thus, further study on larger systems and with twisted boundary conditions could provide further insights here. The success of these twisted boundary conditions in the ATLHM is particularly impressive in that the q-vectors obtained are in strong agreement with other numerical work[117] conducted on substantially larger systems. It

is further striking that the small systems studied here were sufficient to *extend* that work into the $J' \to 0$ region.

As was discussed earlier the effectiveness of the generalized fidelity susceptibilities when applied to the ANNTLHM was somewhat mixed. These quantities did indeed provide valuable information into the relative importance of various forms of correlations. However, the fact that many phases are the result of a competition between different types of correlations means that these results require a degree of interpretation and are thus unpleasantly subjective. However, it remains to be seen to what extent further study could bolster the clarity of interpretation of these quantities.

Suffice it to say that the preceding work has demonstrated a greater variety and value of exact diagonalization as a numerical tool then is commonly expressed. It has been shown that in many ways the restriction to extremely small system sizes required by ED do not entirely doom the method. Clever extensions of the technique can still produce important results. This is very important given that ED is often one of the only techniques available in many classes of systems (i.e. higher-dimensional frustrated quantum systems). Although, no doubt, as research continues on these systems new and improved numerical techniques will be developed. However, this thesis goes part of the way towards showing that exact diagonalization techniques may still have a place a while still.

References

[1] Philip W Anderson et al. More is different. *Science*, 177(4047):393–396, 1972.

[2] Assa Auerbach. *Interacting Electrons and Quantum Magnetism*. Graduate Texts in Contemporary Physics. Springer New York, 1994.

[3] LD Landau. On the theory of phase transitions. *Zh. Eksp. Teoret. Fiz*, 7:19–32, 1937.

[4] LD Landau and VL Ginzburg. On the theory of superconductivity. *Journal of Experimental and Theoretical Physics (USSR)*, 20:1064, 1950.

[5] Kenneth G. Wilson. The renormalization group: Critical phenomena and the kondo problem. *Rev. Mod. Phys.*, 47:773–840, Oct 1975.

[6] Kenneth G. Wilson. The renormalization group and critical phenomena. *Rev. Mod. Phys.*, 55:583–600, Jul 1983.

[7] N. Goldenfeld. *Lectures on Phase Transitions and the Renormalization Group*. Advanced Book Program. Addison-Wesley, Advanced Book Program, 1992.

[8] Lars Onsager. Crystal statistics. i. a two-dimensional model with an order-disorder transition. *Phys. Rev.*, 65:117–149, Feb 1944.

[9] L.P. Kadanoff. Spin-spin correlations in the two-dimensional ising model. *Il Nuovo Cimento B Series 10*, 44(2):276–305, 1966.

[10] L.P. Kadanoff. Scaling laws for Ising models near T(c). *Physics*, 2:263–272, 1966.

[11] Yoichiro Nambu. Quasi-particles and gauge invariance in the theory of superconductivity. *Phys. Rev.*, 117:648–663, Feb 1960.

[12] J. Goldstone. Field theories with superconductor solutions. *Il Nuovo Cimento*, 19(1):154–164, 1961.

[13] Jeffrey Goldstone, Abdus Salam, and Steven Weinberg. Broken symmetries. *Phys. Rev.*, 127:965–970, Aug 1962.

[14] R. Shankar. Renormalization-group approach to interacting fermions. *Rev. Mod. Phys.*, 66:129–192, Jan 1994.

[15] Michael E. Fisher. Renormalization group theory: Its basis and formulation in statistical physics. *Rev. Mod. Phys.*, 70:653–681, Apr 1998.

[16] Michael E. Fisher. The renormalization group in the theory of critical behavior. *Rev. Mod. Phys.*, 46:597–616, Oct 1974.

[17] John B. Kogut. An introduction to lattice gauge theory and spin systems. *Rev. Mod. Phys.*, 51:659–713, Oct 1979.

[18] S. L. Sondhi, S. M. Girvin, J. P. Carini, and D. Shahar. Continuous quantum phase transitions. *Rev. Mod. Phys.*, 69:315–333, Jan 1997.

[19] A. Altland and B.D. Simons. *Condensed Matter Field Theory*. Cambridge books online. Cambridge University Press, 2010.

[20] N. Nagaosa. *Quantum Field Theory in Condensed Matter Physics*. Texts and monographs in physics. U.S. Government Printing Office, 1999.

[21] J.W. Negele and H. Orland. *Quantum Many-particle Systems*. Advanced Books Classics. Westview Press, 2008.

[22] R.P. Feynman and A. Zee. *QED: The Strange Theory of Light and Matter*. Alix G. Mautner memorial lectures. Princeton University Press, 2006.

[23] Guang-Shan Tian and Hai-Qing Lin. Excited-state level crossing and quantum phase transition in one-dimensional correlated fermion models. *Phys. Rev. B*, 67:245105, Jun 2003.

[24] T. Senthil, Ashvin Vishwanath, Leon Balents, Subir Sachdev, and Matthew P. A. Fisher. Deconfined quantum critical points. *Science*, 303(5663):1490–1494, 2004.

[25] T. Senthil, Leon Balents, Subir Sachdev, Ashvin Vishwanath, and Matthew P. A. Fisher. Quantum criticality beyond the landau-ginzburg-wilson paradigm. *Phys. Rev. B*, 70:144407, Oct 2004.

[26] G. H. Wannier. Antiferromagnetism. the triangular ising net. *Phys. Rev.*, 79:357–364, Jul 1950.

[27] G. H. Wannier. Antiferromagnetism. the triangular ising net. *Phys. Rev. B*, 7:5017–5017, Jun 1973.

[28] Leon Balents. Spin liquids in frustrated magnets. *Nature*, 464:199, Mar 2010.

[29] X.G. Wen. *Quantum Field Theory of Many-Body Systems: From the Origin of Sound to an Origin of Light and Electrons*. Oxford Graduate Texts. OUP Oxford, 2007.

[30] A. Goussev, R. A. Jalabert, H. M. Pastawski, and D. Wisniacki. Loschmidt Echo. *ArXiv e-prints*, June 2012.

[31] Asher Peres. Stability of quantum motion in chaotic and regular systems. *Phys. Rev. A*, 30:1610–1615, Oct 1984.

[32] Rodolfo A. Jalabert and Horacio M. Pastawski. Environment-independent decoherence rate in classically chaotic systems. *Phys. Rev. Lett.*, 86:2490–2493, Mar 2001.

[33] Zbyszek P. Karkuszewski, Christopher Jarzynski, and Wojciech H. Zurek. Quantum chaotic environments, the butterfly effect, and decoherence. *Phys. Rev. Lett.*, 89:170405, Oct 2002.

[34] F. M. Cucchietti, D. A. R. Dalvit, J. P. Paz, and W. H. Zurek. Decoherence and the loschmidt echo. *Phys. Rev. Lett.*, 91:210403, Nov 2003.

[35] Fernando Martin Cucchietti, Sonia Fernandez-Vidal, and Juan Pablo Paz. Universal decoherence induced by an environmental quantum phase transition. *Phys. Rev. A*, 75:032337, Mar 2007.

[36] H. T. Quan, Z. Song, X. F. Liu, P. Zanardi, and C. P. Sun. Decay of loschmidt echo enhanced by quantum criticality. *Phys. Rev. Lett.*, 96:140604, Apr 2006.

[37] Lorenzo Campos Venuti and Paolo Zanardi. Unitary equilibrations: Probability distribution of the loschmidt echo. *Phys. Rev. A*, 81:022113, Feb 2010.

[38] Davide Rossini, Tommaso Calarco, Vittorio Giovannetti, Simone Montangero, and Rosario Fazio. Decoherence induced by interacting quantum spin baths. *Phys. Rev. A*, 75:032333, Mar 2007.

[39] Victor Mukherjee, Shraddha Sharma, and Amit Dutta. Loschmidt echo with a nonequilibrium initial state: Early-time scaling and enhanced decoherence. *Phys. Rev. B*, 86:020301, Jul 2012.

[40] Lorenzo Campos Venuti, N. Tobias Jacobson, Siddhartha Santra, and Paolo Zanardi. Exact infinite-time statistics of the loschmidt echo for a quantum quench. *Phys. Rev. Lett.*, 107:010403, Jul 2011.

[41] Paolo Zanardi and Nikola Paunković. Ground state overlap and quantum phase transitions. *Phys. Rev. E*, 74:031123, Sep 2006.

[42] V R Vieira. Quantum information and phase transitions: Fidelity and state distinguishability. *Journal of Physics: Conference Series*, 213(1):012005, 2010.

[43] Huan-Qiang Zhou and John Paul Barjaktarevi. Fidelity and quantum phase transitions. *Journal of Physics A: Mathematical and Theoretical*, 41(41):412001, 2008.

[44] A. Fabricio Albuquerque, Fabien Alet, Clément Sire, and Sylvain Capponi. Quantum critical scaling of fidelity susceptibility. *Phys. Rev. B*, 81:064418, Feb 2010.

[45] Lorenzo Campos Venuti and Paolo Zanardi. Quantum critical scaling of the geometric tensors. *Phys. Rev. Lett.*, 99:095701, Aug 2007.

[46] Bo Wang, Mang Feng, and Ze-Qian Chen. Berezinskii-kosterlitz-thouless transition uncovered by the fidelity susceptibility in the xxz model. *Phys. Rev. A*, 81:064301, Jun 2010.

[47] Uma Divakaran. Three-site interacting spin chain in a staggered field: Fidelity versus loschmidt echo. *Phys. Rev. E*, 88:052122, Nov 2013.

[48] P. D. Sacramento, N. Paunković, and V. R. Vieira. Fidelity spectrum and phase transitions of quantum systems. *Phys. Rev. A*, 84:062318, Dec 2011.

[49] Marek M. Rams and Bogdan Damski. Quantum fidelity in the thermodynamic limit. *Phys. Rev. Lett.*, 106:055701, Feb 2011.

[50] Silvano Garnerone, Damian Abasto, Stephan Haas, and Paolo Zanardi. Fidelity in topological quantum phases of matter. *Phys. Rev. A*, 79:032302, Mar 2009.

[51] Amit Tribedi and Indrani Bose. Entanglement and fidelity signatures of quantum phase transitions in spin liquid models. *Phys. Rev. A*, 77:032307, Mar 2008.

[52] Sheng-Hao Li, Qian-Qian Shi, Yao-Heng Su, Jin-Hua Liu, Yan-Wei Dai, and Huan-Qiang Zhou. Tensor network states and ground-state fidelity for quantum spin ladders. *Phys. Rev. B*, 86:064401, Aug 2012.

[53] Marco Cozzini, Radu Ionicioiu, and Paolo Zanardi. Quantum fidelity and quantum phase transitions in matrix product states. *Phys. Rev. B*, 76:104420, Sep 2007.

[54] Yao Heng Su, Bing-Quan Hu, Sheng-Hao Li, and Sam Young Cho. Quantum fidelity for degenerate ground states in quantum phase transitions. *Phys. Rev. E*, 88:032110, Sep 2013.

[55] L. Campos Venuti, M. Cozzini, P. Buonsante, F. Massel, N. Bray-Ali, and P. Zanardi. Fidelity approach to the hubbard model. *Phys. Rev. B*, 78:115410, Sep 2008.

[56] David Schwandt, Fabien Alet, and Sylvain Capponi. Quantum monte carlo simulations of fidelity at magnetic quantum phase transitions. *Phys. Rev. Lett.*, 103:170501, Oct 2009.

[57] Bo Li, Sheng-Hao Li, and Huan-Qiang Zhou. Quantum phase transitions in a two-dimensional quantum xyx model: Ground-state fidelity and entanglement. *Phys. Rev. E*, 79:060101, Jun 2009.

[58] Shu Chen, Li Wang, Yajiang Hao, and Yupeng Wang. Intrinsic relation between ground-state fidelity and the characterization of a quantum phase transition. *Phys. Rev. A*, 77:032111, Mar 2008.

[59] Wen-Long You, Ying-Wai Li, and Shi-Jian Gu. Fidelity, dynamic structure factor, and susceptibility in critical phenomena. *Phys. Rev. E*, 76:022101, Aug 2007.

[60] S.-J. Gu. Fidelity approach to quantum phase transitions. *International Journal of Modern Physics B*, 24(23):4371, 2010.

[61] Yu-Chin Tzeng, Hsiang-Hsuan Hung, Yung-Chung Chen, and Min-Fong Yang. Fidelity approach to gaussian transitions. *Phys. Rev. A*, 77:062321, Jun 2008.

[62] Bo Wang, Mang Feng, and Ze-Qian Chen. Berezinskii-kosterlitz-thouless transition uncovered by the fidelity susceptibility in the xxz model. *Phys. Rev. A*, 81:064301, Jun 2010.

[63] S. Greschner, A. K. Kolezhuk, and T. Vekua. Fidelity susceptibility and conductivity of the current in one-dimensional lattice models with open or periodic boundary conditions. *Phys. Rev. B*, 88:195101, Nov 2013.

[64] Min-Fong Yang. Ground-state fidelity in one-dimensional gapless models. *Phys. Rev. B*, 76:180403, Nov 2007.

[65] Bogdan Damski. Fidelity susceptibility of the quantum ising model in a transverse field: The exact solution. *Phys. Rev. E*, 87:052131, May 2013.

[66] Yoshihiro Nishiyama. Criticalities of the transverse- and longitudinal-field fidelity susceptibilities for the $d = 2$ quantum ising model. *Phys. Rev. E*, 88:012129, Jul 2013.

[67] Yoshihiro Nishiyama. Critical behavior of the fidelity susceptibility for the transverse-field ising model. *Physica A: Statistical Mechanics and its Applications*, 392(19):4345 – 4350, 2013.

[68] Wing-Chi Yu, Ho-Man Kwok, Junpeng Cao, and Shi-Jian Gu. Fidelity susceptibility in the two-dimensional transverse-field ising and xxz models. *Phys. Rev. E*, 80:021108, Aug 2009.

[69] Yan-Chao Li and Shu-Shen Li. Quantum critical phenomena in the xy spin chain with the dzyaloshinski-moriya interaction. *Phys. Rev. A*, 79:032338, Mar 2009.

[70] N. Tobias Jacobson, Silvano Garnerone, Stephan Haas, and Paolo Zanardi. Scaling of the fidelity susceptibility in a disordered quantum spin chain. *Phys. Rev. B*, 79:184427, May 2009.

[71] Ke-Wei Sun and Qing-Hu Chen. Quantum phase transition of the one-dimensional transverse-field compass model. *Phys. Rev. B*, 80:174417, Nov 2009.

[72] Shi-Jian Gu, Ho-Man Kwok, Wen-Qiang Ning, and Hai-Qing Lin. Fidelity susceptibility, scaling, and universality in quantum critical phenomena. *Phys. Rev. B*, 77:245109, Jun 2008.

[73] Nikola Paunković and Vitor Rocha Vieira. Macroscopic distinguishability between quantum states defining different phases of matter: Fidelity and the uhlmann geometric phase. *Phys. Rev. E*, 77:011129, Jan 2008.

[74] Wen-Long You and Yu-Li Dong. Fidelity susceptibility in two-dimensional spin-orbit models. *Phys. Rev. B*, 84:174426, Nov 2011.

[75] Xiaoguang Wang, Zhe Sun, and Z. D. Wang. Operator fidelity susceptibility: An indicator of quantum criticality. *Phys. Rev. A*, 79:012105, Jan 2009.

[76] N. Tobias Jacobson, Paolo Giorda, and Paolo Zanardi. Transition to chaos of coupled oscillators: An operator fidelity susceptibility study. *Phys. Rev. E*, 82:056204, Nov 2010.

[77] Marko Znidaric and Tomazc Prosen. Fidelity and purity decay in weakly coupled composite systems. *Journal of Physics A: Mathematical and General*, 36(10):2463, 2003.

[78] H.-Q. Zhou. Renormalization group flows and quantum phase transitions: fidelity versus entanglement. *ArXiv e-prints*, April 2007.

[79] Erik Eriksson and Henrik Johannesson. Reduced fidelity in topological quantum phase transitions. *Phys. Rev. A*, 79:060301, Jun 2009.

[80] Shu Chen, Li Wang, Shi-Jian Gu, and Yupeng Wang. Fidelity and quantum phase transition for the heisenberg chain with next-nearest-neighbor interaction. *Phys. Rev. E*, 76:061108, Dec 2007.

[81] Oleg A. Starykh and Leon Balents. Ordering in spatially anisotropic triangular antiferromagnets. *Phys. Rev. Lett.*, 98:077205, Feb 2007.

[82] Sedigh Ghamari, Catherine Kallin, Sung-Sik Lee, and Erik S. Sørensen. Order in a spatially anisotropic triangular antiferromagnet. *Phys. Rev. B*, 84:174415, Nov 2011.

[83] Masashi Hase, Haruhiko Kuroe, Kiyoshi Ozawa, Osamu Suzuki, Hideaki Kitazawa, Giyuu Kido, and Tomoyuki Sekine. Magnetic properties of $Rb_2Cu_2Mo_3O_12$ including a one-dimensional spin-$\frac{1}{2}$ heisenberg system with ferromagnetic first-nearest-neighbor and antiferromagnetic second-nearest-neighbor exchange interactions. *Phys. Rev. B*, 70:104426, Sep 2004.

[84] C K Majumdar. Antiferromagnetic model with known ground state. *Journal of Physics C: Solid State Physics*, 3(4):911, 1970.

[85] Chanchal K. Majumdar and Dipan K. Ghosh. On nextnearestneighbor interaction in linear chain. i. *Journal of Mathematical Physics*, 10(8), 1969.

[86] Chanchal K. Majumdar and Dipan K. Ghosh. On nextnearestneighbor interaction in linear chain. ii. *Journal of Mathematical Physics*, 10(8), 1969.

[87] F. D. M. Haldane. Spontaneous dimerization in the $s = \frac{1}{2}$ heisenberg antiferromagnetic chain with competing interactions. *Phys. Rev. B*, 25:4925–4928, Apr 1982.

[88] R. Chitra, Swapan Pati, H. R. Krishnamurthy, Diptiman Sen, and S. Ramasesha. Density-matrix renormalization-group studies of the spin-$\frac{1}{2}$ heisenberg system with dimerization and frustration. *Phys. Rev. B*, 52:6581–6587, Sep 1995.

[89] T. Tonegawa and I. Harada. Spontaneous dimerization in the $s = \frac{1}{2}$ heisenberg antiferromagnetic chain with competing interactions. *J. Phys. Soc. Jpn.*, 56:2153, 1987.

[90] Sebastian Eggert. Numerical evidence for multiplicative logarithmic corrections from marginal operators. *Phys. Rev. B*, 54(14):R9612–R9615, Oct 1996.

[91] Steven R. White and Ian Affleck. Dimerization and incommensurate spiral spin correlations in the zigzag spin chain: Analogies to the kondo lattice. *Phys. Rev. B*, 54:9862–9869, Oct 1996.

[92] Andreas Deschner and Erik S. Sørensen. Incommensurability effects in odd length $J_1 - J_2$ quantum spin chains: On-site magnetization and entanglement. *Phys. Rev. B*, 87:094415, Mar 2013.

[93] V. L. Berezinskiĭ. Destruction of Long-range Order in One-dimensional and Two-dimensional Systems Possessing a Continuous Symmetry

Group. II. Quantum Systems. *Soviet Journal of Experimental and Theoretical Physics*, 34:610, 1972.

[94] V. L. Berezinskiĭ. Destruction of Long-range Order in One-dimensional and Two-dimensional Systems having a Continuous Symmetry Group I. Classical Systems. *Soviet Journal of Experimental and Theoretical Physics*, 32:493, 1971.

[95] J M Kosterlitz and D J Thouless. Ordering, metastability and phase transitions in two-dimensional systems. *Journal of Physics C: Solid State Physics*, 6(7):1181, 1973.

[96] P.W. Anderson. Resonating valence bonds: A new kind of insulator? *Materials Research Bulletin*, 8(2):153 – 160, 1973.

[97] Rajiv R. P. Singh and David A. Huse. Three-sublattice order in triangular- and kagomé-lattice spin-half antiferromagnets. *Phys. Rev. Lett.*, 68:1766–1769, Mar 1992.

[98] Luca Capriotti, Adolfo E. Trumper, and Sandro Sorella. Long-range néel order in the triangular heisenberg model. *Phys. Rev. Lett.*, 82:3899–3902, May 1999.

[99] Adolfo E. Trumper, Luca Capriotti, and Sandro Sorella. Finite-size spin-wave theory of the triangular heisenberg model. *Phys. Rev. B*, 61:11529–11532, May 2000.

[100] R. Coldea, D. A. Tennant, R. A. Cowley, D. F. McMorrow, B. Dorner, and Z. Tylczynski. Quasi-1d $s = \frac{1}{2}$ antiferromagnet Cs_2CuCl_4 in a magnetic field. *Phys. Rev. Lett.*, 79:151–154, Jul 1997.

[101] R. Coldea, D. A. Tennant, A. M. Tsvelik, and Z. Tylczynski. Experimental realization of a 2d fractional quantum spin liquid. *Phys. Rev. Lett.*, 86:1335–1338, Feb 2001.

[102] R. Coldea, D. A. Tennant, K. Habicht, P. Smeibidl, C. Wolters, and Z. Tylczynski. Direct measurement of the spin hamiltonian and observation of condensation of magnons in the 2d frustrated quantum magnet Cs_2CuCl_4. *Phys. Rev. Lett.*, 88:137203, Mar 2002.

[103] Oleg A. Starykh, Hosho Katsura, and Leon Balents. Extreme sensitivity of a frustrated quantum magnet: Cs_2CuCl_4. *Phys. Rev. B*, 82:014421, Jul 2010.

[104] S. V. Isakov, T. Senthil, and Yong Baek Kim. Ordering in Cs_2CuCl_4: Possibility of a proximate spin liquid. *Phys. Rev. B*, 72:174417, Nov 2005.

[105] Masanori Kohno, Oleg A. Starykh, and Leon Balents. Spinons and triplons in spatially anisotropic frustrated antiferromagnets. *Nat Phys*, 3:790, Nov 2007.

[106] Weihong Zheng, Rajiv R. P. Singh, Ross H. McKenzie, and Radu Coldea. Temperature dependence of the magnetic susceptibility for triangular-lattice antiferromagnets with spatially anisotropic exchange constants. *Phys. Rev. B*, 71:134422, Apr 2005.

[107] Hidekazu Tanaka, Toshio Ono, Hiroko Aruga Katori, Hiroyuki Mitamura, Fumihiro Ishikawa, and Tsuneaki Goto. Magnetic phase transition and magnetization plateau in Cs_2CuBr_4. *Progress of Theoretical Physics Supplement*, 145:101–106, 2002.

[108] Y. Shimizu, K. Miyagawa, K. Kanoda, M. Maesato, and G. Saito. Spin liquid state in an organic mott insulator with a triangular lattice. *Phys. Rev. Lett.*, 91:107001, Sep 2003.

[109] Yang Qi, Cenke Xu, and Subir Sachdev. Dynamics and transport of the Z_2 spin liquid: Application to κ-$(ET)_2cu_2(CN)_3$. *Phys. Rev. Lett.*, 102:176401, Apr 2009.

[110] Hem C. Kandpal, Ingo Opahle, Yu-Zhong Zhang, Harald O. Jeschke, and Roser Valentí. Revision of model parameters for κ-type charge transfer salts: An *Ab Initio* study. *Phys. Rev. Lett.*, 103:067004, Aug 2009.

[111] Dariush Heidarian, Sandro Sorella, and Federico Becca. Spin-$\frac{1}{2}$ heisenberg model on the anisotropic triangular lattice: From magnetism to a one-dimensional spin liquid. *Phys. Rev. B*, 80:012404, Jul 2009.

[112] M. Q. Weng, D. N. Sheng, Z. Y. Weng, and Robert J. Bursill. Spin-liquid phase in an anisotropic triangular-lattice heisenberg model: Exact diagonalization and density-matrix renormalization group calculations. *Phys. Rev. B*, 74:012407, Jul 2006.

[113] Johannes Reuther and Ronny Thomale. Functional renormalization group for the anisotropic triangular antiferromagnet. *Phys. Rev. B*, 83:024402, Jan 2011.

[114] Seiji Yunoki and Sandro Sorella. Two spin liquid phases in the spatially anisotropic triangular heisenberg model. *Phys. Rev. B*, 74:014408, Jul 2006.

[115] T. Pardini and R. R. P. Singh. Magnetic order in coupled spin-half and spin-one heisenberg chains in an anisotropic triangular-lattice geometry. *Phys. Rev. B*, 77:214433, Jun 2008.

[116] Zheng Weihong, Ross H. McKenzie, and Rajiv R. P. Singh. Phase diagram for a class of spin-$\frac{1}{2}$ heisenberg models interpolating between the square-lattice, the triangular-lattice, and the linear-chain limits. *Phys. Rev. B*, 59:14367–14375, Jun 1999.

[117] Andreas Weichselbaum and Steven R. White. Incommensurate correlations in the anisotropic triangular heisenberg lattice. *Phys. Rev. B*, 84:245130, Dec 2011.

[118] Sedigh Ghamari, Catherine Kallin, Sung-Sik Lee, and Erik S. Sorensen. Triangular spin-$\frac{1}{2}$ antiferromagnet : Experiments, theory and numerics. *Physics in Canada*, 68:79–82, Apr 2012.